The zinc-binding group effect: lessons from non-hydroxamic acid vorinostat analogs

Silke Geurs,[a,b] Dorien Clarisse,[b,c] Karolien De Bosscher[b,c] and Matthias D'hooghe[*a]

[a] *SynBioC Research Group, Department of Green Chemistry and Technology, Faculty of Bioscience Engineering, Ghent University, Coupure Links 653, B-9000 Ghent, Belgium; matthias.dhooghe@UGent.be*

[b] *Translational Nuclear Receptor Research, VIB-UGent Center for Medical Biotechnology, Technologiepark-Zwijnaarde 75, FSVMII, Zwijnaarde, Belgium*

[c] *Department of Biomolecular Medicine, Ghent University, Technologiepark-Zwijnaarde 75, FSVMII, Zwijnaarde, Belgium*

[*] *Corresponding author: matthias.dhooghe@ugent.be*

Abstract

Histone deacetylases (HDAC) are enzymes pursued as drug targets in various cancers and several non-oncological conditions, such as inflammation and neurodegenerative disorders. In the past decade, HDAC inhibitors have emerged as relevant pharmaceuticals, with many efforts devoted to the development of new representatives. However, the growing safety concerns regarding the established hydroxamic acid-based HDAC inhibitors tend to drive current research more toward the design of inhibitors bearing alternative zinc-binding groups. This perspective presents an overview of all non-hydroxamic acid zinc-binding groups (ZBGs) that have been incorporated into the clinically approved prototypical HDAC inhibitor SAHA (suberoylanilide hydroxamic acid, vorinostat). This provides the unique opportunity to compare the inhibition potential and biological effects of different ZBGs in a direct way, as the compounds selected for this perspective only differ in their ZBG. To that end, different strategies used to select a ZBG, its properties, activity, and liabilities are discussed.

1. Introduction

Lysine acetylation and deacetylation are vital posttranslational modifications found in diverse organisms, ranging from bacteria to humans.[1, 2] These operations regulate protein function and structure, thereby influencing numerous cellular processes.[3] Lysine deacetylases catalyze the hydrolysis of acetyllysine, which was first discovered to take place on ε-amino groups of lysine residues within histone tails, and consequently these enzymes have been referred to as histone deacetylases (HDACs).[4, 5] Human HDACs occur in eighteen isoforms, also called isozymes, and can be classified into two major groups. Group 1 comprises class I (HDAC1-3 and 8), class IIa (HDAC4, 5, 7 and 9), class IIb (HDAC6 and 10) and class IV (HDAC11), encompassing eleven zinc-dependent isozymes, while group 2 includes class III HDACs or sirtuins, which are NAD^+-dependent.[6] HDACs likely evolved from a common metalloprotein ancestor with arginases, a class of manganese metalloenzymes. These enzyme families both contain a characteristic α/β hydrolase fold and a conserved metal binding site.[7-9]

Lysine deacetylases act upon a much broader substrate scope than just histone tails, which challenges the historical "HDAC" nomenclature and classification. Myriad non-histone proteins,[10, 11] polyamines (HDAC10)[12] and lysine fatty acids (HDAC11)[13, 14] are also substrates of HDAC enzymes. Moreover, class IIa HDACs are weak deacetylases because an essential catalytic tyrosine residue is replaced by a histidine moiety in their active site, and they possibly serve rather as scaffolds in macromolecular complexes.[15-17]

HDACs are upregulated in various types of cancer and are associated with neurodegeneration and immune disorders,[18-24] rendering them important therapeutic targets to inhibit from a pharmaceutical perspective. To date, four HDAC inhibitors (panobinostat, belinostat, vorinostat, romidepsin) have been FDA-approved for use in hematological cancer treatment,[25-28] and tucidinostat (Epidaza) has been approved by the NMPA (formerly CFDA)[29, 30] to treat hematological and breast cancers. In addition, a large number of HDAC inhibitors (HDACi) are currently in clinical trials,[11, 31, 32] and plenty more have been published.[33, 34] Most HDACi bear a hydroxamic acid (HA) functionality to chelate the Zn^{2+} ion in the catalytic pocket of HDACs 1 to 11. Despite their powerful HDAC inhibitory activity, concerns have been raised about the clinical use of HA-based HDAC inhibitors. They exhibit poor pharmacokinetics as a result of rapid clearance and it has been suggested that the observed cardiac adverse side effects upon use of HDACi might be caused by hERG channel inhibition and non-selective metal binding by the powerful HA. The primary concern, however, is the mutagenicity that could result from the transformation of the HA into an isocyanate susceptible to nucleophilic attack by DNA residues.[35, 36] Therefore, there is a high need to identify powerful HA substitutes as a means of providing safer HDACi that could also be included in (long-term) non-oncological applications.

Identifying valuable alternative zinc-binding groups (ZBG) is a challenging task because of the large number of functional groups able to bind metals and the chemical potential to chelate a zinc ion alone does not suffice to ensure activity in a biological setting. The importance of the identity of the ZBG is justified by its contribution to the binding affinity, its influence on the selectivity, and even the binding mode of the inhibitor molecule. Non-hydroxamic acid (non-HA) HDACi that have already been synthesized and evaluated *in vitro* serve as a source of inspiration to many researchers for the design of novel HDACi with an alternative ZBG. The choice of this ZBG, however, has often been based on the comparison of the activity of molecules that not only differ in their ZBG but also in the cap group and the linker unit. Because the latter two components significantly influence the binding of compounds and even the chelation potential of the ZBG, it is impossible to attribute the observed inhibitory activity to the ZBG alone. Consequently, this has hampered the way forward to select the most valuable ZBG.[37] Therefore, in this perspective, we provide an unprecedented overview of alternative zinc-binding

groups that have been incorporated in the clinically-approved prototypical HDAC inhibitor SAHA **1** (suberoylanilide hydroxamic acid, vorinostat, **Figure 1**). SAHA **1** is a nanomolar non-selective, competitive class I and II HDAC inhibitor,[38-40] often used as a pharmacophore for the synthesis of analogs, the introduction of non-hydroxamic acid zinc-binding groups and as a tool compound to investigate the effects of structural modifications on binding, activity and selectivity. Moieties inserted on or near the hydroxamic acid zinc-binding group were not included, as these do not represent alternative ZBGs, but rather a modification to improve binding. Thus, only compounds differing in their ZBG were selected for this perspective, providing a unique opportunity to compare the inhibition potential and biological effects of different ZBGs in a direct way. The rationale to select these functional groups as ZBG candidates is also discussed, as a source of inspiration for medicinal chemists and to make connections with the observed activity.

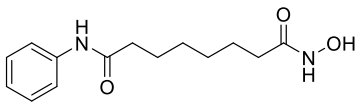

SAHA **1**

*Figure 1 Structure of the prototypical HDAC inhibitor SAHA **1** (suberoylanilide hydroxamic acid, vorinostat).*

2. Catalytic and inhibition mechanism

HDACi can act as transition state or substrate analogs, hence knowledge of the catalytic mechanism provides a strong basis for developing new inhibitors. It is also crucial to understand the inhibition mechanism and the properties underlying the strong binding capacity of hydroxamic acids to identify and select potent substitutes.

2.1 Catalytic mechanism

Crystal structures are essential to understand the molecular properties of HDAC function, selectivity, and inhibition and have been identified for HDACs 1-4,[41-43] 6-8[44-47] and 10.[12] The catalytic mechanism has been mainly elucidated based on structural and enzymological studies of HDAC6 and 8, elaborating on a bacterial homolog-based mechanistic proposal.[48, 49] Comparison of the X-ray crystal structures of the catalytic sites of human HDAC6 (*h*CD1 and 2, *Homo sapiens*) and HDAC6 from zebrafish (*dr*CD1 and 2, *Danio rerio*) indicated that the *dr*HDAC6 is an appropriate substitute for *h*HDAC6, generating crystals of higher quality that are easier to analyze. Crystal structures of *dr*CD2 in the unliganded state and in complex with a fluorogenic peptide substrate provided insights into the catalytic mechanism.[44] In the unliganded state, the nucleophilic water molecule present in the catalytic site forms a hydrogen-donating and a hydrogen-accepting bond with two histidine residues (H573 and H574, *dr*HDAC6 numbering) and coordinates with the Zn^{2+} ion (**Figure 2**, A). Upon substrate binding, the carbonyl moiety binds with the zinc ion without displacing the water molecule, resulting in a penta-coordinated zinc ion (**Figure 2**, B). This scissile carbonyl is further activated for nucleophilic addition of the water molecule by a hydrogen bond with a tyrosine moiety (Y745). Coordination lowers the pKa of the water molecule sufficiently to allow deprotonation by a histidine residue (H573), followed by nucleophilic addition across the carbonyl group. The resulting tetrahedral oxyanion intermediate is stabilized by Zn^{2+} and by hydrogen bonds with neighboring amino acids (**Figure 2**, C). The ultimate collapse of this intermediate into lysine and acetate is initiated by the protonation of the amino group by a histidine residue (**Figure 2**, C, and D).[49] The (de)protonation events by histidine residues differ slightly between HDACs. In HDAC6, a tandem histidine pair ensures a dual general base (H573)-general acid (H574) function (**Figure 2**, B and C), while in HDAC8 H143 serves as a single general base-general acid, and

H142 remains positively charged, functioning as an electrostatic catalyst (**Figure 2**, E and F).[7, 44, 47, 49] In conclusion, a carbonyl group, either from a peptide, ester, ketone, or aldehyde is subjected to hydration in the active site of a zinc hydrolase, as long as the carbonyl moiety is isosteric to the natural substrate.[44]

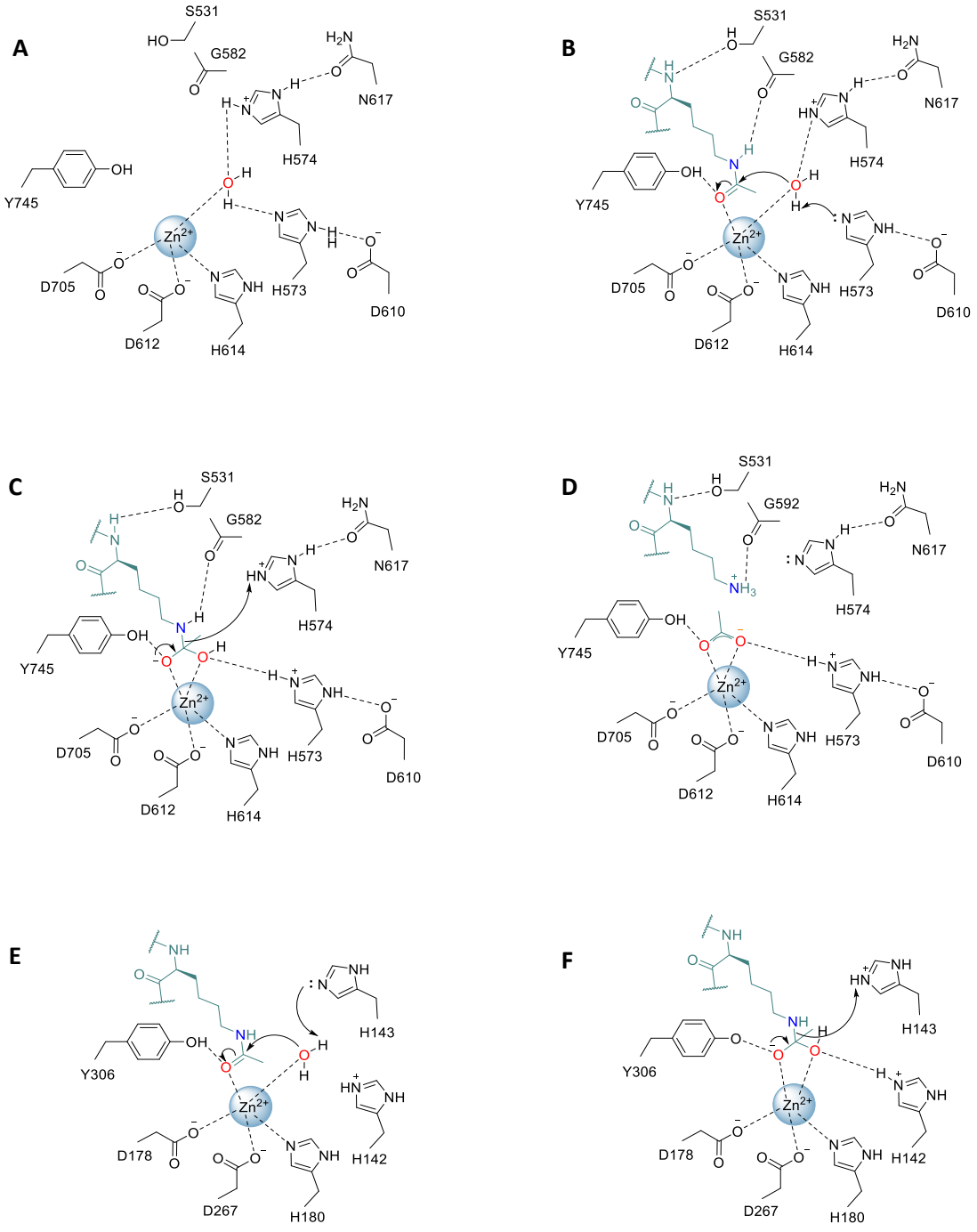

Figure 2 Mechanism of acetyllysine hydrolysis catalyzed by HDACs, exemplified for HDAC6 (A-D) and HDAC8 (E-F). *A) Unliganded state of the catalytic pocket of zebrafish HDAC6 (Danio rerio, drHDAC6). B) Binding of the acetyllysine substrate in the active site of drHDAC6, with indicated activation of the scissile carbonyl function and the nucleophilic water molecule.*

C-D) Collapse of the intermediate and release of reaction products. E-F) In human HDAC8 H143 serves as a single general base-general acid.[44]

2.2 Inhibition of histone deacetylases by hydroxamic acids

Hydroxamic acid (HA)-based structures represent the most studied class of HDACi, owing to their high metal chelating potential. This makes them excellent zinc-binding groups in HDAC inhibitors, resulting in IC_{50} values in the low nanomolar range.[32, 50-53] SAHA is an nonselective inhibitor of both class I and II HDACs (IC_{50} ~ 50 nM),[38, 54] but more recent studies demonstrate a hundred-fold selectivity toward HDAC8 of class I.[55, 56] SAHA is a competitive inhibitor with a fast-on/fast-off binding behavior, resulting in a rapid induction of hyperacetylation with a maximal level after 6 hours of treatment (SH-SY5Y cells). Indeed, the kinetic association rates determined using purified enzymes appeared predictive of the cellular kinetics of histone acetylation.[57, 58] The protonation state of the hydroxamic acid moiety of SAHA upon binding has been, however, under debate for more than a decade. Computational studies by Duca *et al.*[59] have demonstrated a decrease in pKa with ~3.3 units upon complexation of zinc in the active site of the metalloprotease TACE (tumor necrosis factor α converting enzyme), which has an active site similar to HDACs. This could contribute to the excellent inhibition properties of HAs: they are present in neutral form in an aqueous solution (pKa is 9.4 for aliphatic HAs), which results in a small desolvation penalty upon binding. Complexation to zinc lowers the pKa of HAs sufficiently to enable deprotonation by an adjacent histidine in the active site.[60] Some experimental and theoretical studies, however, assume a neutral hydroxamic acid to be present.[61] According to a class-dependent hypothesis,[60] SAHA is deprotonated in class I HDACs due to a conserved tyrosine residue, and is neutral in class IIa HDACs due to a histidine residue that increases binding affinity. This hypothesis has been contested and a metal-dependent mechanism was proposed, describing that the deprotonation of SAHA is mostly modulated by the metal ion (Ca^{2+}/K^{+}) in the second metal site.[62] Models taking into account the second metal site and one or two water molecules constructing hydrogen bonds with SAHA and glycine/tyrosine residues in HDAC2/7/8 show that deprotonated SAHA is much more stable within HDAC7/8, but cannot be theoretically differentiated for HDAC2.[62] For HDAC6, Christianson *et al*. described that a negatively-charged hydroxamate is formed upon binding.[44, 63]

Next to the protonation/deprotonation debate, the stabilities of the different HA conformers and the deprotonation sites (OH and NH) have been studied. Density-functional theory (DFT) studies (B3LYP) identified the 1*Z*-keto form as the most stable form (**Figure 3**). For the metal-free molecule, deprotonation of the NH group is thermodynamically favored, while metal coordination occurs to the *O*-deprotonated 1*Z*-keto HA (**Figure 4**).[64] This is corroborated by the C-O and C-N bond lengths of 1.223 Å and 1.315 Å, determined from the crystal structure of SAHA in complex with Danio rerio HDAC6 (PDB: 5EEI), which correspond to what is expected for the keto form.[44, 65]

Z-keto (1*Z*) | *E*-keto (1*E*) | *Z*-iminol (2*Z*) | *E*-iminol (1*E*)

Figure 3 E and Z isomers of the keto and enol forms of hydroxamic acids.[66]

SAHA binds the Zn^{2+} ion present in the catalytic site in a bidentate manner through its carbonyl group and oxyanion, constituting a stable five-membered ring, as was observed in crystal structures of zebrafish HDAC6 (*Danio rerio*, *dr*HDAC6)[44] and an HDAC8 homolog.[46, 48] Monodentate coordination has been observed for other HA-based HDACi, for example in crystal structures of inhibitors with a phenyl linker unit.[11, 67, 68] Upon bidentate coordination, the Zn^{2+}-associated water molecule is displaced, while the oxyanion and carbonyl group of the deprotonated hydroxamic acid interact with H573 and Y745, respectively, and the NH forms a hydrogen bond with H574 (**Figure 4**, *dr*HDAC6 numbering). A very similar binding mode is observed in X-ray studies of the hydroxamic acid analog of N^8-acetylspermidine

in complex with HDAC10.[69] The high affinity of HA-based HDAC inhibitors likely results from this specific constellation of hydrogen bonds and metal interactions.[63]

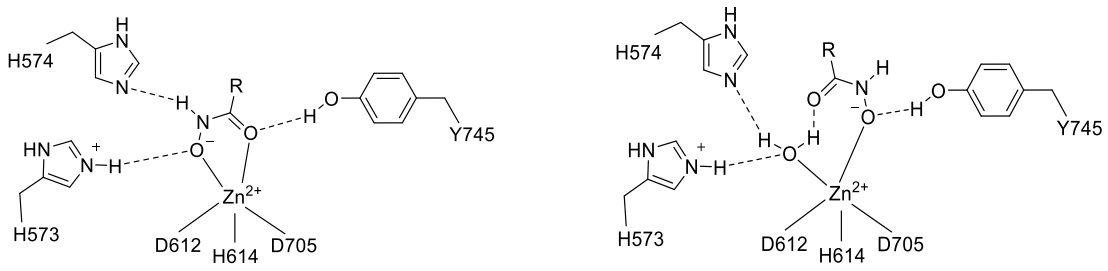

Figure 4 Bidentate (A) and monodentate (B) binding modes of hydroxamate anion in the catalytic cavity of Danio rerio HDAC6. Dashed lines: hydrogen bonds, solid lines Zn^{2+}: metal-coordination interactions.[67]

Two types of molecular geometries of the Zn^{2+}-inhibitor interactions are common in most zinc enzymes: tetrahedral, as a result of the substitution of the non-protein fourth zinc ligand (a hydroxide ion or water molecule) by the inhibitor, and trigonal-bipyramidal, after addition of the inhibitor to the zinc coordination sphere, in which the zinc ion is coordinated by the three protein ligands, a water molecule and the inhibitor (**Figure 4**).[70]

Based on the catalytic and inhibition mechanisms, a number of strategies can be identified to replace the hydroxamic acid as a ZBG to overcome therapeutic limitations, i.e. the introduction of (i) a stable structure incorporating the favorable structural features of the unstable transition state conformation, which are not present in the ground state,[71] (ii) analogs of the natural substrate, (iii) hydroxamic acid mimics, serving as bidentate ligands, and (iv) functional groups that can engage in extensive hydrogen bonding and strong metal chelation in the catalytic site. For example, thiol-containing moieties can be viable alternatives considering the thiophilic nature of the zinc ion. Next to these, inspiration for the selection of alternative zinc-binding groups may arise from existing bioactive and natural molecules.

3. Overview of potential alternative zinc-binding groups

Table 1 Overview of SAHA analogs containing a non-hydroxamic acid zinc-binding group evaluated against HDAC-containing nuclear extract (typically rich in class I HDACs), and/or selected recombinant human HDAC isozymes and corresponding inhibitory potencies (IC_{50}, in µM). The IC_{50} determined for SAHA 1 in the same experiment is mentioned as a reference to enhance the comparability of the results.

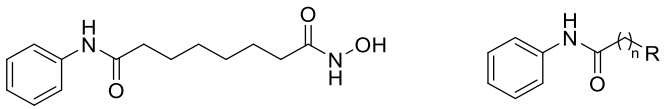

SAHA **1**

Entry	Compound number	R	n	HDAC[a]	IC_{50} (µM)[b]	IC_{50} SAHA (µM)	Opportunities/Liabilities	Reference
1	**2**		6	HeLa nuclear extract	> 100	0.28	Micromolar activity against HDACs after optimization of cap and linker groups.	[72]
2	**6**	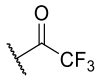	6	HDAC1/2 from K562 extract	6.7	ND[c]	Selectivity for class IIa over class I is possible. Readily reduced to the inactive alcohol in biological environments.	[73]
3	**9**	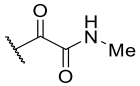	6	HeLa nuclear extract	0.34	ND[c]	Readily reduced to the inactive alcohol in biological environments.	[74, 75]
4	**12**	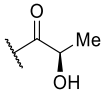	6	HeLa nuclear extract HDAC6	8.9 > 300	0.099 0.033	Selectivity over HDAC6. Non-selective antiproliferative effect on *Plasmodium falciparum* and Jurkat, K562, and HEK293 human cell lines that could be HDAC-independent.	[37] [37]
5	**13**	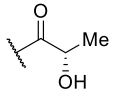	6	HeLa nuclear extract HDAC6	77.1 > 300	0.099 0.033		[37] [37]
6	**14**	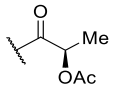	6	HeLa nuclear extract HDAC6	63.8 > 300	0.033 0.033		[37] [37]
7	**15**	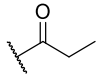	6	HeLa nuclear extract HDAC6	> 100 > 300	0.099 0.033		[37] [37]
8	**16**		6	HeLa nuclear extract	> 40	0.37		[76]

		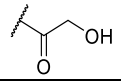		HDAC8	> 40	0.82		76
9	**23**	-SH	6	HeLa nuclear extract	0.21	0.28	Zinc is thiophilic.	77-79
				HeLa nuclear extract	0.058	0.055	Prone to dimerization.	80
				HDAC1	0.218	0.136	A prodrug is required to enhance cell penetration.	80
				HDAC6	0.074	0.082		80
10	**24**	-SAc	6	HeLa nuclear extract	7.1	0.28	Only moderate cancer cell growth inhibition by *S*-acetyl prodrug.	77-79
11	**25**	-SMe	6	HeLa nuclear extract	> 100	0.28		77-79
12	**26**		6	HeLa nuclear extract	> 40	0.37		76
				HDAC8	> 40	0.82		
13	**27**		6	HeLa nuclear extract	> 40	0.37		76
				HDAC8	> 40	0.82		
14	**29**	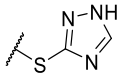	5	HeLa nuclear extract	8.1	0.051 (HDAC1) 0.172 (HDAC2)		81
15	**30**	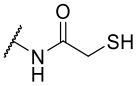	4	HeLa nuclear extract	2.80	0.060	Functional mimic of HA. Inherent selectivity for HDAC6.	82
			5	HeLa nuclear extract	1.10	0.060	Selectivity for *Schistosoma mansoni* over human HDAC8.	82
				HeLa nuclear extract	0.39	0.28		79
			6	HeLa nuclear extract	2.44	0.37	Antiparasitic activity.	76
				HDAC8	3.89	0.82	*In vitro* neuroprotection without toxicity. Prone to dimerization. A prodrug is required to enhance cell penetration.	76
16	**33**	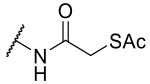	5	HeLa nuclear extract	22	0.28		79
					20.1	0.37		76
17	**35**	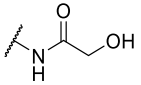	5	HeLa nuclear extract	> 100	0.28		77,79
				HeLa nuclear extract	> 40	0.37		76
				HDAC8	> 40	0.82		76
18	**36**	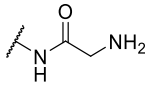	5	HeLa nuclear extract	>100	0.28		77,79

19	**37**	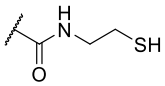	4	HeLa nuclear extract	1.50	0.06		[82]
			5	HeLa nuclear extract	2.50	0.06		[82]
			6	HeLa nuclear extract	2.35	0.06		[82]
20	**38**	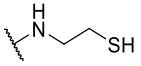	6	HeLa nuclear extract	> 100	0.28		[78]
21	**39**	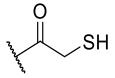	6	HeLa nuclear extract	0.15	0.37	Potential not further explored.	[76]
				HDAC8	0.69	0.82		[76]
22	**40**	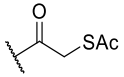	6	HeLa nuclear extract	0.081	0.37		[76]
				HDAC8	0.19	0.82		[76]
23	**41**	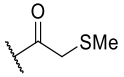	6	HeLa nuclear extract	> 40	0.37		[76]
				HDAC8	>40	0.82		[76]
24	**44**	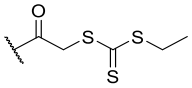	6	HeLa nuclear extract	0.050	0.079	Lacks cellular activity. Structural optimization delivered nanomolar HDAC6-selective inhibitors.	[83]
25	**50**	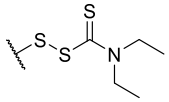	5	HeLa nuclear extract	0.7	ND	Possibly acts as a prodrug for thiols.	[81]
				HDAC1	0.046	0.051		
				HDAC2	0.18	0.17		[81]
				HDAC6	0.068	0.017		
				HDAC10	0.14	0.080		
26	**51**		6	HeLa nuclear extract	230	0.28		[79]
27	**52**	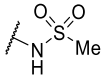	5	HeLa nuclear extract	7500	0.28		[79]
28	**53**	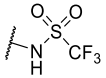	5	All HDAC isoforms	NA[c,d]	ND[e]		[84]
29	**54**	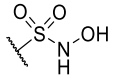	6	HeLa nuclear extract	> 100	0.28		[79]
30	**55**		6	HeLa nuclear extract	48	0.28	A partial negative charge on oxygen could enable potent zinc coordination.	[85]
31	**56**	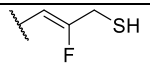	4	HeLa nuclear extract	0.51	1.1	Non-hydrolyzable.	[86]

			5	HeLa nuclear extract	0.36	1.1	Increased lipophilicity. π-system can interact with hydrophobic environment Prone to dimerization. No cellular data.	86
32	**57**	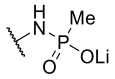	5	HeLa nuclear extract	2000	0.11	Cytotoxic effect possibly due to off-target effects or inhibition of HDAC isozymes not included in assay.	54
				HDAC8	280	0.27		
33	**58**	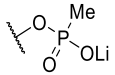	5	HeLa nuclear extract	6100	0.11		54
				HDAC8	390	0.27		
34	**59**	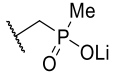	5	HeLa nuclear extract	8200	0.11		54
				HDAC8	390	0.27		
35	**60**	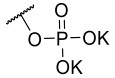	4	HeLa cell extract	2200	0.2	No cellular data.	
				HDAC8	ND[e]	1		
				HDAC3	ND[e]	0.24		
			5	HeLa cell extract	60	0.2		87
				HDAC8	179	1		
				HDAC3	690	0.24		
			6	HeLa cell extract	3900	0.2		
				HDAC8	ND[e]	1		
				HDAC3	ND[e]	0.24		
36	**61**	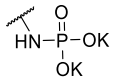	4	HeLa cell extract	360	0.2		
				HDAC8	ND[e]	1		
				HDAC3	ND[e]	0.24		
			5	HeLa cell extract	70	0.2		87
				HDAC8	129	1		
				HDAC3	240	0.24		
			6	HeLa cell extract	490	0.2		
				HDAC8	ND[e]	1		
				HDAC3	ND[e]	0.24		
37	**62**	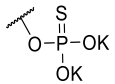	5	HeLa cell extract	50	0.2		87
				HDAC8	49	1		
				HDAC3	103	0.24		
38	**63**	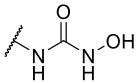	5	HeLa nuclear extract	80	0.28	Similar binding mode to HA. High desolvation penalty.	79, 88

39	**64**	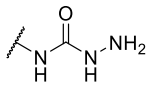	5	HeLa nuclear extract	150	0.28		[79]
40	**65**	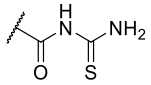	4				Bidentate chelation, stable six-membered coordination complex.	
			5	Only cytotoxicity	ND[e]	ND[e]	Dose-dependent cytotoxicity, limited effect on healthy cells. No HDAC inhibition data.	[89]
41	**66**	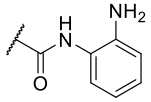	4	HeLa nuclear extract	238	ND[e]	High selectivity for HDAC1-3.	[90]
				HeLa nuclear extract	78	ND[e]	Active in *in cellulo* and *in vivo* models of Friedreich's ataxia and Huntington's disease, but results are contested. More persistent histone hyperacetylation. Metabolic liabilities.	[90]
			5	HDAC1	1.51	ND[e]		[91]
				HDAC2	2.23	ND[e]		
				HDAC3	0.25	ND[e]		
				HDAC8 and class II	> 50	ND[e]		
			6	HeLa nuclear extract	120	0.28		[79]
					87	ND[e]		[90]
42	**68**	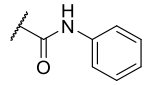	5	HeLa nuclear extract	204	ND[e]		[90]
43	**69**	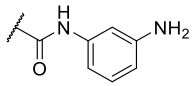	5	HeLa nuclear extract	500	ND[e]		[90]
			6	HeLa nuclear extract	85	ND[e]		[90]
44	**70**	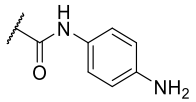	5	HeLa nuclear extract	123	ND[e]		[90]
			6	HeLa nuclear extract	186	ND[e]		[90]
45	**71**	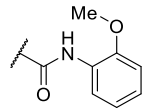	5	HeLa nuclear extract	54	ND[e]		[90]
			6	HeLa nuclear extract	470	ND[e]		[90]
46	**72**	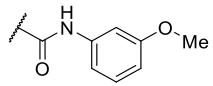	5	HeLa nuclear extract	> 1 mM	ND[e]		[90]
47	**73**	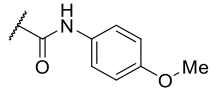	5	HeLa nuclear extract	438	ND[e]		[90]

48	**74**	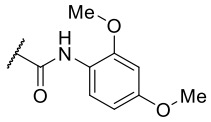	5	HeLa nuclear extract	387	ND[e]		90
49	**75**	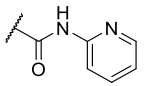	5	HeLa nuclear extract	140	ND[e]		90
			6	HeLa nuclear extract	99	ND[e]		90
50	**76**	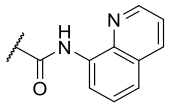	5	HeLa nuclear extract	17	ND[e]		90
51	**77**	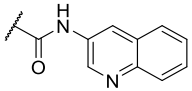	5	HeLa nuclear extract	84	ND[e]		90
52	**80**	-SeCN	6	HeLa nuclear extract	8.9. 10^{-3}	0.20	Selenium interferes in cell cycle progression pathways.	92
53	**81**	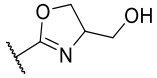	6	HDAC[f]	> 1	ND[e]	No cytotoxic effect on different cancer cell lines.	93
54	**98**	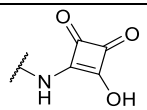	4 5 6	HDAC[f]	> 1	ND[e]		88
55	**99**	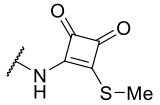	4 5 6	HDAC[f]	> 1	ND[e]	No cytotoxic effect on different cancer cell lines.	88
56	**100**	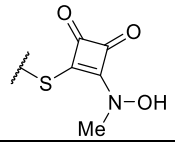	4 5 6	HDAC[f]	> 1	ND[e]		88

[a] Substrate used in the assay to determine the inhibitory activity of the SAHA analogs.

[b] The standard deviations were < 30% of the IC_{50} values.

[c] NA: No activity

[d] Tested against all HDAC isoforms at 10 µM and 100 µM, at which no or very limited inhibition was observed.

[e] ND: Not determined

[f] Not specified how the assay was performed.

Table 2 Overview of the SAHA analogs containing a non-hydroxamic acid zinc-binding group evaluated against all recombinant human zinc-dependent HDAC isoforms, i.e. class I (HDAC1-3 and 8), class IIa (HDAC4, 5, 7, and 9) and class IIb (HDAC6 and 10). The standard deviations were < 30% of the IC_{50} values.

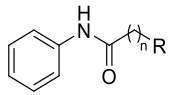

Entry	Compound number	n	R	IC_{50} (μM) HDAC											Opportunities/Liabilities	Ref
				1	2	3	4	5	6	7	8	9	10	11		
1	**1**		SAHA[b]	0.021	0.032	0.028	24.0	50.0	0.051	70.0	3.0	> 100	0.11	0.03		
2	**6**	6		7.8	1.4	0.3	0.04	0.9	2.2	0.6	1.7	5.9	19.0	100.0	See Table 1.	
3	**10**	6		2.7	6.0	0.6	> 100	> 100	18.0	> 100	27.0	ND[a]	5.0	57.0	Stable geminal diol. Low micromolar inhibition of HDAC1-3 and 10, high selectivity over HDAC4,5,7 and 11. Increased lipophilicity. No info on metabolic stability.	84
4	**1**		SAHA[c]	0.061	0.24	0.25	0.21	0.15	0.10	2.48	0.18	0.02	0.15	0.1		
5	**19**	6	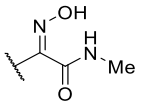	56.7	100	18.6	65.7	59.3	> 100	36.2	22.6	30.7	> 100	> 100	*N*-methyl substituent is responsible for the activity. No cellular data.	94
6	**1**		SAHA[d]	0.044	0.089	0.14	6.86	> 10	0.17	> 10	1.53	7.37	0.24	> 10		
7	**66**	6	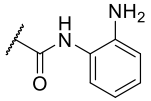	0.83	0.53	0.38	> 10	> 10	> 10	> 10	> 10	> 10	> 10	> 10	See Table 1.	
8	**79**	6	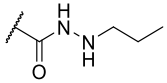	0.045	0.12	0.020	> 10	> 10	> 10	> 10	> 10	> 10	> 10	> 10	Interaction with the allosteric site. No zinc-binding.	95
9	**86**		TSA[e,f]	ND[a]	ND[a]	ND[a]	ND[a]	ND[a]	0.0004	0.09	ND[a]	ND[a]	ND[a]	ND[a]		96

10	**82**	4	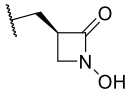	> 1000	> 1000	> 1000	> 1000	> 1000	132	> 1000	> 1000	> 1000	> 1000	> 1000	
11	**83**	4	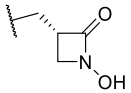	> 1000	> 1000	> 1000	> 1000	> 1000	174	> 1000	> 1000	> 1000	> 1000	> 1000	High selectivity for HDAC6 Selectivity can be switched by changing the substituent on the nitrogen atom. No cellular data.
12	**84**	4	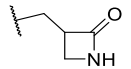	> 1000	> 1000	> 1000	> 1000	> 1000	74.5	> 1000	> 1000	> 1000	> 1000	> 1000	
13	**85**	4	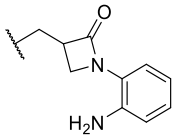	> 1000	> 1000	> 1000	> 1000	> 1000	> 1000	> 1000	> 1000	> 1000	> 1000	> 1000	

[a] ND: Not determined.

[b] Fluorogenic substrate used: Leu-Gly-Lys(Ac)-AMC for HDAC1-3, 6 and 11. Ac-Leu-Gly-Lys(TFA)-AMC for HDAC4-5 and 7-9, Ac-Arg-His-Lys(Ac)-Lys(Ac)-AMC for HDAC10. AMC = aminomethylcoumarin, TFA = trifluoroacetyl.

[c] Fluorogenic substrate used: Ac-Lys(TFA)-AMC for HDAC4, 5, 7, and 9. Arg-His-Lys-Lys(Ac), for the other HDACs. HDAC inhibition fluorescence assay was conducted as described by Hanessian *et al*[97]. and Galletti *et al.*[96]

[d] Fluorogenic substrate used: Boc-Lys(Ac)-AMC for HDAC1-3 and 6 . Boc-Lys(TFA)-AMC for HDAC4-5 and 7-9. AMC = aminomethylcoumarin, TFA = trifluoroacetyl. No specification of the substrates used to determine HDAC10 and 11 inhibition could be found. HDAC inhibition fluorescence assay was conducted as described by Li *et al*.[98]

[e] Trichostatin A (TSA) was used as a reference compound. It is a low nanomolar inhibitor of class I and II HDACs.[99]

[f] Fluorogenic substrate used: Arg-His-Lys-Lys(Ac)

3.1. Boronic acids

The introduction of a boronic acid functionality in bioactive molecules has been demonstrated to improve selectivity, physicochemical and pharmacokinetic properties, and activity.[100-104] It is a strong Lewis acid, despite the presence of two hydroxy groups, owing to the empty p-orbital of the sp^2-hybridized boron atom (**Figure 5**). This enables boronic acid compounds to form reversible covalent bonds with amino acids, a trait exploited by the blockbuster drug Bortezomib for the treatment of the hematological cancer multiple myeloma.[105, 106] In addition, boronic acid is also able to bind diol units as present in saccharides and is considered to be a bioisostere for carboxylic acids in drug design.[107, 108] Hence, this functional group has drawn considerable attention from medicinal chemists.[109] The use of boronic acid as a chelator of active site metals to induce inhibition of the enzyme of interest seems to be studied to a lesser extent, but was done for metallo-β-lactamases, coordinating zinc and acting as tetrahedral intermediate, which proved to be successful.[110]

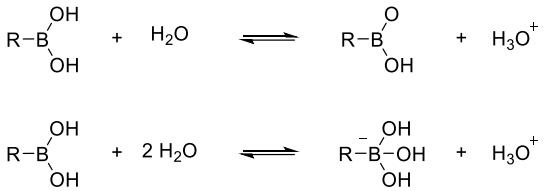

Figure 5 Ionization equilibrium of boronic acids in water, when acting as a Bronsted acid (top) or as a Lewis acid (bottom).[111]

The acidity of boronic acid is influenced by the substituent attached to the boron atom, with a pKa ranging from 4-10 in water. The most electrophilic boron atom is present in the most acidic boronic acids and can best form and stabilize a hydroxyboronate anion.[112] Therefore, with the appropriate substituent, boronic acids can be converted from a neutral and trigonal planar sp^2 hybridization to an anionic tetrahedral sp^3-hybridized boron atom under physiological conditions (**Figure 5**).[111, 113-115] Considering that breaking an amide bond, as done by HDACs, requires the conversion of an sp^2 carbon atom to a tetrahedral sp^3 carbon atom, boronic acids may represent a suitable transition state analog for the inhibition of HDACs.[116-118]

The boronic acid analog of SAHA **2** should be capable of coordinating zinc when hydrated, for which both bidentate (**Figure 6**) and monodentate binding modes have been proposed (**Figure 7**).[85, 119] For the monodentate model, it was suggested that two hydrogen bonds are formed with tyrosine and histidine residues in HDAC1, contributing to the inhibitory strength (**Figure 7**).[119]

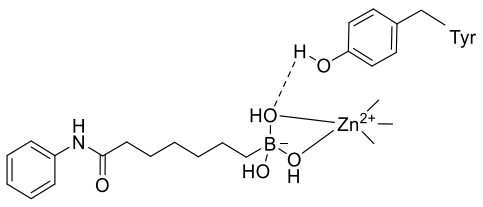

Figure 6 Model for the bidentate binding of hydrated boronic acid with a zinc ion as present in the catalytic site of histone deacetylases. Dashed lines: hydrogen bonds, solid lines Zn^{2+}: metal-coordination interactions [85]

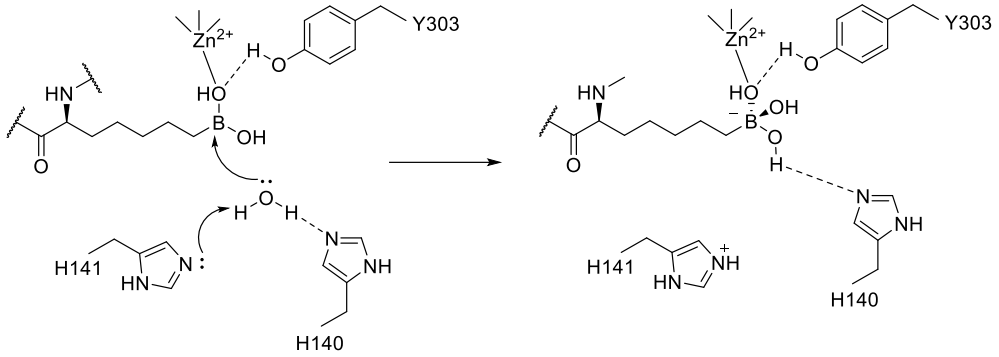

Figure 7 Proposed mechanism of inhibition of HDACs by boronic acids (HDAC1 numbering), showing monodentate binding of the hydrated boronic acid to the zinc ion. Dashed lines: hydrogen bonds, solid lines Zn^{2+}: metal-coordination interactions [119]

Despite the analogies and coordination potential, replacing the hydroxamic acid moiety in SAHA with a boronic acid appeared to be detrimental to its activity (Table 1, compound **2**, IC_{50} HeLa nuclear extract > 100 µM). Enhancing the binding capacity by changing the cap group and linker unit, however, did lead to functional inhibitors with low micromolar activity against HDACs from HeLa nuclear extract and/or human recombinant HDAC1, 2, 8, 6.[119]

Herbst-Gervasoni *et al*. determined the crystal structure of N^8-acetylspermidine boronic acid analog **3** in complex with zebrafish HDAC10 (*Danio rerio*, *dr*HDAC10) and compared it with its hydroxamic acid counterpart **4** (**Figure 8**). The boronic acid moiety was present in this complex as a tetrahedral boronate anion, formed after hydration of the boronic acid, presumably by the Zn^{2+}-bound water molecule, thereby mimicking the first step in the hydrolysis of substrate N^8-acetylspermidine. The boronic acid analog displayed little activity (IC_{50} *dr*HDAC10 = 400 µM), in contrast to the hydroxamic acid (IC_{50} = 120 nM).[69]

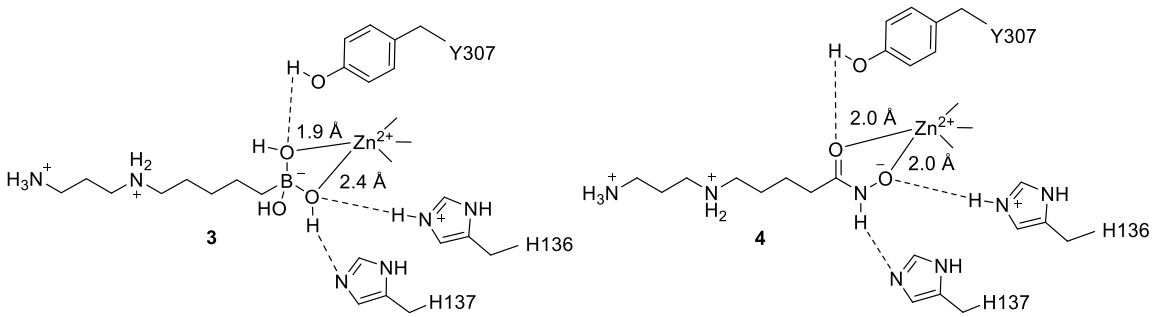

*Figure 8 Binding modes of N^8-acetylspermidine boronic acid analog **3** and hydroxamic acid analog **4**, determined from the crystal structure of the respective drHDAC10/inhibitor complexes. Dashed lines: hydrogen bonds, solid lines Zn^{2+}: metal-coordination interactions.*[69]

The loss of activity upon replacing the hydroxamic acid with a boronic acid was also observed in potent bicyclic tetrapeptides[120] and a phenyl-based HDAC6i screening.[121] Taken together, boronic acid might not represent a potent hydroxamic acid alternative for zinc complexation in HDAC inhibitors, but micromolar inhibition can be achieved after optimization of the cap group and linker unit, inferring improved interaction with the protein surface and the channel to the catalytic site.

3.2. Electrophilic ketones

Electrophilic ketones are known to act as inhibitors of several hydrolytic enzymes, including aspartyl and serine proteases, and zinc-dependent enzymes such as metallo-β-lactamase and carboxypeptidase A. They mimic the substrate transition state as hydrates (geminal diols) and can coordinate the active

site zinc ion (**Figure 9**). This instigated interest in the development of non-hydroxamic acid HDACi bearing an electrophilic ketone.[77, 122-124]

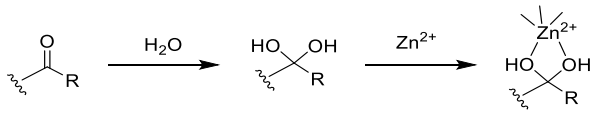

Figure 9 Hydration of electrophilic ketones, followed by coordination with the Zn^{2+} ion.[77]

3.2.1. Trifluoromethyl ketones

The use of trifluoromethyl ketones (TFMKs) as a zinc-binding moiety in HDAC inhibitors was pioneered by Frey *et al.*, inspired by the success of TFMKs as inhibitors of phospholipases, aspartyl, cysteine, and serine proteases, and zinc-dependent enzymes such as metallo-β-lactamases and carboxypeptidase A.[122, 125-132]

α-Fluorinated ketones are more electrophilic compared to other ketones, as a result of the strong electron-withdrawing effect of the fluorine atoms. Consequently, trifluoromethyl ketones (TFMK) are hydrated in aqueous solutions at physiological pH. The resulting tetrahedral geminal diol is a transition state analog of the HDAC catalysis mechanism. Work by the Christianson group showed, using the TFMK analog of N^8-acetylspermidine, that the TFMK hydrate **5** can bind in a bidentate manner and non-symmetrically with the zinc ion in the active site of zebrafish HDAC6 (*Danio rerio*), at a distance of 2.0 Å between Zn^{2+} and O1, and 2.5 Å between Zn^{2+} and O2 (**Figure 10**). The stronger interaction of Zn^{2+} and O1 can indicate that ionization to an oxyanion has occurred, which would be inductively stabilized by the adjacent trifluoromethyl moiety. Moreover, these oxygens atoms engage in hydrogen bonds with amino acid residues of the catalytic site, more specifically O1 with Y745 and O2 with tandem histidine residues H573 and H574, that fulfill general acid-base functions in catalysis (HDAC6 numbering). This binding is similar to the interactions for the binding of the acetate product after *N*-acetyl lysine hydrolysis.[44] A very similar binding mode has also been observed for TFMK analogs of N^8-acetylspermidine in HDAC10, determined by X-ray analysis of the crystal complex.[69]

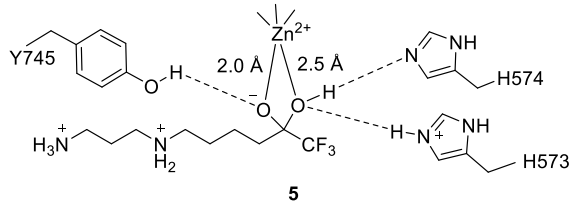

5

Figure 10 Interaction of the hydrated trifluoromethyl ketone with the zinc ion and amino acid residues present in the catalytic site of Danio rerio HDAC6. Dashed lines: hydrogen bonds, solid lines: metal-coordination interactions.[12]

The trifluoromethyl ketone derivative of SAHA **6** exhibits an overall good to strong inhibition of all HDAC isoforms (**Table 1** and **Table 2**), outcompeting the HA in inhibiting HDAC4, HDAC5, HDAC7 (IC_{50}= 0.04 - 0.9 µM) and HDAC9 (IC_{50}= 5.9 µM) and low micromolar inhibition of HDACs 1-3, 6, 8 and 10.[73, 84] Selectivity of TFMKs for class IIa over class I HDACs could be expected, since sequence alignments and modeling suggested that the TFMK binding pocket would be larger in HDACs 1-3 with less favorable contacts compared to class IIa enzymes.[43] The TFMK analog of N^8-acetylspermidine did not exhibit this selectivity profile and was more potent in inhibiting HDAC10 than its HA counterpart (IC_{50} zebrafish HDAC10 = 80 nM and 120 nM, respectively).[69] This can be explained by the substrate used in the biochemical assays. For analysis of the N^8-acetylspermidine analogs, an acetylpolyamine hydrolysis assay was employed,[69] while the potencies of the SAHA analogs were determined with a peptide-based assay.[84] The former appears to be a more reliable method,[133] considering HDAC10 is characterized as a polyamine deacetylase.[12] Bisthiazole-based trifluoromethyl ketone HDACi demonstrated similar potencies against HDACs 1, 3, 4 and 6.[134] Isoform-selectivity and activity can thus be enhanced and

even altered via the cap group and/or linker unit, which was also observed in a series of 5-aryl-2-(trifluoroacetyl)thiophene analogs that inhibited HDAC4 and HDAC6 in nanomolar concentrations, while maintaining a hundred-fold selectivity toward HDAC1.[135] Also, the introduction of a thiophene linker furnished class II selective HDACi with low micromolar to nanomolar activity.[136, 137]

The importance of the trifluoromethyl moiety compared to less or more fluorine substitutions has been investigated by employing thiophene-based HDACi **7** evaluated against HDACs 1, 3, 4, and 6 (**Table 3**). Di- and trifluoromethyl and pentafluoroethyl analogs were prepared and incorporated in the same inhibitor. Double fluorine substitution significantly decreased activity against HDACs 3 and 4 but enhanced HDAC6 inhibition over ten-fold. Surprisingly, this compound was not further pursued as a potential HDAC6-selective inhibitor. The introduction of the pentafluoroethyl group eliminated the inhibition of HDAC4 and HDAC6. The drop in inhibition of HDAC4 can be explained by the size of the cavity surrounding the zinc ion (X-ray crystal of HDAC4). The trifluoromethyl group fits in there tightly, approaching a proline residue within Van der Waals distance at the bottom of the cavity. The pentafluoroethyl group is more sterically hindered, hence the loss in activity.[136] The activity of the pentafluoroethyl ketone analog of SAHA was assessed against HDAC1 and HDAC2 (prepared from K562 erythroleukemia cell extract), but this molecule proved to be inactive.[125]

Table 3 Inhibitory activity of thiophene-based fluorinated HDAC inhibitors.

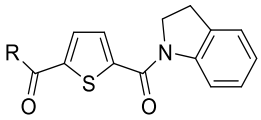

7

	HDAC IC_{50} (µM)			
R	**1**	**3**	**4**	**6**
CF_3	2	1.7	0.13	0.2
CHF_2	9.7	42% inhibition at 10 µM	7.6	0.015
CF_2CF_3	4.2	2.9	NA[a]	NA[a]

[a]NA: No activity at 10 µM

The incorporation of TFMK as ZBG has also been performed for HDAC6 inhibitors with an aryl linker. Unfortunately, only low inhibition (< 30% at 10 µM) of the enzyme could be observed and the inhibitors were ineffective *in cellulo* and *in vivo*, possibly due to the reduction of the ketone moiety to the inactive alcohol by carbonyl reductases present in the cells.[138] Indeed, it has previously been observed that the trifluoromethyl alcohol is inactive in cellular assays.[125, 134, 136]

Taken together, TFMKs show potent activity against HDACs when combined with an alkyl- or thiophene-based linker. Unfortunately, the SAHA-based TFMK with an optimized cap group and other TFMK-containing inhibitors displayed metabolic liabilities and a poor pharmacokinetic profile. The half-life is only 30 minutes, the intravenous exposure in mice at a dose of 10 mg/kg is poor and the ketone is transformed to the inactive alcohol upon incubation with cells or whole blood and *in vivo*. Linker modifications, such as the introduction of heteroatoms in the beta position to the ketone function or insertion of unsaturation or a cyclopropane ring next to the ketone carbonyl, were to no avail.[125] The introduction of an amido group adjacent to the TFMK, resulting in trifluoromethyl pyruvate, might

represent a strategy to obtain metabolically more stable alternatives for TFMKs. The additional electron withdrawing group is expected to stabilize the hydrate form, preventing the reduction of the ketone moiety to the inactive alcohol. Investigation of the metabolic stability of a TFMK-based HDACi and its trifluoromethyl pyruvate counterpart was performed using the S9 fraction of human liver extract, which contains both cytosolic and microsomal enzymes. The TFMK was completely reduced within 15 minutes, whereas the trifluoromethyl pyruvate remained unaffected in the 2 hour timeframe of the assay.[139]

3.2.2. α-Keto amides

The α-keto amide system has been reported as a functional group in inhibitors of lipases and serine and cysteine proteases. This motif is present in many natural products and represents a privileged structure in drug discovery.[140] It is readily hydrated like TFMKs [74] and resembles both a scissile amide and ester bond, making it a potentially suitable warhead in the design of novel HDACi. α-Keto amides have been shown to possess superior pharmacokinetic properties compared to other dicarbonyl derivatives, such as α-keto acids (improved membrane permeance) and α-keto esters (enhanced stability toward plasma esterases), and are reported to be more resistant against proteolytic cleavage.[140] Wada *et al.* investigated different α-keto amides **8** (**Table 4**), of which methyl amide was the most potent. Alkylation of the amide nitrogen appeared to be essential for activity.[74]

Table 4 Screening of different α-keto amides against HDAC1/2.

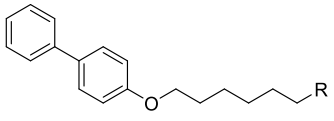

8

R	HDAC1/2 IC50 (μM)[a]
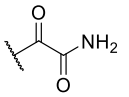	> 50
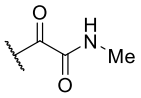	0.11
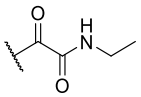	4.9
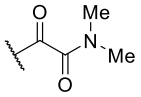	> 5
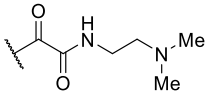	> 50
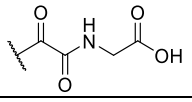	> 50

[a] Mixture of HDAC1 and HDAC2 from nuclear extraction of K562 erythroleukemia cells.

N-methyl-α-keto amide has been introduced into the SAHA structure, producing a fairly potent inhibitor **9**, exhibiting an IC_{50} of 0.34 μM (Table 1). Additional improvements of the cap group lowered the IC_{50} values to the nanomolar range (IC_{50} < 10 nM). This optimized inhibitor, however, showed a short half-life *in vivo*, in cell culture, and in whole blood, as a result of its rapid reduction to the inactive α-hydroxy amide. [74, 75]

Overall, electrophilic ketones show good to excellent inhibition in biochemical assays but are readily reduced to the corresponding inactive alcohols in biological environments, eliminating inhibitory activity.

3.3. Silane diols

Silane diol has been extensively studied as a functional part of (peptidomimetic) metalloprotease inhibitors and as an isostere of the tetrahedral geminal diol, formed upon peptide bond hydrolysis.[84, 141-143] The inhibition occurs via the chelation of the metallic center, whereas in the case of HIV protease, hydrogen bonding with aspartic residues in the active site of the enzyme ensures inhibition.[144] The silicon atom of a silane diol is most stable in a tetrahedral configuration, and the hydroxy groups can serve as potent hydrogen bond donors and acceptors.[141, 143] Also, theoretical studies point out that silane diols are capable of coordinating zinc with a similar affinity as that of hydroxamic acids.[68, 84] Simple silane diols are prone to polymerization, but sterically hindered diols can be stable.[145]

Replacement of a carbon atom by a silicon atom can create benefits in terms of druglike properties. The silicon switch, as this bioisosteric replacement is called, retains the required properties because of the similarities between carbon and silicon, but at the same time, offers advantageous differences. Increased lipophilicity can lead to improved cell penetration and consequently enhanced potency. Geminal diols on carbon are not stable, whereas silane diol is not dehydrated to silanone since silicon favors sp^3 hybridization over sp^2, making it a suitable transition state mimic.[145] Moreover, the ability of silicon to extend its coordination number from four to six due to the presence of empty 3d orbitals, is useful in the formation of coordination complexes.[145] A quantum chemical study has been performed with silane diol, using a tridentate complex of Zn^{2+} with an exchangeable water molecule in which amino acid residues are mimicked by ammonia and imidazole ligands. This showed that the silane diol group forms a hexacoordinated intermediate complex with a bidentate bonding to the oxygen atoms of the silane diol group, displacing the Zn^{2+}-bound water molecule (**Figure 11**, A). One exception was observed, when modeling the back-side attack, i.e. when the silane diol approaches from the side opposite to the water molecule, establishing a monodentate binding in a trigonal bipyramidal structure with a penta-coordinated zinc atom (**Figure 11**, B).[68]

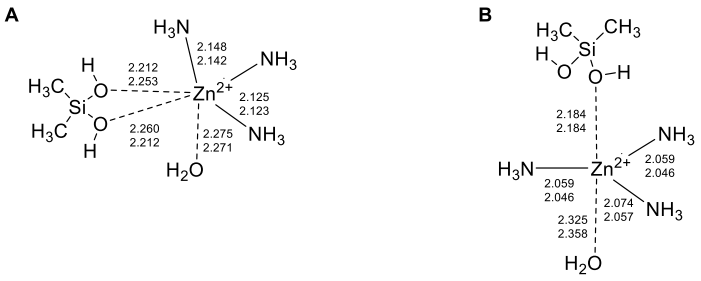

Figure 11 Modelled binding mode of dimethyl silane diol with Zn^{2+}, showing bidentate (A) and monodentate (B) binding, with ammonia ligands.[68]

The silane diol derivative of SAHA **10** displayed activities in the lower micromolar range against HDACs 1, 2, 3, and 10, no inhibition of HDACs 4, 5, and 7, and an intermediate activity against the other HDACs (**Table 2**). Comparison of silane diol derivatives of SAHA with their trifluoromethyl ketone counterparts shows that the latter exhibited superior HDAC inhibition, but silane diols do not suffer from reduction to an inactive form as the TFMKs do.[84] Despite the loss of activity compared to the HA counterparts, silane diols represent a potential substitute for the contested hydroxamic acid as a zinc-binding group in HDACi, exhibiting low micromolar IC_{50}'s. Pharmacyclics, part of Abbvie, patented several silane diol derivatives, including the SAHA analog, for use as a therapeutic against cancer and bipolar disorders.[146] However, *in vivo* data or clinical trials assessing these compounds are currently unavailable.

3.4. Hydroxyketones

The interest in hydroxyketones as HDAC inhibitors originated from the discovery of the cyclic tetrapeptide FR235222 **11**, isolated from the broth of the fungi *Acremonium* (**Figure 12**). This natural product inhibited *Toxoplasma gondii* proliferation at low nanomolar level (IC_{50}= 28.6 nM) and abolished the infectious capacity of Toxoplasma cysts, by targeting HDAC3. It showed class I versus class IIb selectivity, and the hydroxyketone showed increased potency compared to its ethyl ketone analog (IC_{50}= 172 nM).[147, 148]

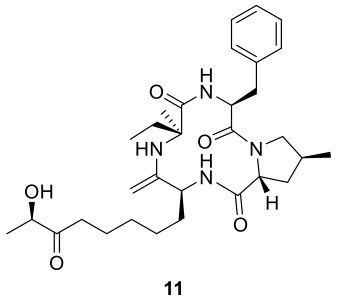

11

Figure 12 Structure of FR235222, the natural product that inspired introduction of hydroxyketones as zinc-binding group in HDACi.[147, 148]

Replacing the HA in SAHA with an α-hydroxyketone, resulted in compound **12**, decreased the potency to the low micromolar range (**Table 1**). High selectivity over HDAC6 was attained, which was not observed for SAHA, indicating the ZBG induced a selectivity for class I versus class IIb HDACs (IC_{50} > 33 µM). Docking and molecular dynamics studies were performed to explain this selectivity. The strong affinity of the hydroxamic acid for Zn^{2+} enabled strong inhibition of all HDAC isoforms by SAHA and coordinated the zinc ion of both HDAC1 (**Figure 13**, A) and HDAC6 (**Figure 14**, B) in a bidentate manner. The hydroxyketone was a weaker ZBG and coordinated Zn^{2+} in a bidentate manner in HDAC1 (**Figure 13**, B), resulting in potent inhibition, while monodentate coordination was observed in HDAC6 (**Figure 14**, B), possibly explaining the class I selectivity.[37] However, the crystal structures of trapoxin A and HC toxin, two cyclic tetrapeptides structurally related to FR235222, in complex with HDAC8 and HDAC6, respectively, revealed that even unactivated ketones can be hydrated in the active site. This was also observed in X-ray analysis of other alkyl and aryl ketone-containing inhibitors bound to HDAC2.[149] As was concluded from the discussion of the catalytic mechanism (see section 2.1), the active site of HDACs has evolved to enable hydration of practically any carbonyl group, resulting in a stabilized tetrahedral configuration mimicking the transition state.[44, 150] The selectivity and activity of the α-hydroxyketone SAHA analog could thus be a result of differences in the active site-*gem*-diol(ate) interaction patterns between HDACs or as a consequence of the positioning of active site residues enabling the hydration of the carbonyl.

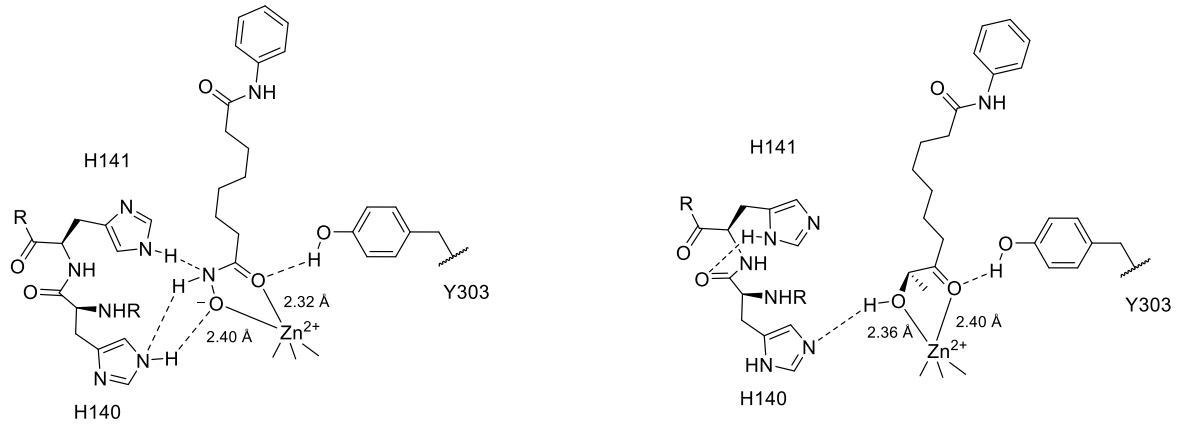

*Figure 13 Binding of SAHA (left) and compound **12** (right) in the catalytic domain in HDAC1, determined by molecular dynamics simulations. The average distances between the hydroxy oxygen atom and Zn^{2+} and the carbonyl oxygen atom and Zn^{2+} are, respectively, 2.40 and 2.32 Å for SAHA and 2.36 and 2.40 Å for compound **12**. Dashed lines: hydrogen bonds, solid lines: metal-coordination interactions.[37]*

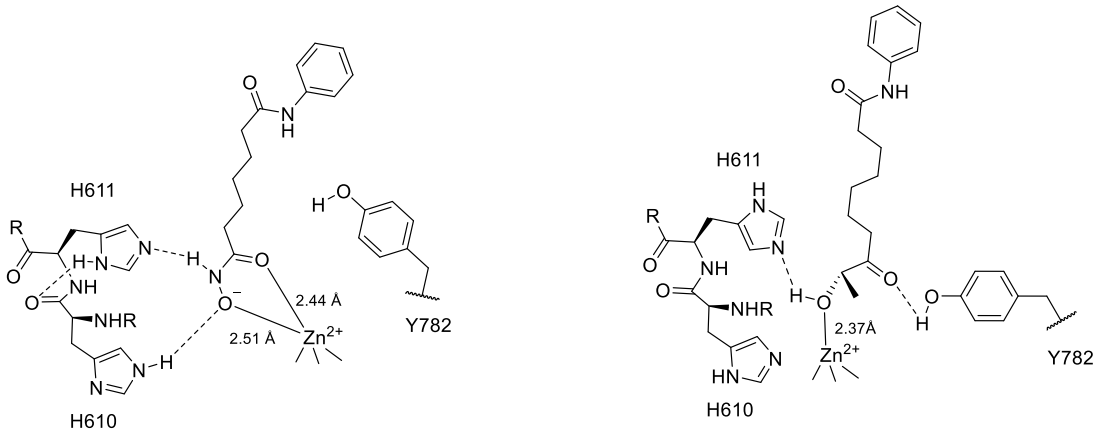

*Figure 14 Binding of SAHA (left) and compound **12** (right) in the catalytic domain in HDAC6, determined by molecular dynamics simulations. The average distances between the hydroxy oxygen atom and Zn^{2+} and the carbonyl oxygen atom and Zn^{2+} are, respectively, 2.51 and 2.44 Å for SAHA, and 2.37 and 3.91 Å for compound **12**. Dashed lines: hydrogen bonds, solid lines: metal-coordination interactions.[37]*

Conversion to the (*S*)-enantiomer **13** resulted in weaker HDAC inhibition (IC_{50} = 77.1 µM), and acetylation of the alcohol **14** induced a similar decrease. Removing the hydroxy group abolished HDAC inhibition (compound **15**, IC_{50} > 100 µM),[37] as did the removal of the methyl group from the chiral center (compound **16**, IC_{50} > 40 µM, **Table 1**).

Assessment of the antiproliferative activity (GI_{50}) of the α-hydroxyketone SAHA analog **12** showed micromolar activity against *Plasmodium falciparum*, Jurkat, K562, and HEK293 human cell lines, thus lacking selectivity in terms of cytotoxicity between P. falciparum and the human cell lines. No activity was observed against HeLa cells, in contrast to the significant HDAC inhibitory activity observed in HeLa nuclear extracts, indicating that the observed antiproliferative effects could be HDAC-independent.[37]

3.5. Oximes

Oximes, or hydroxy-imine derivatives, are widely known as a powerful antidote for organophosphate poisoning since they can reverse cholinesterase inhibition. They also demonstrate antibacterial, anti-fungal, anti-inflammatory, antioxidant, and anti-cancer activities.[151] Oxime complexes with various

metals (Pt(II), Cu(II), Mn(II)) are stable and gave rise to compounds with antitumor activity.[94, 152, 153] This instigated the evaluation of this motif as a ZBG in HDAC inhibitors.

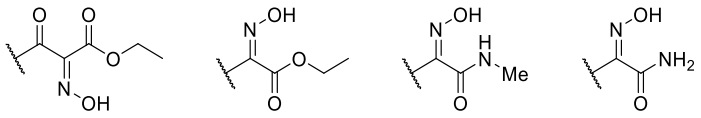

Figure 15 Oxime derivatives that were combined with the cap group and linker unit of SAHA and evaluated for their HDAC inhibitory activity.

α-Oxime esters and α-oxime amides have been introduced into the SAHA structure as they were expected to mimic the natural substrate's chelating characteristics (**Figure 15** and **Table 2**). The α-keto oxime ester **17** and the α-oxime ester **18** were inactive. Methylated oxime amide **19** showed micromolar activity against HDACs 1-5 and HDACs 7-9 (IC_{50}= 22-100 µM), while no inhibition of HDACs 6, 10, and 11 was observed. The substituent on the amide nitrogen appeared to be vital for the inhibition of the HDAC catalytic site since removal of the methyl substituent (compound **20**) decreased the activity. This trend was also observed for the α-keto amide series of SAHA analogs (see 3.2.2).[74] Considering the natural HDAC substrate also contains an acetamide, a methyl-substituted amide likely engages in similar interactions with the catalytic site, increasing the inhibitory activity.[94] Docking and DFT studies showed that the best accommodation in the catalytic site is obtained when the amide oxygen and oxime nitrogen interact with the zinc ion through a five-membered ring coordination geometry (**Figure 16)**. The positioning of the ZBG affects the placement of the cap group on the enzyme surface, thereby significantly influencing the inhibition potential and selectivity profile of compound **19**. HDAC3, for example, contains an additional aromatic residue in the binding region on the protein surface, that engaged in π-π interactions with the phenyl ring of the cap group, which is not possible in the other HDAC isozymes.[94] No cellular assays were performed with this SAHA analog.

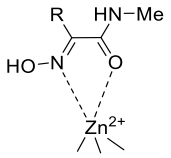

*Figure 16 Complex of compound **19** and Zn^{2+} optimized at DFT level (B3LYP).[94]*

3.6. Sulfur-based zinc-binding groups

The FDA-approved HDACi romidepsin **21** (FR901228, FK228) has been isolated from a broth culture of *Chromobacterium violaceum* and showed low nanomolar inhibition of class I HDACs and antitumor activity. It is a macrocyclic depsipeptide with a thiol as a zinc-binding moiety, which is naturally present as an intramolecular disulfide (**Figure 17**).[154-156] Reduction after uptake into cells releases the thiolate, resulting in an active inhibitor.[157] Largazole **22**, a marine natural depsipeptide structurally related to romidepsin, is also an HDACi. The free mercapto group is liberated by thioester hydrolysis, cleaving off the lipophilic side chain (**Figure 17**). Crystal structures of hydrolyzed Largazole showed that the thiol side chain extends into the active site tunnel and coordinates the Zn^{2+} ion in a monodentate manner, with a nearly perfect tetrahedral geometry.[157, 158] Zinc ions are inherently thiophilic,[159] and thiol-containing compounds have been reported as inhibitors of other zinc-dependent enzymes as well, such as angiotensin-converting enzyme and matrix metalloproteases.[160, 161] Consequently, thiols and sulfur-containing functional groups have been extensively studied as substitutes for the hydroxamic acid ZBG.

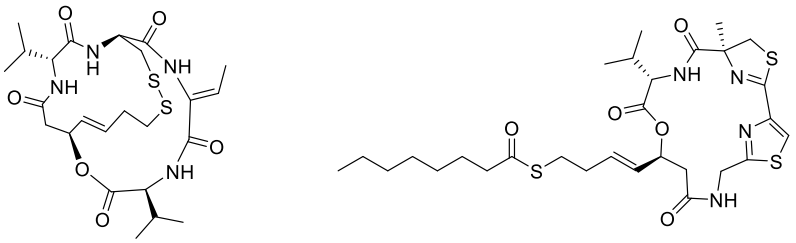

Romidepsin
21

Largazole
22

*Figure 17 Natural HDAC inhibitors with a thiol zinc-binding group, masked as an intamolecular disulfide in romidepsin **21**, and as a thioester in Largazole **22**.*

3.6.1. Thiols

Inspired by the success of romidepsin **21**, a simple thiol has been introduced into the SAHA structure as a ZBG. While it was assumed that monodentate ZBGs are inferior to bidentate ZBGs, the thiol analog **23** of SAHA exhibited much higher activity against HDAC1/2 (IC_{50} HeLa nuclear extract = 0.058-0.21 µM, **Table 1**) compared to other, bidentate, non-hydroxamic acid ZBGs such as *o*-aminoanilides **66** (IC_{50} = 120 µM) and trifluoromethyl ketones **6** (IC_{50} = 6.7 µM)[73] and a similar activity as SAHA (IC_{50} = 0.055-0.21 µM).[78] Thiol **23** was as potent as SAHA against recombinant human HDACs 1 and 6 (**Table 1**)[80] and engaged in competitive inhibition versus the acetylated lysine substrate, with an inhibition constant (K_i) of 0.11 µM.[79]

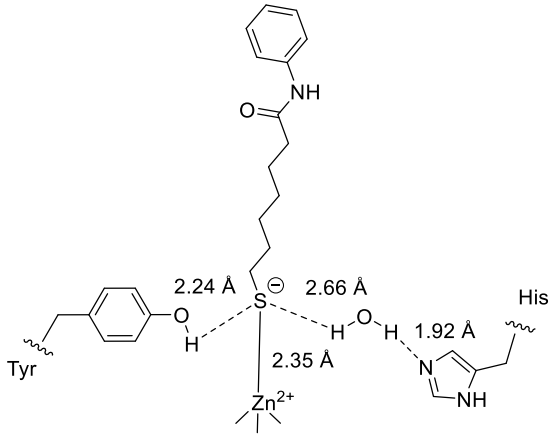

*Figure 18 Proposed model for the binding of thiol derivative **23** of SAHA in the catalytic site of HDAC8, obtained as a low energy conformation in docking studies. Dashed lines: hydrogen bonds, solid lines: metal-coordination interactions.[77]*

Docking studies suggested that the thiolate anion generated under physiological conditions interacts strongly with the zinc ion located in the active site, forming a tetrahedral complex (**Figure 18**). This was also observed in the crystal structure of a thiol analog of N^8-acetylspermidine in complex with HDAC10.[69]

The rate of thiol ionization correlates with the inhibitory potency. This was demonstrated by transforming the thiol functionality to thioacetate **24**, which increased the IC_{50} to the low micromolar range, and methylsulfide **25**, which was detrimental to the inhibition of the enzymatic activity (**Table 1**).[79] The potential of masking the thiol as a thiirane has been investigated to overcome unwanted metal binding and oxidative and metabolic transformations of inhibitors of gelatinases, which are Zn^{2+}-containing matrix metalloproteases.[76, 162, 163] The superior activity of the thiirane moiety relative to an oxirane prompted Gu *et al.*[76] to conduct a similar comparative study by incorporating these moieties in SAHA (**Table 1**, compounds **26** and **27**). Both appeared to lack HDAC inhibitory activity (IC_{50} > 40 µM),

probably because the active thiolate could not be released from the thiirane. In the gelatinase inhibitors, the thiirane ZBG was attached to a methyl sulfonyl moiety (compound **28**, **Figure 19**). The sulfone installs hydrogen bonds in the gelatinase catalytic site and activates the adjacent methylene hydrogens for deprotonation. As a result, the thiol is liberated, enabling potent monodentate coordination to the active site zinc ion, which is missing in the SAHA analog.[162]

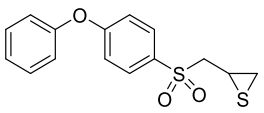

28

Figure 19 Structure of the gelatinase inhibitor that served as an inspiration for the synthesis of HDACi with a thiirane ZBG. The methyl sulfonyl part appeared to be essential for the liberation of the thiolate from the thiirane.[162, 163]

Assessment of the cancer cell growth inhibition induced by thiol **23** in human lung cancer NCI-H460 cells showed only weak potency (EC_{50} > 50 µM), despite the good results in an enzymatic assay. Possibly, the polar character limited membrane penetration. A prodrug approach could overcome these limitations and therefore the corresponding disulfide and *S*-acetyl **24** were prepared. In contrast to what is observed for the disulfide romidepsin **21**, which is reduced in the cellular environment and releasing the free thiol as the active species, the disulfide prodrug of **23** failed to inhibit growth in NCI-H460 cells (EC_{50} > 50 µM). Acetylated analog **24** did show moderate growth inhibition (EC_{50} = 36 µM), suggesting prodrug **24** penetrated the cell membrane more efficiently than thiol **23**.[79] In a similar SAR study a thiol, methyl sulfide, and thioester were introduced into the same cap-modified SAHA analog and evaluated via an MTT assay for their cell growth inhibition potential against HCT-116, HT-29, MCF-7, MDA-MB-231, A549, PC-3, AsPC-1 and HEK-293 cells. Herein, it was also observed that activity was lost upon methylation of the sulfur atom, but the free thiol, the corresponding dimer, and the thioester all showed micromolar growth inhibition of most cell lines, with the dimer as the most potent compound (GI_{50}= 5-27 µM) inhibiting cell growth in all studied cell lines. HDAC inhibition by the thiol and the dimer was also validated in HCT-116 cells, in which the dimer was more potent in inducing an increase in histone H3 and α-tubulin acetylation.[80]

Another prodrug strategy consisted of the addition of a triazolyl group to the sulfur atom (6-[(1*H*-1,2,4-triazol-3-yl)thio]-*N*-phenylhexanamide **29**), which demonstrated low micromolar inhibition of HDACs (**Table 1**, HeLa nuclear extract, IC_{50}= 8.1 µM) and antiproliferative activity against 293T, MCF-7, HeLa and K562 cell lines (IC_{50} = 11.08 - 31.95 µM, assessed by MTT assay). This activity was lost upon extension of the linker to six or seven carbon atoms.[81]

3.6.2. Mercaptoalkylamides, -amines and -ketones

The natural product lead romidepsin **21**,[154-156] the crystal structure of HDAC enzymes,[46, 48] the deacetylation mechanism[46, 48] and the key elements of inhibitor-enzyme interaction served as an inspiration to include a mercaptoacetamide (MAA) as a ZBG in SAHA (compound **30**). This approach was investigated by three research groups at the same time.[79, 82, 164] Docking studies and molecular dynamics simulation using the HDAC homology model predicted that the HDAC binding site could accommodate the mercaptoacetamide and that the binding mode could be similar to that found for SAHA, chelating the zinc ion via the sulfur and oxygen atom of the carbonyl function.[164] Docking of **30** in the crystal structure of HDAC8 showed that the sulfur and oxygen atom of the MAA group are situated at a distance of 2.44 Å and 2.04 Å from the zinc ion, respectively. The water molecule required for the deacetylation of the acetylated lysine substrate is positioned at a distance of 4.95 Å from the zinc ion in the catalytic center. These values indicate that the zinc ion is expected to be chelated in a

bidentate manner, which is realized through the removal of the water molecule, without hydrolysis of the MAA (**Figure 20**).[77]

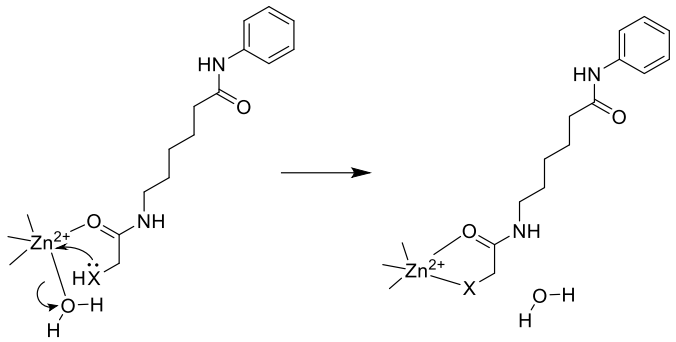

Figure 20 Model for the binding of heteroatom-containing SAHA analogs with the zinc ion present in the catalytic site of HDACs, X= S, NH, O.[77]

The MAA analog of SAHA (SAHA-MAA) **30** showed low micromolar inhibition of HDACs (HeLa nuclear extract) and HDAC8, tolerating different linker lengths (n= 4-6, **Table 1**).[76, 77, 79] In other inhibitors, a similar potency and a selectivity for HDAC6 was observed when comparing a MAA (e.g. **31**, HDAC1 IC_{50} = 5.7 µM, HDAC6 IC_{50} = 0.26 µM) and HA derivative (e.g. **32**, HDAC1 IC_{50} = 3.0 µM, HDAC6 IC_{50} = 0.18 µM). This indicated that the MAA moiety might represent a potent alternative ZBG, with some inherent HDAC6 selectivity. The small difference in activity between compounds **31** and **32** could be explained by the extra hydrogen bond between the HA and the enzyme. The NH of HA can engage in a hydrogen bond with a histidine residue in the active site of HDACs, which is not possible with the MAA ZBG (**Figure 21**).[164-167]

Figure 21 HDAC inhibitors with the same cap group and linker unit, enabling comparison of the mercaptoacetamide-based zinc-binding group and the hydroxamic acid.

In parallel with the observations made for the thiol ZBG, the transformation of the MAA to the thioacetate **33** (**Table 1**) led to a 55-fold less potent inhibitor in enzymatic assays.[76, 79] Thioesters are however beneficial as prodrugs to improve cell penetration, releasing the active thiols once inside the cells, and facilitating use in *in vivo* studies.[156, 168-170] Disulfide MAA prodrugs have also been explored, again reasoning that the highly reducing cell cytosol would favor conversion to the free MAA. As for the thiol ZBG, this strategy was successful in some cases[169] but failed in others.[121] Hassig *et al.* discussed that the thioester prodrugs of thiols hydrolyze more rapidly under basic conditions than under neutral and acidic conditions and undergo facile enzymatic hydrolysis by esterases. Nonhydrolyzable analogs of the series were found to be inactive in biochemical and cell-based assays, indicating that the free thiol is the active species; however, data was not shown.[171] This is also reflected in the work by Kalin *et al.*, in which lower concentrations of the thioester prodrug were required to induce neuroprotection compared to the free thiol compound, while devoid of HDAC activity in enzyme-based assays.[167]

Oxidative dimerization of MAA HDACi could present a problem in enzyme-based activity profiling, despite the probable reduction to the monomers within cells.[167] Therefore, Kalin *et al.* introduced α-methyl groups relative to the thiol in MAA-based SAHA analogs, with a modified cap group. Mono-α-methyl MAA dimerized at a much lower rate than the MAA, and the addition of a second methyl group further decreased the rate of dimerization, however less significant than instalment of the first methyl

group. The introduction of an α-methyl group resulted in a highly selective HDAC6 inhibitor while maintaining good activity (IC_{50} HDAC6 = 1.1 µM). Isolation of the enantiomers showed that the (*S*)-enantiomer is inactive, whereas the (*R*)-enantiomer demonstrated the same activity as its MAA parent (IC_{50} HDAC6 = 0.28 µM) while maintaining selectivity over all isoforms. Molecular docking of the compounds in HDAC2, HDAC4, and a homology model of HDAC6-DD2 showed that only the (*R)*-isomer was able chelate zinc in a bidentate manner while enabling a hydrogen bond between the sulfur atom and a tyrosine residue. Moreover, the arrangement of the ZBG influenced the interaction exploited by the cap group and linker unit, further contributing to activity and selectivity. The addition of two methyl groups is detrimental to the activity with respect to all HDAC isoforms, likely due to steric interactions in the catalytic site. Indeed, although HDACs can accommodate some bulky groups, the second methyl group probably directs the conformation in such a way that it clashes with active site residues.[167]

The activity of SAHA-MAA **30** has also been evaluated against *Schistosoma mansoni* HDAC8 (*sm*HDAC8, 42% identical to human HDAC8), demonstrating an increased inhibition (IC_{50}= 50 µM) compared to human HDAC8 (*h*HDAC8, IC_{50}= 200 µM). The first crystal structure of an HDACi containing a MAA ZBG was obtained from *sm*HDAC8 in a complex with SAHA-MAA (**Figure 22** and **Figure 24**). Unlike the docking study performed with *h*HDAC8, crystallographic data of the complex *sm*HDAC8/SAHA-MAA demonstrated a monodentate coordination of the thiol to zinc, while the carbonyl moiety interacted with Y341 (**Figure 22**). The zinc ion coordination was tetrahedral, which likely contributed significantly to the HDAC8/SAHA-MAA affinity. Upon binding of SAHA-MAA **30** in contrast to SAHA,[172] F151 adopts an unusual flipped-in conformation and forms a hydrophobic tunnel together with F216 that accommodates a slightly kinked linker. Thus, the binding of the MAA to zinc results in different positioning of the hydrophobic linker and cap group.[168] This explains that re-optimization of cap group and linker unit after installation of a novel ZBG is likely required to further improve inhibition potential and that a specific ZBG can induce selectivity, in this case against *sm*HDAC8 or *h*HDAC8.[168]

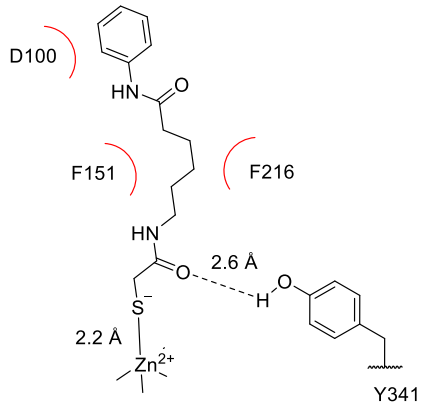

*Figure 22 Structural insight into the smHDAC8 inhibition by the mercaptoacetamide inhibitor **30**, with a schematic representation of the interactions formed by the inhibitor and the smHDAC8 active-site zinc ion and residues. Dashed lines: hydrogen bonds, solid lines: metal-coordination interactions.[168]*

Four years later, in 2018, the X-ray crystal structure of a SAHA-analog containing a MAA as ZBG and a modified cap group (compound **34**, **Figure 23**) in complex with the HDAC6 catalytic domain 2 (HDAC6-DD2) from *Danio rerio* (zebrafish) was presented (**Figure 24**). The zebrafish active site is identical to the human HDAC6-DD2 and superior for X-ray crystallographic studies.[173] Compound **34** inhibited HDAC6 240 times more potently than HDAC8. The negatively charged thiolate displaced the zinc-bound water molecule and coordinated to the zinc ion in a monodentate manner. This resulted in a slightly distorted tetrahedral geometry, similar to the coordination geometry of thiolate-bearing HDACi such

as the depsipeptide Largazole in complex with HDAC8[157, 158] and polyamine N^8-acetylspermidine analogs in complex with HDAC10.[63, 69]

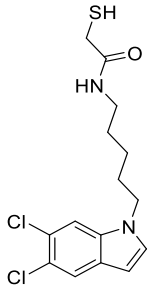

34

*Figure 23 Compound **34** assessed in X-ray studies in complex with HDAC6-DD2.*

Comparison of the crystal structure of SAHA-MAA **30** in complex with HDAC8 and MAA-based compound **34** in complex with HDAC6-DD2 showed similar interactions (**Figure 24**). The zinc-bound thiolate group accepts a hydrogen bond from a histidine residue (H573 in HDAC6, H141 in *sm*HDAC8), while the carbonyl oxygen engages with the hydroxy group of a tyrosine residue (**Figure 24**, C and D). The latter mimics the activation of the scissile carbonyl group of acetylated lysine. In both cases, the carbonyl oxygen is not able to coordinate the zinc ion, which is required to activate the scissile amido group for hydrolysis, rendering the amido group of the MAA chemically inert when bound in the HDAC6 active site. A major difference between both complexes was found in the NH group. In HDAC6, the MAA NH group forms a hydrogen bond with H574, which requires that the side chain of H574 is present in the neutral form. In *sm*HDAC8, however, the distance is too large for hydrogen bonding, possibly because the side chain of H142 is present as the imidazolium cation.[173]

The MAA **34** binds in a similar constellation of hydrogen bond interactions and metal coordination as SAHA, in which the hydroxamate NH donates a hydrogen bond to H574 (**Figure 24**, A and C), making

the MAA a functional mimic of the HA without the potential mutagenicity associated with the HA via the Lossen rearrangement.[44, 173]

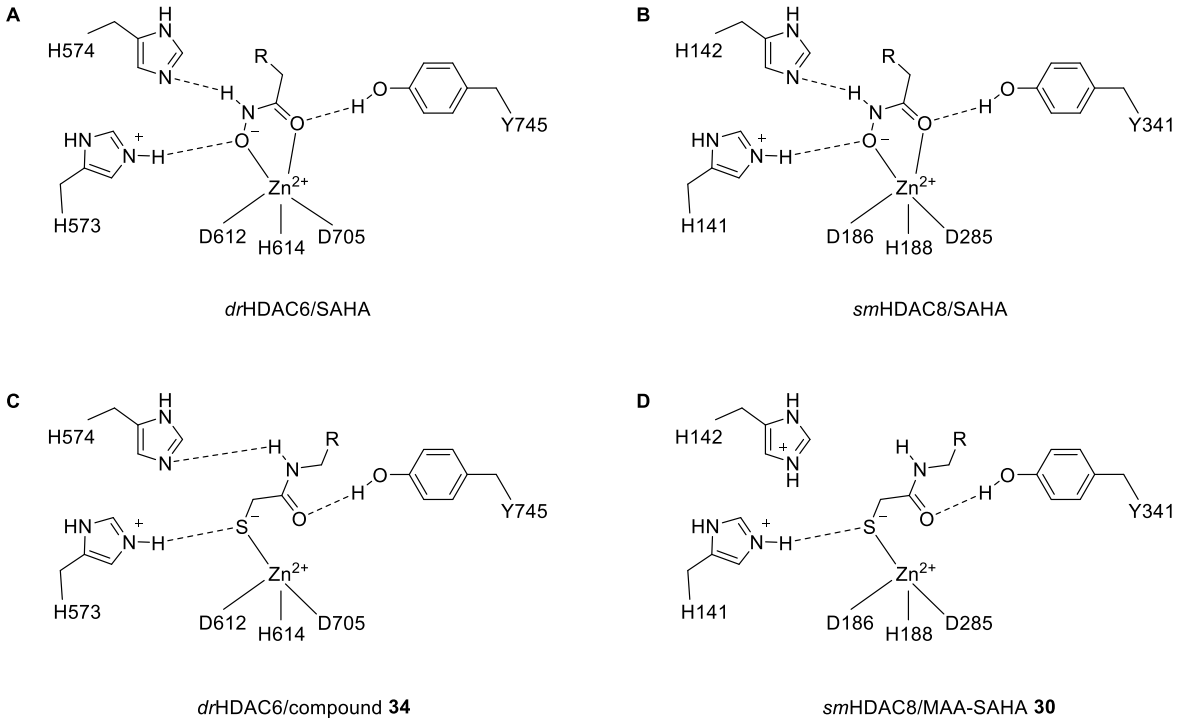

*Figure 24 Comparison of the interactions of SAHA (hydroxamic acid HDACi) and the mercaptoacetamide analog of SAHA **30** and mercaptoacetamide-based SAHA derivative **34** in the active site of drHDAC6/smHDAC8 based on crystal structures of inhibitor/HDAC complexes. (A) SAHA in complex with drHDAC6-DD2, (B) SAHA in complex with smHDAC8, (C) Compound **34** in complex with HDAC6-DD2, (D) Mercaptoacetamide analog of SAHA **30** in complex with smHDAC8. drHDAC6: Danio rerio HDAC6-DD2, smHDAC8: Schistosoma mansoni HDAC8, dashed lines: hydrogen bonds, solid lines Zn^{2+}: metal-coordination interactions.*[168, 172, 173]

Antiparasitic activity of MAA **30** has been investigated by treating cultured *schistosomula* with the corresponding thioester **33** (10, 20, 50 µM, 1-5 days treatment), resulting in a dose- and time-dependent decrease in viability.[168] A patent application for MAA **30** and related compounds was filed in 2005 but was later abandoned.[174]

MAA-based SAHA derivatives with a modified cap group provided effective neuroprotection at 10 µM in an *in vitro* model of oxidative-stress-induced neurodegeneration based on glutathione depletion, protecting cortical neurons to approximately untreated control levels. Some of the HA counterparts also showed neuroprotection, but all of the HA compounds displayed toxicity, underpinning the superiority of MAA-based HDACi.[166] Neurotoxicity probably stems from HDAC1 inhibition, since HAs generally exhibit good inhibition of this isozyme, and it was shown that HDAC1 is essential for the survival of cerebella granule neurons, underscoring the need for isoform-selective HDAC inhibitors, especially in the framework of neuroprotective strategies. The MAA-HDACi on the other hand can protect neurons from oxidative stress-induced death without any inhibitor-associated toxicity and show HDAC6 selectivity. The possibility that the protection results from radical trapping by the sulfur group was ruled out by the evaluation of simple thiol antioxidants such as *N*-acetyllysine and lipoic acid, which only induced a therapeutic effect at 100 µM - 1 mM concentrations. This indicated that the inhibitor concentrations used were well below the antioxidant level.[166] Some of the MAA-HDACi,

however, were also effective in preventing glutathione depletion independent from their HDAC6 inhibitory activity, suggesting an additional neuroprotective mechanism for these compounds.[167]

Inspired by the potential of MAA in HDACi, it was expected that other hetero atom-containing substrate analogs such as compounds **35** and **36** (**Table 1**) would inhibit HDACs in a similar way.[79] Evaluation of their HDAC-targeting potential, however, showed that replacing the thiol with an amine or alcohol abrogated activity (HeLa nuclear extract, IC_{50} > 100 µM).[77, 79] Adjustment of the mercaptoacetamide to a mercaptoethylamide furnished a low micromolar inhibitor **37** (for n= 6, HeLa nuclear extract, IC_{50}= 2.35 µM), which similar to MAA, functioned as a bidentate Zn^{2+} chelator (**Figure 25**).[82] Removal of the amide carbonyl, resulting in mercaptoethylamine **38**, disrupted activity, confirming the importance of the amide carbonyl in zinc complexation and inhibition.[78, 82] Gu *et al*. questioned the contribution of the nitrogen atom in the amido function and replaced it with a carbon atom. The 2-mercaptoethan-1-one **39** was over 15 times more potent against HDACs (HeLa nuclear extract) and HDAC8, and potency was even more enhanced upon the acetylation of the mercapto group (compound **40**, **Table 1**). Again, alkylation of the thiol (**41**) abrogated enzyme inhibition.[76]

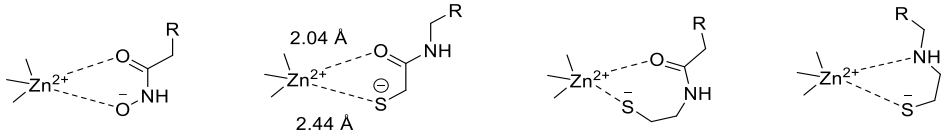

Figure 25 Bidentate chelation of Zn^{2+} by a hydroxamic acid, mercaptoacetamide, mercaptoethylamide, and mercaptoethylamine ZBG. Distances of the sulfur and oxygen atom of the mercaptoacetamide from the zinc ion in a complex of compound x in HDAC8 are indicated.

In summary, installation of an (α-methylated) MAA can induce (i) selectivity for parasitic over human HDAC8 by a differential positioning of linker unit and cap group as a result of the specific MAA binding mode, (ii) selectivity for HDAC6 over other HDACs, (iii) potent inhibition of HDACs, even superior to hydroxamic counterparts, (iv) potent neuroprotection without toxicity. As a result of these characteristics, MAA has been included as a ZBG in several HDAC6-selective inhibitors.[121, 164-170, 173, 175]

Overall, if a ZBG contains a thiol as a coordinating moiety, it is observed that protection of the thiol moiety by acetylation is needed to ensure cellular activity, but it abrogates activity in enzymatic assays, except in mercaptoketones. Alkylation of the thiol always results in loss of activity. Masking the thiol as a thiirane could entail a promising strategy, in combination with an activated α-methylene moiety and an active site-associated base. Together, it shows that the ability to ionize to the free thiolate is required for potent inhibition by thiol-based ZBGs.

3.6.3. Di- and trithiocarbonates and dithiocarbamates

Tert-butyl-phenylacetyl trithiocarbonates **42** and **43** (**Figure 26**) have been identified as hits in a high throughput screening campaign to identify new starting points for the development of HDACi.[83] These compounds exhibited submicromolar inhibition of HDACs present in HeLa cell nuclear extract (HDACs 1-3, 5, 8), with moderate cytotoxicity. First, different alkyl substituents were screened, which serve as an affix to the trithiocarbonate head and which could improve activity by exploiting the cavity underneath the binding site. Substitution of the *tert*-butyl group was well tolerated as different alkyl and aryl substituents retained HDAC inhibitory activity. The cytotoxic activity, however, was enhanced for methyl and ethyl substitutions.

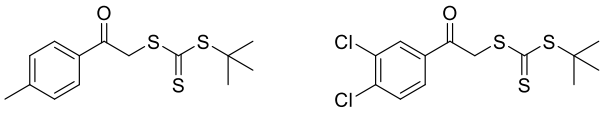

42 43

Figure 26 Trithiocarbonate hits resulting from a high throughput screening to identify novel HDAC inhibitors.[83]

Since the ethyl trithiocarbonate demonstrated superior chemical stability in aqueous media, it was selected for incorporation into the SAHA core structure (**Table 1**). This trithiocarbonate SAHA analog **44** (HeLa nuclear extract, pIC_{50}= 7.3 µM) was as potent as SAHA (HeLa nuclear extract, pIC_{50}= 7.1 µM) in HDACs 1-3, 5 and 8 inhibition, but lacked cellular activity, exhibiting only 40% inhibition of proliferation of HeLa cells at 25 µM, possibly due to the high lipophilicity and high protein binding.[83]

A stepwise SAR study was performed with compound **45** as a basis (**Figure 27**). Comparison of HDAC inhibition and cytotoxic activity of compounds **45**, **46**, and **47** demonstrated that the trithiocarbonates act as HDAC inhibitors themselves, not as a prodrug for the corresponding thiols. The methyl carbonyl moiety is essential for HDAC inhibition. It was assumed that the trithiocarbonate motif complexes Zn^{2+} in the HDAC active site, but this was not further investigated, nor was the role of the methyl carbonyl moiety in binding.

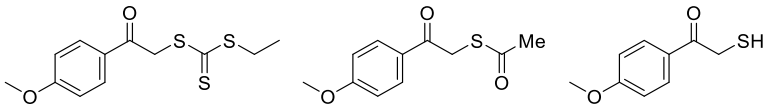

45 46 47

Figure 27 Stepwise SAR study performed to investigate the inhibitory mode of action of trithiocarbonates.[83]

Broadening of the HDAC isozyme scope showed that the most potent inhibition by compound **45** was observed for HDAC6 and that this motif can bind in the active site of HDAC class I and II enzymes.[83] Further structural optimization and analysis of the enzymatic and cellular effects furnished substrate competitive, HDAC6-selective inhibitors with nanomolar potency.[176] Exchanging the trithiocarbonate (HeLa nuclear extract, IC_{50}= 0.375 µM) for a dithiocarbonate was tolerated but reduced the potency (HeLa nuclear extract, IC_{50}= 0.811 µM).[176]

A decade later, in 2019, the SAHA analogs ethyl dithiocarbonate **48**, diethyldithiocarbamate **49**, and diethyldithiocarbamate coupled as a disulfide **50** were synthesized (**Figure 28**), varying the linker length from five to seven carbon atoms. Disulfide **50** displayed nanomolar inhibition of HDACs (**Table 1**) without pronounced selectivity, and potent antiproliferative activity against 293T, MCF-7, HeLa, K562, Kasumi-1, and BV173 cell lines (IC_{50} = 3.44 - 21.05 µM, MTT assay). No proliferation inhibition was observed for the other analogs (IC_{50} > 20 µM) with either linker length, while HDAC inhibition was not assessed. Diethylcarbamo(dithioperoxo)thioate **50** was claimed to be a new excellent ZBG, but it was not examined whether it serves as a zinc-binding group, or rather as a prodrug for the thiol. [81] The lack of activity can possibly be explained by the missing carbonyl methyl motif, which was identified as essential by Dehmel *et al.* and present in the trithiocarbonate **44**.[83]

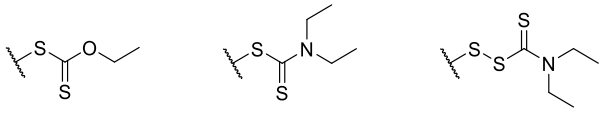

48 49 50

Figure 28 Thiocarbonyl ZBGs introduced into the SAHA structure.[81]

3.6.4. Sulfones and sulfoxides

Sulfone **51**, sulfonamide **52**, and trifluoromethylsulfonamide **53** have been designed as transition state analogs (**Table 1**) since it had been suggested that a sulfonamide sterically and electronically resembles the transition state of amide bond hydrolysis.[177] Although the geometry is distorted relative to the tetrahedral state of the native hydrate,[84] these ZBG were expected to bind the catalytic zinc ion in a bidentate manner (**Figure 29**).[79]

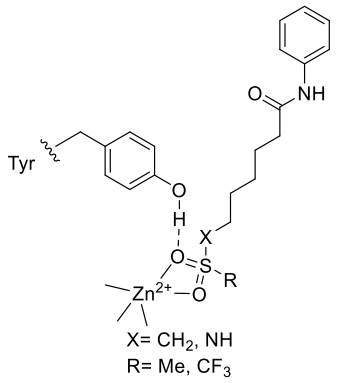

Figure 29 Model for binding of sulfone SAHA derivatives with the zinc ion in the active site of HDACs. Dashed lines: hydrogen bonds, solid lines Zn^{2+}: metal-coordination interactions.[85]

Despite the similarities, HDAC1/2 inhibition (HeLa extract) was lost upon installation of sulfone as a ZBG (IC_{50} > 100 µM).[79] Sulfonamide **52** elicited limited inhibition, less than 50% of all HDAC isoforms at 100 µM, except for HDAC5, for which 60% inhibition was achieved. Similar observations were made for the trifluoromethylated derivative **53**, only inhibiting HDAC11 for more than 50% at 100 µM.[84]

Hydroxysulfonamide **54** (**Table 1**) was explored because it was expected to chelate the zinc ion and form hydrogen bonds with tyrosine and histidine residues similar to SAHA. This model for interaction was based on the binding of hydroxamic acid rather than the negatively-charged hydroxamate. Again, no inhibitory activity was observed (IC_{50} > 100 µM).[79, 119]

Methyl sulfoxide was introduced as a monodentate ZBG (compound **55**, **Table 1**), as the partial negative charge on the oxygen was expected to enable potent zinc chelation. With an IC_{50} of 48 µM, the oxidized sulfur was inferior to its thiol counterpart.[85]

3.7. Fluoroalkenes

Osada *et al*. suspected that the amide bond in mercaptoacetamide may be sensitive to hydrolytic cleavage and therefore replaced the amido functionality with a mimetic structure. They proposed (*Z*)-fluoroalkene as a nonhydrolyzable (s-*Z*)-amide surrogate, which had been incorporated into peptidomimetics.[86, 178] Indeed, fluoroethylene is a stable, isosteric, and isoelectronic mimic, albeit with a lower dipolar moment value, of the amide bond (**Figure 30** and **Figure 31**). The fluoroalkene can also act as a hydrogen bond acceptor, with lower capability than the amide bond, while increasing the lipophilicity of the compound. Moreover, it can improve the metabolic stability of bioactive molecules, as shown by a significant increase in the half-life in human serum compared to the amide parent compound.[179]

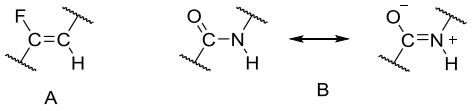

Figure 30 Fluoroalkene (A) as an (s, Z)-amide (B) surrogate.[86]

This resulted in potent inhibitors **56** (HeLa nuclear extract, IC_{50}= 0.36 µM), superior to SAHA (HeLa nuclear extract, IC_{50}= 1.10 µM), with a small fraction of the corresponding disulfides present in the end products.[86] It was assumed that the fluoroalkene interacts with zinc in a monodentate manner and that its π-system interacts with the hydrophobic environment.[86]

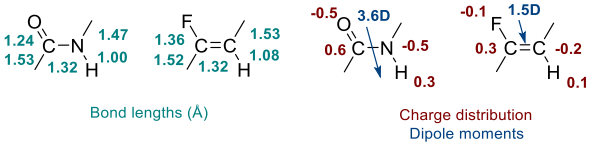

Figure 31 Steric and electronic analogies, with dipole moments and vectors illustrating the isosterism between the amide and the fluoroethylene function.[179-181]

3.8. Phosphorus-based zinc-binding groups

Phosphorus peptide analogs have been identified as effective inhibitors of several zinc peptidases already more then four decades ago, in the search for transition state analogs of amide bond hydrolysis.[71, 177, 182] In phosphonamidates, specifically, the phosphorus center is tetrahedral, the positioning of the heteroatoms mimics the tetrahedral amide bond hydrolysis transition state, and the phosphorus-heteroatom bonds are longer than carbon-heteroatom bonds in the ground state and thus capable of mimicking the longer bonds of the transition state (**Figure 32**).[71] Considering HDAC deacetylation is also an amide bond hydrolysis process involving a tetrahedral transition state, it was proposed that phosphorus-based zinc-binding groups could be included in potent HDACi.[48, 54] Analogous to the known metalloprotease inhibitors, phosphonamidate **57**, phosphonate **58**, and phosphinate **59** SAHA derivatives were synthesized and evaluated as HDAC inhibitors (**Table 1**). All three phosphorus-SAHA analogs lacked potent inhibitory activity, demonstrating millimolar IC_{50}s, as evaluated using HeLa nuclear extracts and recombinant human HDAC8. Although activity against HDAC8 increased over ten-fold compared to activity against the mixture of nuclear HDACs, SAHA is still over 1000-fold more potent. The effect of preincubation (10 h) was investigated to assess possible slow binding behavior of the inhibitors, as slow binding inhibition had been observed for all three types of phosphorus moieties in thermolysin inhibitors. The IC_{50} of the phosphonamidate changed from 2 mM to 0.57 mM (HeLa nuclear extract), indicating a possible slow-binding mode, whereas the IC_{50} of the phosphonate and phosphinate remained the same.[54]

Compounds **57**-**59** were also tested for cell growth inhibition in human ovarian A2780 cells. Surprisingly, here the phosphorus analogs were equally potent as SAHA (IC_{50} = 110 -120 µM), possibly due to off-target effects or inhibition of other HDAC isozymes. Phosphinate **59** is one atom shorter than phosphonamidate **57** and phosphonate **58**, which could influence its binding potential.[54]

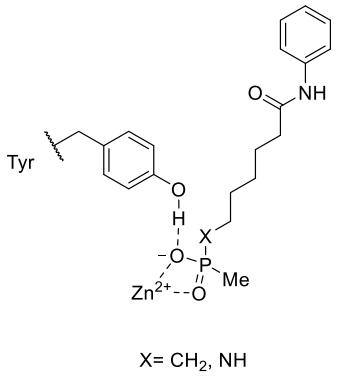

Figure 32 Model for binding of phosphonamidate and phosphinate ZBG with the zinc ion in the active site of HDAC1.[54]

Inspired by the work of Kapustin *et al*., Pun *et al*. investigated phosphate, phosphoramidate, and phosphorthiolate groups as ZBG and screened the resulting SAHA analogs **60**-**62** for inhibition of HDAC activity in HeLa cell lysates, and inhibition of HDAC3 and HDAC8 (**Table 1**). An eight hour incubation was required to detect significant inhibitory activity, in accordance with the slow-binding behavior of the phosphonamidate inhibitor.[54, 87] A five-carbon linker furnished the most potent inhibitors of HDACs present in HeLa cell extract for all three ZBG (IC_{50}= 50-70 µM). Phosphorthiolate **62** was the most potent inhibitor of HDAC3 and HDAC8, with a two-fold selectivity for HDAC3. Phosphate **60** and phosphoramidate **61** were less potent but showed some selectivity for HDAC8 over HDAC3. These motifs are more potent compared to the phosphonamidate **57**, phosphonate **58**, and phosphinate **59** SAHA analogs, while still considerably less potent than SAHA.[87]

3.9. Urea-based zinc-binding groups

Hydroxyurea **63** and semicarbazide derivative **64** (**Table 1**) have been designed to mimic the bidentate chelation and hydrogen bonding pattern established by hydroxamic acid HDACi.[48, 61, 79, 85] Concurrently, Vanommeslaeghe *et al*. identified *N*'-hydroxyurea as one of the best possible replacements for the HA via a DFT study including acetohydroxamic acid and *N*-methyl-*N*'-hydroxyurea.[183] This identification stemmed from the almost identical binding mode of *N*-methyl-*N*'-hydroxyurea compared to acetohydroxamic acid, a very similar binding mode to the hydroxamate moiety in the then available X-ray structures of HDAC(8)/SAHA complexes and the chemical similarities to hydroxamate.[46, 48] On the contrary, the calculated large energetic penalty upon desolvation may have a detrimental effect on binding affinity, consistent with its presumed high polarity.[183] The inhibitory activity towards HDACs of these urea-based compounds (HeLa nuclear extract, IC_{50} **63** = 80 µM, IC_{50} **64** = 150 µM) was comparable to *o*-amino anilide derivatives **66**, but considerably less effective than SAHA. Hanessian *et al*. studied the influence of the linker length (n= 5,6,7) since the active site can accommodate a limited number of carbon atoms in an acyclic chain, and this might have influenced the results of Suzuki *et al*.[46, 48, 93] None of the hydroxyurea analogs showed HDAC inhibitory activity below 1 µM and no cytotoxicity on different, although unspecified, tumor cell lines was observed below 20 µM.[93] Adaptation of the cap group to a bisthiazole did not furnish potent inhibitors either (IC_{50} HDAC1, 3, 4, 6 > 10 µM), while the hydroxamic acid and trifluoromethyl ketone counterparts were nanomolar inhibitors.[134]

Acyl thiourea was also explored as a non-HA ZBG (compound **65**), rationalized by the coordination potential, which can be either bidentate or monodentate (**Figure 33**).[89] Anionic *S,O*-chelation is the most common for transition metals, resulting in very stable six-membered coordination complexes. Monodentate coordination through a neutral *S*-atom is only observed with softer metal cations such as Au(I), Cu(I), Ag(I), Hg(II), Cd(II), Re(I), Ru(II), Pt(II) and Pd(II).[184] The interest in this ligand has

increased following its successful use in pharmacological, biological and agricultural applications such as anticancer, antifungal and herbicidal products.[184] HDAC inhibition was not determined, only docking experiments were performed showing that the binding affinities of **65** are comparable to or better than SAHA in HDAC2 and 7. Assessment of the antiproliferative potential in carcinoma cell lines (HRT-18 and HC-04) and epithelial cells (HBL-100) demonstrated a dose-dependent effect for the cancer cell lines (IC_{50} HRT-18= 30.42 and 24.12 µM, IC_{50} HC-04= 30.42 and 24.12 µM, for n= 4 and 5, respectively) with limited effect on healthy cells (< 12% inhibition at 100 µM).[89]

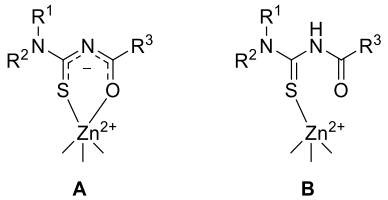

Figure 33 Proposed bidentate (A) and monodentate (B) coordination of Zn^{2+} by acyl thiourea.[89]

3.10. *o*-Aminoanilides

The *o*-aminoanilide (OAA) analog of SAHA **66** (SAHA-OAA, with n= 5) has been synthesized following the identification of histacin (*hist*one *ac*etylation *in*ducer) as a selective HDAC1-3 inhibitor (**Figure 34**). Histacin was the hit compound found after screening a library of compounds, containing 1,3-dioxane as a central core. Treatment of A549 cells with histacin (20 µM) significantly augmented lysine acetylation of histones, without any effect on α-tubulin acetylation.[185-187]

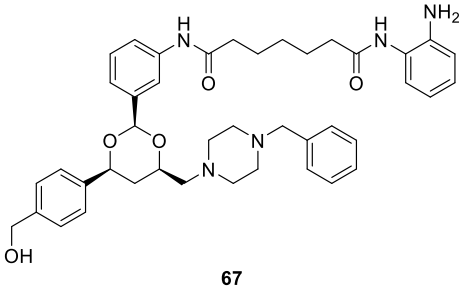

*Figure 34 Structure of histacin **67**, a 1,3-dioxane with an o-aminoanilide zinc-binding group.*

The OAA-based HDAC inhibitors are often described as the benzamide family. However, benzamide OAAs refer to a specific sub-category of the larger *o*-aminoanilide family (**Figure 35**).[188] Tucidinostat (Epidaza), approved by the NMPA for the treatment of hematological and breast cancers, contains a benzamide as a ZBG.[29, 30]

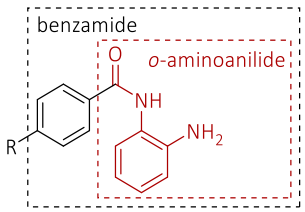

Figure 35 Difference between benzamides and o-aminoanilides.[188]

SAHA-OAA **66** (n= 6) displayed moderate inhibition of HDACs present in HeLa nuclear extracts (IC_{50}= 120 µM, Table 1),[79] but appeared more potent in biochemical assays with HDACs 1, 2 and 3 (1.51 µM, 2.23 µM, and 0.25 µM, respectively). In agreement with the selectivity observed for histacin, no activity was detected against HDAC8 or the class IIa/b enzymes up to 50 µM.[91] Western blot analysis showed

that SAHA-OAA **66** (n= 5) could indeed induce an increase in histone acetylation, without affecting the level of tubulin acetylation in A549 cells (20, 50, 100 µM).[185, 186] In an attempt to optimize the activity of SAHA-OAA **66**, a series of analogs were synthesized by Herman *et al.*, varying the linker length, the nature of the ZBG rings and the type and position of substituents on the ring (**Table 1**).[90] IC_{50} values were determined using HeLa nuclear extract and structure-activity relationships concerning HDAC inhibition could be deduced from the systematic structural changes. The optimal linker length depended on the position and nature of the aromatic substituent and could significantly influence the inhibitory activity. A five-atom linker (IC_{50}= 78 µM) is somewhat preferred over six carbon atoms (IC_{50}= 87 µM), as was also observed by Wong *et al*.[186] Some OAA derivatives, on the other hand, seemed to be more or less insensitive to changes in linker length. Removal of the *o*-amino group lowered activity, but not as dramatically as one might expect (IC_{50} **68** = 204 µM) considering that in the OAA, this *o*-amino group coordinated the active site zinc ion and engaged in hydrogen bonds. When this amino group was moved to the meta position, the inhibitory activity was impaired (IC_{50} **69** = 500 µM) for a five-carbon linker while activity remained for n= 6. Similarly, *p*-aminoanilide **70** derivatives were less potent than the *ortho*-parent compounds **66**. The activity was only moderately affected when the *o*-amino was replaced with an *o*-methoxy group for n= 5 (IC_{50} **71** = 54 µM) but was lost upon extending the linker with one methylene unit, changing the position or adding a second methoxy substituent (compounds **72**-**74**, IC_{50}> 380 µM). When the benzyl moiety was replaced with pyridine (**75**), no large change in activity occurred. *N*-(quinolin-8-yl)amide **76**, however, induced a four-fold increase in potency compared to the OAA **66**, whereas no change in activity was observed upon introduction of *N*-(quinolin-3-yl)amide as a ZBG (**77**).[90]

Modification of the cap group of SAHA-OAA to a tolyl moiety (**Figure 36**) resulted in a nanomolar inhibitor **78** of HDAC1 (IC_{50}= 13 nM) and HDAC3 (IC_{50}= 380 nM).[189]

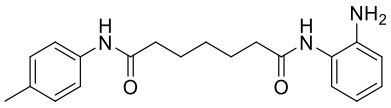

78

Figure 36 Tolyl derivative of o-aminoanilide-based SAHA.[189]

The lack of inhibition of HDAC8 and class II HDACs can be attributed to the differences in the active sites. The residues at the bottom of the tunnel leading to the active site differ between HDACs 1-3 on the one hand and HDAC8 and class II HDACs on the other hand. In HDAC8, the replacement of a leucine residue, present in HDACs 1-3, by a voluminous tryptophane residue (Trp141) interferes with the binding of the bulky OAA. This Trp residue is located near the zinc-binding domain and impedes the optimal chelation geometry of the OAA. The reduced activity of *o*-aminoanilides towards class II HDACs stems from the limited size of the active site of this class.[190] Moreover, HDACs 1-3 contain a secondary pocket next to the catalytic Zn^{2+}-ion, which can accommodate the bulky OAA ZBG, increasing its inhibitory potential against HDACs 1-3.[61, 191, 192]

SAHA-OAA derivatives **66** and the closely related tolyl analog **78** have been evaluated in cell and mouse models of Friedreich's ataxia (FRDA)[90, 91, 189, 193] and Huntington's disease.[91, 194] FRDA is characterized by abnormally low levels of the essential mitochondrial protein frataxin. In a lymphoid cell model for FRDA (GM15850), SAHA-OAA **66** (n= 6) and tolyl derivative **78** were able to increase acetylated histone levels and reverse the deficit in frataxin mRNA levels. The concentration required to induce HDAC inhibition (1-5 µM) did not affect viability or proliferation in the lymphoid cells, in contrast to SAHA. Remarkably, SAHA did not affect the frataxin levels, even though it was more effective in enhancing acetylated histone levels (total acetylated H3 and H4). Rai *et al.* reasoned that the discrepancy between the potent HDAC inhibitory activity of SAHA and the inability to restore frataxin levels on the one hand and

the ability of SAHA-OAA analogs **66** to promote frataxin levels while being less potent HDACi, on the other hand, is due to a difference in kinetics. SAHA-OAA analogs **66** are characterized by unique slow-on slow-off kinetics, which results in a more persistent histone hyperacetylation than induced by the very potent SAHA.[189, 195] This was also observed for other OAA-containing HDACi and benzamide-based inhibitors.[58] Bressi *et al.* proposed that these kinetics could result from the intramolecular hydrogen bond between the *ortho*-NH_2 group and the carbonyl oxygen, present in the unbound state.[192] In the bound conformation (**Figure 37**, modeled in human HDAC2), the nitrogen of the *ortho*-NH_2 and the carbonyl oxygen interact with the zinc ion. The hydrogens of the *ortho*-NH_2 form hydrogen bonds with H145 and H146, whereas the carbonyl oxygen forms a hydrogen bond with Y29. These interactions outweigh the ligand desolvation penalty and the disruption of the intramolecular hydrogen bond upon binding in the HDAC catalytic site. The anilide nitrogen seems to function as a surrogate for the water molecule that hydrolyzes the natural acetylated lysine substrate.

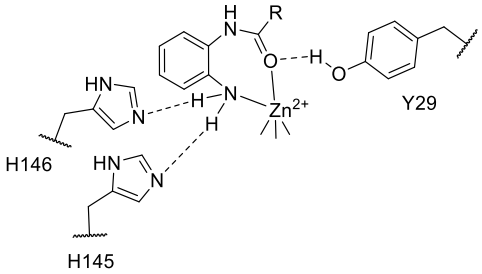

Figure 37 Proposed binding of the anilide ligand in the active site of human HDAC2, based on semi-empirical calculations. Dashed lines: hydrogen bonds, solid lines Zn^{2+}: metal-coordination interactions.[192]

Herman *et al.* analyzed the series of SAHA-OAA derivatives **66** (**Table 1**) for the activation of frataxin transcription, which was monitored by RT-qPCR of the frataxin mRNA levels. From this, it was apparent that no correlation existed between HDAC inhibition, determined with HeLa nuclear extracts as a source of HDACs, and the ability of compounds to enhance transcription of the frataxin gene. The authors explained this observation by pointing to the HDAC isozyme composition in HeLa nuclear extracts, which they expected to be poor in the true target HDAC isozyme involved in silencing the frataxin gene.[90]

Beconi *et al*. revealed that the OAA ZBG can undergo cyclization to an inactive benzimidazole product, especially under acidic conditions (**Figure 38**). They performed an extensive evaluation of the ADME profile of SAHA-OAA and unveiled important metabolic liabilities. It is very unstable in plasma ($T_{1/2}$= 1.9 h) and liver microsomes ($T_{1/2}$= 1.9 h, NADPH as cofactor), with M1 and M2 as main metabolites (**Figure 38**). These metabolites are not capable of HDAC inhibition. SAHA-OAA **66** serves as a P-glycoprotein 1 substrate, resulting in a high systemic clearance and efficient transport out of the brain. SAHA-OAA was consequently regarded as unsuitable for *in vivo* studies in mice by oral administration,[91] contesting the results obtained by Thomas *et al*. in Huntington's disease mice models.[194]

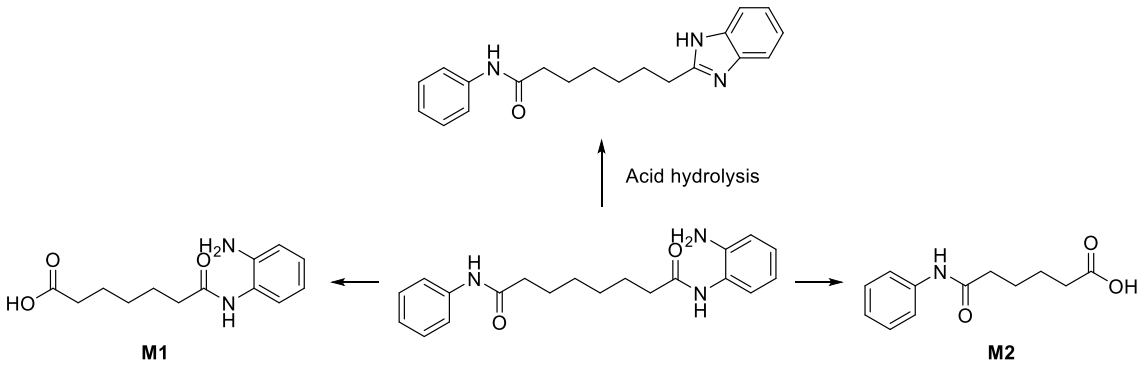

Figure 38 Product formed after acid hydrolysis of SAHA-OAA (top) and the two main inactive metabolites M1 and M2, resulting from amide hydrolysis.[91]

Compared to SAHA, OAA offers the advantage of high selectivity for HDACs 1-3 and possibly more persistent histone hyperacetylation, but faces metabolic liabilities, and the induced biological effect in disease models appears independent of HDAC inhibition. Compounds incorporating an OAA as a ZBG could be useful as selective probes. For therapeutic use, however, the ADME liabilities need to be addressed.

3.11. Hydrazides

Hydrazide emerged as a potential ZBG in HDACi from a high-throughput screening, which delivered a benzoylhydrazide as a lead compound. It selectively inhibited HDACs 1, 2, and 3 in nanomolar concentrations.[196] Intrigued by these powerful results, an extensive set of potent hydrazide-containing HDACi have been synthesized and evaluated by the Chou research group. These compounds exhibited high potency, class I selectivity, and a favorable pharmacokinetics profile.[39, 98, 197] Antidepressants and antituberculosis agents containing a hydrazine/hydrazide motif have been used in the clinic for decades.[98, 198] To compare the profile of hydroxamic acid and hydrazide as ZBGs, the latter was incorporated into the SAHA structure. Hydrazide **79** showed potent inhibition of class I HDACs (IC_{50}= 20-120 nM, **Table 2**), comparable to SAHA (IC_{50}= 43-145 nM), and displayed nanomolar anti-proliferative activity against leukemia cells (MV4-11, IC_{50}= 0.59 µM), with a potency similar to SAHA.[95] Evaluation of the protein-small molecule kinetics showed mixed inhibition kinetics, involving both competitive and non-competitive sites. Hydrazide HDACi thus also interact with an allosteric site, which was confirmed by docking studies in allosteric and catalytic sites of HDAC1 and HDAC3 and which was also observed for other hydrazide-based HDACi.[39, 98, 197] Inspection of the docking results clarifies that the hydrazide does not act as a zinc-binding group and that the inhibition is the result of the hydrogen bonding and hydrophobic interaction profile of the molecule.

To characterize the binding kinetics, dilution experiments were performed, in which it was expected that the complex of a tight-binding inhibitor and the target enzyme would be resistant to dilution. The release profile was assessed by Western blot, after washing out the inhibitor after a three-hour treatment and subsequently incubating the cells with fresh culture medium for different durations (0.5h, 1h, 3h, 6h). Together, this characterized compound **79** as a slow-on-slow-off tight binding inhibitor, in contrast to SAHA, which is a fast-on-fast-off reversible HDACi.[95]

3.12. Selenocyanates

As discussed in section 3.6, romidepsine **21** (FK228) is a powerful HDAC inhibitor containing a disulfide bond, which is reduced in the cellular environment, liberating the free thiol as the active species.[157]

Desai *et a*l. reasoned that a selenol moiety could similarly inhibit HDACs and synthesized the SAHA analogs containing this ZBG in a prodrug form, i.e. the selenium dimer bis(5-phenylcarbamoylpentyl) diselenide ([B(PCP)-2Se], also SelSA-1) and 5-phenylcarbamoylpentyl selenocyanide (PCP-SeCN, also SelSA-2) **80.** It was hypothesized that both species would be reduced in the cellular environment and free SeH would be released as the active form. Both the selenocyanate **80** and the selenium dimer were potent inhibitors of HDAC activity in HeLa nuclear extract, exhibiting 81% and 95% inhibition at 50 nM, respectively. The IC_{50} of the selenocyanate-based compound was established at 8.9 nM, showing superior inhibitory activity compared to SAHA (IC_{50}= 196 nM). The IC_{50} of selenium dimer was not determined but was expected to be in the same range.[92]

In a study performed by Gowda *et al*., cell killing efficacy of these selenium-containing SAHA analogs was investigated against melanoma (various cell lines, see below), pancreatic (MiaPaca-2), breast (MDA-MD-231), prostate (PC-3), and sarcoma (HT-1080) cell lines. It was found that these compounds could reduce the viability of cancer cells more efficiently than normal human cells (IC_{50}= 0.30-3.28 µM versus IC_{50}= 5.27 to > 40 µM) and more potently than SAHA. HDAC activity was higher in melanocytic lesion cell lines (WM35, WM3211, WM115, and WM278.1), which were also more sensitive to HDAC inhibition compared with metastatic melanoma (A375M and UACC 903). A dose-dependent (0.1-1.0 µM) decrease in endogenous HDAC activity in WM35 nuclear extract was observed upon treatment with SelSA-1 and SelSA-2 **80**, which was significantly more potent than SAHA. Western blot analysis of acetylated histone H3 and H4 levels demonstrated similar gains in protein levels upon treatment (0.25-2.0 µM) for SelSA-1, SelSA-2 **80**, and SAHA. Topical application of these selenium SAHA derivatives established a decrease in melanoma tumor development by 87% with negligible toxicity on skin cellular constituents. Besides the HDAC inhibitory activity, however, these compounds also displayed selenium-mediated inhibitory properties that decreased PI3 kinase pathway activity, increasing cellular apoptosis rates.[199] A similar observation was made by Yun *et al*., who examined the potential of these inhibitors in human lung cancer cell lines (A549, H2126, H1299, H226, H460, H522, H23, and H441). Again, it was found that SelSA-1 and SelSA-2 inhibited cell growth to a larger extent than parent-compound SAHA in a dose-dependent manner, exhibiting IC_{50} values in low micromolar concentrations. Mechanistically, it was found that SelSA-1 and SelSA-2 interfered with ERK and PI3K-AKT signaling pathways, while simultaneously increasing autophagy in A549 cells.[200]

Thus, despite exhibiting beneficial off-target effects in particular biological settings, the higher efficacy of selenium-based HDAC inhibitors in cancer research is not fully related to the enhancement of the HDAC inhibition potency but rather based on interference of the selenium moiety in cell cycle progression pathways.

3.13. (Hydroxymethyl)oxazolines

The (hydroxymethyl)oxazoline core has been explored as a zinc-binding group in the context of MMP inhibitors by Cook *et al.*, who synthesized inhibitors demonstrating low micromolar activity against MMP-9, a zinc-dependent gelatinase.[201] It was originally hypothesized that the oxazoline group would engage in a strong complex with the zinc ion of the active site and the functional group present in position X (**Figure 39**). R^1 substituents could be installed to provide selectivity over other zinc enzymes. Moreover, the rigidity of the ring might be beneficial for the drug-likeness of the inhibitors by restricting bond rotations [201]

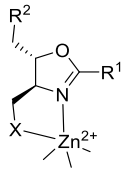

Figure 39 Hypothetical binding mode for the coordination of the active site zinc ion by oxazoline-based ZBG.[201]

Alcohol and thiol substituents on the X position were evaluated for their activity against MMPs. Improved binding of the thiols was expected compared to the alcohols since zinc is thiophilic and it was expected to form stronger bonds.[159] These sulfur derivatives showed some inhibition, but were less active than their alcohol counterparts, indicating that the 5-oxazoline substituent is probably not chelating the zinc ion and is most likely pointing out of the active site of MMP enzymes. This was corroborated by the observation that the size and electronic nature of the substituent could be varied without significant change in activity.[201] Nevertheless, this inspired Hanessian *et al*. to incorporate this ZBG in HDAC inhibitors.[93]

The incorporation of hydroxymethyl-substituted oxazoline as a ZBG in SAHA **81** (**Table 1**) did not result in a potent HDAC inhibitor. No inhibitory activity lower than 1 µM was observed and there was no cytotoxic effect on different cancer cell lines. Unfortunately, the biological analyses lacked experimental data.[93]

3.14. β-lactams

β-Lactams, or azetidin-2-ones, comprise an essential part of antibiotics such as penicillins and cephalosporins, in which this ring is fused to a five- or six-membered heterocycle. Such a bicyclic β-lactam system has been reported in compounds able to inhibit HDACs as well.[202] Monocyclic β-lactams also demonstrate potent biological activities, as antibiotics against resistant bacteria[203] and as enzyme inhibitors, for example as matrix metalloprotease inhibitors.[96, 204] Analysis of the *in vitro* inhibitory activity of compounds **82**-**84** against the 11 human HDACs (**Table 2**) demonstrated an unexpected selectivity against HDAC6 (IC_{50}= 74.5-174 µM) and no inhibition of the other HDACs (IC_{50} > 1000 µM). The two stereoisomers only differed slightly in their potency. Removal of the *N*-hydroxy group increased activity to an IC_{50} of 74.5 µM, whereas addition of an aminophenyl group (**85**) abrogated all activity.

Table 5 Overview of the SAR performed by Galletti et al.[96] to investigate β-lactams as potential zinc-binding group in HDAC inhibitors.

Entry	Compound number	Structure	IC_{50} HDAC6 (µM)	IC_{50} HDAC8 (µM)
1	**86**[a]	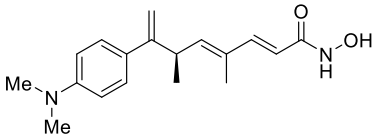	0.0004	0.09
2	**87**	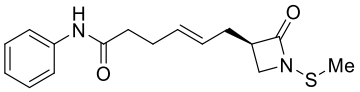	> 1000	34.3
3	**88**	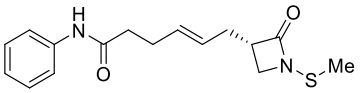	> 1000	11.6
4	**89**	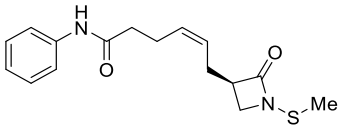	> 1000	33.1
5	**90**	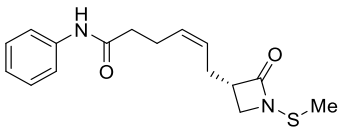	> 1000	9.6
6	**91**	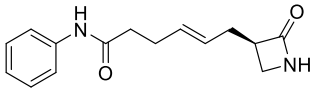	132.0	> 1000

7	**92**	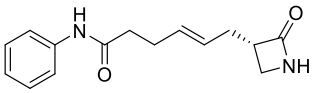	64.1	> 1000
8	**93**	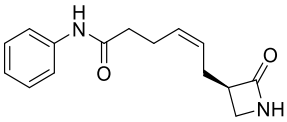	76.0	> 1000
9	**94**	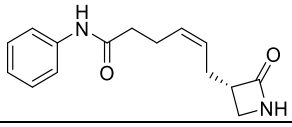	90.0	> 1000

[a] Trichostatin A (TSA) was used as a reference compound. It is a low nanomolar inhibitor of class I and II HDACs.[99]

Comparison of the SAHA analogs containing a β-lactam ZBG and a double bond in the linker, showed a complete switch in selectivity upon introduction of an *N*-thiomethyl group (**Table 5**), from inhibition of HDAC6 to HDAC8, whereas still no inhibition of other HDACs was observed. Replacing the *N*-hydroxy group in compounds **82**-**84** could thus also induce a similar change in selectivity.

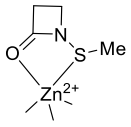

Figure 40 Calculated bidentate coordination geometry of 1-(methylthio)azetidin-2-one and Zn^{2+}.[96]

Galletti *et al*.[96] computationally investigated the binding mode of *N*-thiomethyl-β-lactam in HDAC2, 7 and 8 in order to explain the observed selectivity. Energy and geometry calculations of the zinc ion in complex with unsubstituted 1-(methylthio)azetidin-2-one demonstrated a bidentate coordination geometry (**Figure 40**). Computational analysis using the co-crystal structures of HDAC7 (PDB: 3C0Z) and HDAC8 (PDB: 1T67) and a 3D structural model of HDAC2 with hydroxamic acid-based inhibitors, demonstrated that the bidentate interaction was lost in all complexes upon superposition of the 1-(methylthio)azetidin-2-one on the hydroxamic acid moiety of these inhibitors. This was the result of a steric clash between two conserved glycine residues on the one hand and the methyl group and the CH_2 on the C4 position of the azetidinone ring on the other hand. Consequently, 1-(methylthio)azetidin-2-one was modeled as a monodentate ligand and a water molecule was added as a zinc-coordinating group. With this model, molecular dynamics simulations were performed, which showed that HDAC2 can accommodate a larger ZBG, owing to a more accessible space in the catalytic centre. The small S-Me group, however, cannot engage in favorable interactions in this larger site, which could explain the lack of activity. In HDAC7, the S-Me group clashes with a proline residue, which causes the inhibitor to adopt a different conformation, in which the sulfur atom coordinates the Zn^{2+} ion. In HDAC8, the carbonyl group of methylthiolated β-lactams coordinated the zinc ion.

Together, this demonstrates that substituted β-lactams can be implemented as a zinc-binding moiety in HDACi, but would require further optimization to enhance activity. The selectivity could be directed towards HDAC6 or HDAC8 by careful selection of the substituents on the nitrogen atom of the β-lactam ring.

3.15. Squaric acid and derivatives

Squaric acid, also known as quadratic acid (3,4-dihydroxycyclobut-3-ene-1,2-dione), has a unique pseudo-aromatic character, rendering an unusually high double acidity (pKa1= 0.54, pKa2= 3.5) due to the resonance-stabilization of the squarate dianion (**Figure 41**).[205-208]

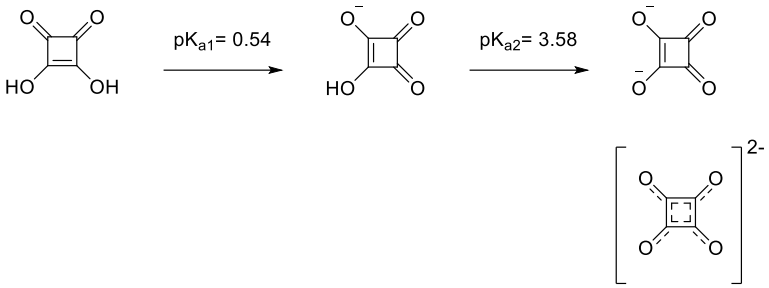

Figure 41 Double acidity of squaric acid and the resulting resonance stabilized squarate dianion, which has an aromatic character.[208]

The conjugate base of squaric acid can serve as an electrostatic mimic of negatively charged groups, such as carboxylates and phosphates. Therefore, squaric acid and its analogs are used as non-classical isosteric replacements for these functionalities, providing potent enzyme inhibitors and receptor antagonists.[206] Squaramides have historically been mainly considered as thiourea and urea substitutes, but have also been used in bioisosteric approaches to drug design for hydroxamic acid and amide moieties.[209] As Chasák *et a*l. reviewed, this scaffold and related analogs are undergoing a revival with several squaramides in (pre)clinical trials, despite mistrust by medicinal chemists because of potential *in vivo* toxicity originating from the reactive functional groups.[208] Squaramides **95** have been synthesized as vinylogous hydroxamic acids derived from squaric acid and were shown to bind iron(III) in an aqueous medium (**Figure 42**).[210] This prompted Onaran *et al*. to investigate their potential as inhibitors of the zinc-dependent metalloprotease-1 (MMP-1).[206] It was expected that the *N*-hydroxy squaramide **95** would coordinate the zinc ion in a bidentate manner, establishing a six-membered coordination ring (**Figure 43**, left). Incorporation of a methyl or isopropyl group at R^1 was preferred over larger groups (cyclohexyl, benzyl) or no substitution (R^1= H). No potent inhibition could be observed, with IC_{50} values in the high micromolar to the millimolar range.[206] The corresponding squaric acid analog **96** also lacked activity (IC_{50} > 200 µM); not surprisingly, since the bite angle between the two oxygen atoms in squaric acid is too large to coordinate Zn^{2+} in a strong five-membered manner (**Figure 43**, right). A third derivatization performed by Onaran *et al.* consisted of the conversion of a carbonyl group on the 3-cyclobutene-1,2-dione core to a thiocarbonyl (**97**) to enhance the potency of the inhibitors. Some compounds were 2-18 times more potent upon sulfur incorporation, while others showed similar IC_{50} values.[206] In spite of the limited inhibitory potencies, this work sparked interest in investigating the potential of these ZBGs as potential HDAC inhibitors.[88]

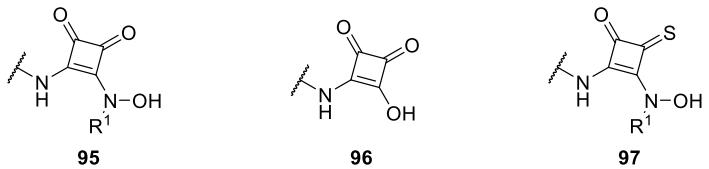

*Figure 42 Squaric acid and derivatives explored as MMP-1 inhibitors: squaramide as vinylogous HA **95**, the squaric acid derivative of the vinylogous HA **96**, and the thiocarbonyl analog of the vinylogous HA **97**.*

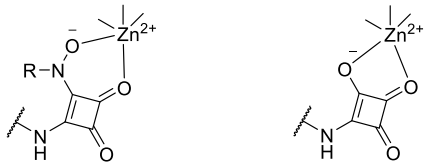

95 98

Figure 43 (Left) Proposed binding mode of the squaric acid N-hydroxyamide derivative, as suggested by molecular modeling. (Right) Five-membered zinc chelation model for the squaric acid ZBG.[206, 210]

Hanessian *et al.*[93] synthesized SAHA-analogs containing squaric acid **98**, thiol-based squaric acid **99** and the vinylogous HA **100** as ZBG (**Table 1**). The length of the aliphatic chain was varied to optimize accommodation in the active site since the zinc-binding geometry might differ from hydroxamic acids. None of the squaric acid analogs showed HDAC inhibitory activity below 1 µM, and no cytotoxic effect was observed on different cancer cell lines below 20 µM. The authors provided no experimental information on the biological testing. The activity could potentially be improved by optimization of the *N*-alkyl group for increased HDAC binding. Indeed, the *N*-methyl group was the result of a selection procedure of squaric acid derivatives to optimize binding in MMP-1. It should be assessed whether this methyl substituent is also preferred for HDAC binding. Replacement of the carbonyl group in the vinylogous HA **100** engaging in zinc-binding by a thiocarbonyl could induce an increase in inhibition potential as well.[206]

4. Conclusions and future perspectives

Identification of valuable alternative zinc-binding groups currently represents the focal point of current HDAC inhibition research efforts. Indeed, HDACs are increasingly recognized as essential to cellular function and a wide range of diseases, and safety concerns associated with the hydroxamic acid zinc-binding group are growing. Inhibitors of several (zinc-dependent) metalloproteases also exhibit this trend. This Perspective provides an overview of zinc-binding groups introduced into the well-known SAHA (vorinostat) structure, enabling comparison of various approaches and outcomes and demonstrating that it is possible to obtain non-hydroxamic acid HDAC inhibitors with an improved or similar inhibitory activity and/or lower toxicity toward healthy cells compared to the HA counterpart.

A variety of strategies to select an alternative zinc-binding group (ZBG) have been employed before incorporation into the SAHA structure. Natural products provide a valuable source of information regarding the activity of a ZBG in a biological environment and the corresponding requirements (e.g. prodrugs for thiol-based ZBG) and selectivity (e.g. hydroxyketones). High-throughput screenings can identify active inhibitors, but the resulting compounds often show cellular liabilities, such as weak cellular activity (trithiocarbonates) and allosteric inhibition (hydrazides). The introduction of transition state mimics as hydroxamic acid substitutes gave rise to both active (trifluoromethyl ketones, α-keto amides, silane diols) and inactive (sulphonamides, phosphonamidates) compounds. When translating structural inspiration from metalloprotease inhibitors to HDAC inhibitors, it is crucial to disseminate the key features responsible for potent inhibition, metal complexation and the ones inducing selectivity for (specific) metalloproteases.

Bidentate coordination does not necessarily produce potent inhibitors, as was observed for boronic acids, sulfones and sulfonamides, while monodentate complexes (e.g. thiols) can demonstrate strong inhibitory activity. Thiol, (α-methylated) mercaptoacetamide and 2-mercaptoethan-1-one are potent inhibitors, but require transformation into a prodrug for cellular activity. Optimization of the type of prodrug could further increase activity and selectivity.

Some ZBG show an inherent selectivity for a specific HDAC isozyme or class, as the result of additional interactions in the catalytic site (e.g. fluoroalkenes), the size of the cavity, and/or a steric clash with specific amino acid residues. The size of the catalytic site can influence selectivity in two ways, it can be too small to accommodate certain groups that fit in other isozymes (e.g. *o*-aminoanilides), or it can be too large to form hydrogen bonds or hydrophobic interactions with small ZBGs. The ZBG's substitution pattern, therefore, can play a crucial role in enhancing potency and selectivity. For example, *N*-methyl substitution in amide-based natural substrate mimics appears to be essential for activity and probably engages in similar interactions with the catalytic site as the acetylated lysine substrate. Moreover, a ZBG's differential positioning can disrupt the optimal interaction of the inhibitor with the protein surface and/or catalytic tunnel, resulting in the need to reoptimize the cap group and the linker unit.

Equipotent HDAC inhibitors can elicit different cellular effects as a result of distinct binding kinetics, leading to more persistent hyperacetylation in cellular assays, as observed for *o*-aminoanilides. A ZBG demonstrating moderate activity when introduced into the SAHA structure can be a valuable substitute for HA. Combining it with an appropriate cap group and linker unit can result in a potent, highly selective inhibitor with an improved pharmacological profile. Weak but selective ZBGs may be more interesting than highly powerful ones in that regard.

In screening platforms for HDAC inhibitory activity, HeLa nuclear cell extracts are often used as a source of HDACs. This seems like a reasonable approach for screening for inhibitors of class I HDACs, but it overlooks potential candidates with inherent selectivity for a specific HDAC isozyme or class II HDACs. Also, a fluorogenic, acetylated peptide substrate is most often used for the assessment of the HDAC inhibitory activity of compounds. As HDAC10 is a polyamine deacetylase and HDAC11 is a lysine fatty acid deacetylase, this can cause false-negative results, and substrates used in the analysis should be adjusted accordingly. Thus, the inhibition potential should rather be determined using recombinant HDAC enzymes and appropriate substrates, so as not to miss any inhibitory effects. In addition, it is imperative to verify the substrate(s) used for activity measurements when interpreting HDAC inhibitory results from literature.

Some of the compounds demonstrated double inhibitory mechanisms, some by allosteric inhibition (hydrazides), and others by concurrent interference with a cell survival pathway (selenium-containing ZBGs). When evaluating the HDAC inhibitory activity *in cellulo* or *in vivo*, analyses should be included to differentiate between HDAC-related effects and allosteric and/or off-target therapeutic effects. It is also important to consider effects induced by degradation products or metabolites, before attributing observed therapeutic effects to HDAC inhibition.

In summary, the following guidelines can be considered for the selection of a non-hydroxamic acid zinc-binding group in the context of (HDAC) enzyme inhibitor research. A ZBG should be able to engage in hydrophobic and hydrogen bonding interactions, as well as exploit differences in size and composition of the active site to promote activity and selectivity. Additionally, the desolvation penalty and lipophilicity should be taken into account. The zinc-coordinating atom should be able to ionize in the catalytic site or bear a partial negative charge and the ZBG should form a stable coordination complex with Zn^{2+}. Moderately active ZBGs can be valuable alternatives to hydroxamic acid, but assays used to determine inhibitory and/or therapeutic activity should be critically assessed. The optimal positioning of an alternative ZBG candidate in the catalytic site can be determined using docking studies or, better, crystal structures of the candidate-ZBG combined with a simple or flexible linker in complex with the HDAC isoform of interest. An optimized linker and cap group can then be added to enhance activity, which should interact with the catalytic tunnel and protein surface, respectively, while maintaining the ZBG in its optimal orientation.

The binding kinetics has only been assessed for a few non-HA SAHA analogs. More research in that regard would be valuable as it could be predictive of the cellular kinetics as has been observed for SAHA[58] and even of functional and therapeutic effects.[211] Knowledge on the kinetic inhibition properties is also important for the setup of experiments and analysis. Slow associating/dissociating inhibitors, for example, may not have reached equilibrium within the timeframe of IC_{50} determination.[58]

Potent HDACi devoid of a ZBG have been reported recently,[212-214] reminiscent of the "cap-less" HDACi introduced by Wagner *et al.*,[215] questioning the typical HDACi pharmacophore. In contrast to the non-zinc-binding inhibitors which rely on a culmination of weak interactions, the ZBG provides a stronger interaction with the protein. The presented work shows that ZBGs can induce specific selectivity, enhance or decrease activity, change binding kinetics and could thus be used to optimize or change the inhibition characteristics. We expect that a combination of a selected ZBG with a cap group and linker unit tailored to this specific ZBG, allowing the ZBG to bind in its optimal conformation and maximizing interactions with the protein surface and catalytic tunnel would furnish superior HDACi.

Valuable additional and/or supportive insights would result from the introduction of zinc-binding groups in SAHA that are present in emerging, potent and selective non-HA HDACi. 2-Methylthiobenzamide, for example, could be incorporated in SAHA to investigate to which extent the observed HDAC3 selectivity results from this specific ZBG, and how it compares to *o*-aminoanilides.[216] Oxadiazoles are emerging as ZBG in HDAC6-selective inhibitors and a dissemination of the characteristics when incorporated in SAHA would provide valuable information on the intrinsic features responsible for the observed beneficial activity and selectivity, possible opportunities to enhance or adapt these and the preferred substitutions.[217, 218]

Acknowledgements

The authors acknowledge the Research Foundation - Flanders (FWO) and the Ghent University Special Research Fund (BOF) for financial support.

Biographies

Silke Geurs

Silke Geurs is pursuing a PhD at the Department of Green Chemistry and Technology at Ghent University and at the VIB-UGent Center for Medical Biotechnology, under the guidance of Matthias D'hooghe, Dorien Clarisse and Karolien De Bosscher. She studied HDAC6 inhibition in her Master's thesis (2017), and continued to investigate it in her PhD research, combining chemical synthesis and analysis with biochemical and cell-based assays. She has been focused on the design and synthesis of novel HDAC6 inhibitors and evaluation of their activity against multiple myeloma, introduction and evaluation of non-hydroxamic acid zinc-binding groups and carboxylic acid bioisosteres in HDAC6 inhibitors, interrogation of mechanistic and phenotypic aspects of HDAC6 as a molecular target by use of chemical probes and establishment of structure-activity relationships.

Dorien Clarisse

Dorien Clarisse holds two Master's degrees, one in Chemistry and one in Biochemistry and Biotechnology. Ensuing, she obtained her PhD in Health sciences in 2018, under the supervision of Prof. Karolien De Bosscher, at the VIB Center for Medical Biotechnology and the Department of Biomolecular Medicine (Ghent University, Belgium). She continued as a postdoctoral researcher on a translational 'Stand up to Cancer' project (2018-2021). Supported by her interdisciplinary research profile, she also embarked in 2020 on a research project revolving around the crosstalk between

nuclear receptors and how therapeutic targeting thereof can improve efficacy and reduce side effects. She is collaborating with Prof. Matthias D'hooghe on this project, which is at the interface between chemistry and biology.

Karolien De Bosscher

Karolien De Bosscher (Ph.D degree at UGent, Belgium, in 2000) secured a competitive research professorship grant in 2013. In 2019 she reeled in both a full professorship position via the fast-track system and an appointment as expert scientist at the VIB Center for Medical Biotechnology. K. De Bosscher has a long-standing focus on the anti-inflammatory and anti-cancer action mechanisms ofvarious small molecules with a focus on nuclear receptor ligands. In recent years her team zooms in on the benefit of nuclear receptor crosstalk mechanisms (GR, MR) in hematological cancers. She has been collaborating with the team of Matthias D'hooghe since the past 7 years; her team has developed and implemented bio-assays to test the anti-inflammatory and anti-cancer activities of various new chemical entities.

Matthias D'hooghe

Matthias D'hooghe received his Master's diploma in 2001 and his PhD degree in 2006 at Ghent University (Belgium). In 2007, he became postdoctoral assistant, and in 2009 he performed a short postdoctoral stay at Eindhoven University of Technology (The Netherlands). In 2010, he was promoted to Professor at Ghent University, and he was granted tenure in 2015. His main research interests include the chemistry of small-ring azaheterocycles and the synthesis and assessment of bioactive heterocyclic compounds with applications in different fields (cancer, antibiotics, inflammation...). Prof. D'hooghe is the author of >170 publications in international journals and the recipient of several awards. He is a member of the Bioheterocycles International Scientific Committee and organized and chaired the international Bioheterocycles conference in 2019.

Abbreviations

ADME, absorption, distribution, metabolism, and excretion; CFDA, China food and drug administration; DFT, density-functional theory; FDA, U.S. food and drug administration; FRDA, Friedreich's ataxia; HA, hydroxamic acid; HDAC, histone deacetylase; HDACi, histone deacetylase inhibitors; hERG, human ether-a-go-go related gene; MAA, mercaptoacetamide; MMP, matrix metalloprotease; MTT, 3-(4,5-dimethylthiazol-2-yl)-2,5-diphenyltetrazolium bromide; NMPA, national medical products administration; OAA, o-amino anilide; PD, pharmacodynamics; PK, pharmacokinetics; qRT-PCR, real-time quantitative reverse transcription polymerase chain reaction; SAHA, suberoylanilide hydroxamic acid; SAHA-MAA, mercaptoacetamide analog of suberoylanilide hydroxamic acid; SAHA-OAA, o-amino anilide analog of suberoylanilide hydroxamic acid; SAR, Structure-activity relationship; SelSA-1, bis(5-phenylcarbamoylpentyl) diselenide; SelSA-2, 5-phenylcarbamoylpentyl selenocyanide; smHDAC8, Schistosoma mansoni histone deacetylase 8; TFMK, trifluoromethyl ketone; ZBG, zinc-binding group

References

1. Yang, X.-J.; Seto, E., The Rpd3/Hda1 family of lysine deacetylases: from bacteria and yeast to mice and men. *Nat. Rev. Mol. Cell Biol.* **2008,** *9* (3), 206-218.
2. Haberland, M.; Montgomery, R. L.; Olson, E. N., The many roles of histone deacetylases in development and physiology: implications for disease and therapy. *Nat. Rev. Genet.* **2009,** *10* (1), 32-42.
3. Choudhary, C.; Kumar, C.; Gnad, F.; Nielsen, M. L.; Rehman, M.; Walther, T. C.; Olsen, J. V.; Mann, M., Lysine acetylation targets protein complexes and co-regulates major cellular functions. *Science* **2009,** *325* (5942), 834-40.

4. Allfrey, V. G.; Faulkner, R.; Mirsky, A. E., Acetylation and Methylation of Histones and Their Possible Role in the Regulation of Rna Synthesis. *Proc. Natl. Acad. Sci. USA* **1964,** *51*, 786-94.
5. Gershey, E. L.; Vidali, G.; Allfrey, V. G., Chemical studies of histone acetylation. The occurrence of epsilon-N-acetyllysine in the f2a1 histone. *J Biol Chem* **1968,** *243* (19), 5018-22.
6. Seto, E.; Yoshida, M., Erasers of Histone Acetylation: The Histone Deacetylase Enzymes. *Cold Spring Harb. Perspect. Biol.* **2014,** *6* (4), a018713.
7. Lombardi, P. M.; Cole, K. E.; Dowling, D. P.; Christianson, D. W., Structure, mechanism, and inhibition of histone deacetylases and related metalloenzymes. *Curr. Opin. Struct. Biol.* **2011,** *21* (6), 735-743.
8. Ouzounis, C. A.; Kyrpides, N. C., On the evolution of arginases and related enzymes. *J. Mol. Evol.* **1994,** *39* (1), 101-4.
9. Kanyo, Z. F.; Scolnick, L. R.; Ash, D. E.; Christianson, D. W., Structure of a unique binuclear manganese cluster in arginase. *Nature* **1996,** *383* (6600), 554-7.
10. Narita, T.; Weinert, B. T.; Choudhary, C., Functions and mechanisms of non-histone protein acetylation. *Nat. Rev. Mol. Cell Biol.* **2019,** *20* (3), 156-174.
11. Ho, T. C. S.; Chan, A. H. Y.; Ganesan, A., Thirty Years of HDAC Inhibitors: 2020 Insight and Hindsight. *J. Med. Chem.* **2020,** *63* (21), 12460-12484.
12. Hai, Y.; Shinsky, S. A.; Porter, N. J.; Christianson, D. W., Histone deacetylase 10 structure and molecular function as a polyamine deacetylase. *Nat. Commun.* **2017,** *8*.
13. Kutil, Z.; Novakova, Z.; Meleshin, M.; Mikesova, J.; Schutkowski, M.; Barinka, C., Histone Deacetylase 11 Is a Fatty-Acid Deacylase. *ACS Chem. Biol.* **2018,** *13* (3), 685-693.
14. Moreno-Yruela, C.; Galleano, I.; Madsen, A. S.; Olsen, C. A., Histone Deacetylase 11 Is an ε-N-Myristoyllysine Hydrolase. *Cell Chem. Biol.* **2018,** *25* (7), 849-856.e8.
15. Melesina, J.; Simoben, C. V.; Praetorius, L.; Bülbül, E. F.; Robaa, D.; Sippl, W., Strategies To Design Selective Histone Deacetylase Inhibitors. *ChemMedChem* **2021,** *16* (9), 1336-1359.
16. Hudson, G. M.; Watson, P. J.; Fairall, L.; Jamieson, A. G.; Schwabe, J. W. R., Insights into the Recruitment of Class IIa Histone Deacetylases (HDACs) to the SMRT/NCoR Transcriptional Repression Complex. *J. Biol. Chem.* **2015,** *290* (29), 18237-18244.
17. Desravines, D. C.; Serna Martin, I.; Schneider, R.; Mas, P. J.; Aleksandrova, N.; Jensen, M. R.; Blackledge, M.; Hart, D. J., Structural Characterization of the SMRT Corepressor Interacting with Histone Deacetylase 7. *Sci. Rep.* **2017,** *7* (1), 3678.
18. Ropero, S.; Esteller, M., The role of histone deacetylases (HDACs) in human cancer. *Mol. Oncol.* **2007,** *1* (1), 19-25.
19. Li, G.; Tian, Y.; Zhu, W.-G., The Roles of Histone Deacetylases and Their Inhibitors in Cancer Therapy. *Front. Cell Dev. Biol.* **2020,** *8* (1004).
20. Simões-Pires, C.; Zwick, V.; Nurisso, A.; Schenker, E.; Carrupt, P.-A.; Cuendet, M., HDAC6 as a target for neurodegenerative diseases: what makes it different from the other HDACs? *Mol. Neurodegener.* **2013,** *8* (1), 7.
21. Chuang, D.-M.; Leng, Y.; Marinova, Z.; Kim, H.-J.; Chiu, C.-T., Multiple roles of HDAC inhibition in neurodegenerative conditions. *Trends Neurosci.* **2009,** *32* (11), 591-601.
22. Falkenberg, K. J.; Johnstone, R. W., Histone deacetylases and their inhibitors in cancer, neurological diseases and immune disorders. *Nat. Rev. Drug Discov.* **2014,** *13* (9), 673-91.
23. Arrowsmith, C. H.; Bountra, C.; Fish, P. V.; Lee, K.; Schapira, M., Epigenetic protein families: a new frontier for drug discovery. *Nat. Rev. Drug Discov.* **2012,** *11* (5), 384-400.
24. Rodrigues, D. A.; Pinheiro, P. d. S. M.; Sagrillo, F. S.; Bolognesi, M. L.; Fraga, C. A. M., Histone deacetylases as targets for the treatment of neurodegenerative disorders: Challenges and future opportunities. *Med. Res. Rev.* **2020,** *40* (6), 2177-2211.
25. Mann, B. S.; Johnson, J. R.; Cohen, M. H.; Justice, R.; Pazdur, R., FDA approval summary: vorinostat for treatment of advanced primary cutaneous T-cell lymphoma. *Oncologist* **2007,** *12* (10), 1247-52.
26. Raedler, L. A., Farydak (Panobinostat): First HDAC Inhibitor Approved for Patients with Relapsed Multiple Myeloma. *Am. Health Drug Benefits* **2016,** *9* (Spec Feature), 84-7.

27. Lee, J.; Hong, E. C.; Jeong, H.; Hwang, J. W.; Kim, H.; Bae, E. K.; Ahn, J. K.; Choi, Y. L.; Han, J.; Cha, H. S.; Koh, E. M., A novel histone deacetylase 6-selective inhibitor suppresses synovial inflammation and joint destruction in a collagen antibody-induced arthritis mouse model. *Int. J. Rheum. Dis.* **2015,** *18* (5), 514-23.
28. https://www.fda.gov/Drugs/InformationOnDrugs/ApprovedDrugs/default.htm (accessed 03/12/2021).
29. Lu, X.; Ning, Z.; Li, Z.; Cao, H.; Wang, X., Development of chidamide for peripheral T-cell lymphoma, the first orphan drug approved in China. *Intractable Rare Dis. Res.* **2016,** *5* (3), 185-191.
30. Yao, X.; Ding, J.; Liu, Y.; Li, P., The New Drug Conditional Approval Process in China: Challenges and Opportunities. *Clin. Ther.* **2017,** *39* (5), 1040-1051.
31. http://pharma.globaldata.com/Drugs/NewAdvExport (accessed 23/02/2022).
32. Bondarev, A. D.; Attwood, M. M.; Jonsson, J.; Chubarev, V. N.; Tarasov, V. V.; Schiöth, H. B., Recent developments of HDAC inhibitors: Emerging indications and novel molecules. *Br. J. Clin. Pharmacol.* **2021,** *87* (12), 4577-4597.
33. He, X.; Li, Z.; Zhuo, X. T.; Hui, Z.; Xie, T.; Ye, X. Y., Novel Selective Histone Deacetylase 6 (HDAC6) Inhibitors: A Patent Review (2016-2019). *Recent Pat. Anticancer Drug Discov.* **2020,** *15* (1), 32-48.
34. Shen, S.; Kozikowski, A. P., A patent review of histone deacetylase 6 inhibitors in neurodegenerative diseases (2014-2019). *Expert Opin. Ther. Pat.* **2020,** *30* (2), 121-136.
35. Shen, S.; Kozikowski, A. P., Why Hydroxamates May Not Be the Best Histone Deacetylase Inhibitors--What Some May Have Forgotten or Would Rather Forget? *ChemMedChem* **2016,** *11* (1), 15-21.
36. Strevel, E. L.; Siu, L. L., Cardiovascular toxicity of molecularly targeted agents. *Eur. J. Cancer* **2009,** *45*, 318-331.
37. Traoré, M. D. M.; Zwick, V.; Simões-Pires, C. A.; Nurisso, A.; Issa, M.; Cuendet, M.; Maynadier, M.; Wein, S.; Vial, H.; Jamet, H.; Wong, Y.-S., Hydroxyl Ketone-Based Histone Deacetylase Inhibitors To Gain Insight into Class I HDAC Selectivity versus That of HDAC6. *ACS Omega* **2017,** *2* (4), 1550-1562.
38. Marks, P. A., Discovery and development of SAHA as an anticancer agent. *Oncogene* **2007,** *26* (9), 1351-1356.
39. McClure, J. J.; Zhang, C.; Inks, E. S.; Peterson, Y. K.; Li, J.; Chou, C. J., Development of Allosteric Hydrazide-Containing Class I Histone Deacetylase Inhibitors for Use in Acute Myeloid Leukemia. *J. Med. Chem.* **2016,** *59* (21), 9942-9959.
40. Richon, V. M., Cancer biology: mechanism of antitumour action of vorinostat (suberoylanilide hydroxamic acid), a novel histone deacetylase inhibitor. *Br. J. Cancer* **2006,** *95* (1), S2-S6.
41. Wagner, F. F.; Weïwer, M.; Steinbacher, S.; Schomburg, A.; Reinemer, P.; Gale, J. P.; Campbell, A. J.; Fisher, S. L.; Zhao, W.-N.; Reis, S. A.; Hennig, K. M.; Thomas, M.; Müller, P.; Jefson, M. R.; Fass, D. M.; Haggarty, S. J.; Zhang, Y.-L.; Holson, E. B., Kinetic and structural insights into the binding of histone deacetylase 1 and 2 (HDAC1, 2) inhibitors. *Biorg. Med. Chem.* **2016,** *24* (18), 4008-4015.
42. Watson, P. J.; Fairall, L.; Santos, G. M.; Schwabe, J. W. R., Structure of HDAC3 bound to co-repressor and inositol tetraphosphate. *Nature* **2012,** *481* (7381), 335-340.
43. Bottomley, M. J.; Lo Surdo, P.; Di Giovine, P.; Cirillo, A.; Scarpelli, R.; Ferrigno, F.; Jones, P.; Neddermann, P.; De Francesco, R.; Steinkühler, C.; Gallinari, P.; Carfí, A., Structural and Functional Analysis of the Human HDAC4 Catalytic Domain Reveals a Regulatory Structural Zinc-binding Domain*. *J. Biol. Chem.* **2008,** *283* (39), 26694-26704.
44. Hai, Y.; Christianson, D. W., Histone deacetylase 6 structure and molecular basis of catalysis and inhibition. *Nature Chemical Biology* **2016,** *12* (9), 741-747.
45. Schuetz, A.; Min, J.; Allali-Hassani, A.; Schapira, M.; Shuen, M.; Loppnau, P.; Mazitschek, R.; Kwiatkowski, N. P.; Lewis, T. A.; Maglathin, R. L.; McLean, T. H.; Bochkarev, A.; Plotnikov, A. N.; Vedadi, M.; Arrowsmith, C. H., Human HDAC7 Harbors a Class IIa Histone Deacetylase-specific Zinc Binding Motif and Cryptic Deacetylase Activity*. *J. Biol. Chem.* **2008,** *283* (17), 11355-11363.

46. Somoza, J. R.; Skene, R. J.; Katz, B. A.; Mol, C.; Ho, J. D.; Jennings, A. J.; Luong, C.; Arvai, A.; Buggy, J. J.; Chi, E.; Tang, J.; Sang, B.-C.; Verner, E.; Wynands, R.; Leahy, E. M.; Dougan, D. R.; Snell, G.; Navre, M.; Knuth, M. W.; Swanson, R. V.; McRee, D. E.; Tari, L. W., Structural Snapshots of Human HDAC8 Provide Insights into the Class I Histone Deacetylases. *Structure* **2004,** *12* (7), 1325-1334.
47. Porter, N. J.; Christianson, N. H.; Decroos, C.; Christianson, D. W., Structural and Functional Influence of the Glycine-Rich Loop G302GGGY on the Catalytic Tyrosine of Histone Deacetylase 8. *Biochemistry* **2016,** *55* (48), 6718-6729.
48. Finnin, M. S.; Donigian, J. R.; Cohen, A.; Richon, V. M.; Rifkind, R. A.; Marks, P. A.; Breslow, R.; Pavletich, N. P., Structures of a histone deacetylase homologue bound to the TSA and SAHA inhibitors. *Nature* **1999,** *401* (6749), 188-193.
49. Porter, N. J.; Christianson, D. W., Structure, mechanism, and inhibition of the zinc-dependent histone deacetylases. *Curr. Opin. Struct. Biol.* **2019,** *59*, 9-18.
50. De Vreese, R.; D'hooghe, M., Synthesis and applications of benzohydroxamic acid-based histone deacetylase inhibitors. *Eur. J. Med. Chem.* **2017,** *135*, 174-195.
51. De Vreese, R.; Galle, L.; Depetter, Y.; Franceus, J.; Desmet, T.; Van Hecke, K.; Benoy, V.; Van Den Bosch, L.; D'hooghe, M., Synthesis of Potent and Selective HDAC6 Inhibitors Bearing a Cyclohexane- or Cycloheptane-Annulated 1,5-Benzothiazepine Scaffold. *Chem. Eur. J.* **2017,** *23* (1), 128-136.
52. De Vreese, R.; Verhaeghe, T.; Desmet, T.; D'hooghe, M., Potent and selective HDAC6 inhibitory activity of N-(4-hydroxycarbamoylbenzyl)-1,2,4,9-tetrahydro-3-thia-9-azafluorenes as novel sulfur analogues of Tubastatin A. *Chem Commun* **2013,** *49* (36), 3775-7.
53. Citarella, A.; Moi, D.; Pinzi, L.; Bonanni, D.; Rastelli, G., Hydroxamic Acid Derivatives: From Synthetic Strategies to Medicinal Chemistry Applications. *ACS Omega* **2021,** *6* (34), 21843-21849.
54. Kapustin, G. V.; Fejér, G.; Gronlund, J. L.; McCafferty, D. G.; Seto, E.; Etzkorn, F. A., Phosphorus-Based SAHA Analogues as Histone Deacetylase Inhibitors. *Org. Lett.* **2003,** *5* (17), 3053-3056.
55. Estiu, G.; Greenberg, E.; Harrison, C. B.; Kwiatkowski, N. P.; Mazitschek, R.; Bradner, J. E.; Wiest, O., Structural Origin of Selectivity in Class II-Selective Histone Deacetylase Inhibitors. *J. Med. Chem.* **2008,** *51* (10), 2898-2906.
56. Khan, N.; Jeffers, M.; Kumar, S.; Hackett, C.; Boldog, F.; Khramtsov, N.; Qian, X.; Mills, E.; Berghs, Stanny C.; Carey, N.; Finn, Paul W.; Collins, Laura S.; Tumber, A.; Ritchie, James W.; Jensen, Peter B.; Lichenstein, Henri S.; Sehested, M., Determination of the class and isoform selectivity of small-molecule histone deacetylase inhibitors. *Biochemical Journal* **2007,** *409* (2), 581-589.
57. Schäker-Hübner, L.; Haschemi, R.; Büch, T.; Kraft, F. B.; Brumme, B.; Schöler, A.; Jenke, R.; Meiler, J.; Aigner, A.; Bendas, G.; Hansen, F. K., Balancing Histone Deacetylase (HDAC) Inhibition and Drug-likeness: Biological and Physicochemical Evaluation of Class I Selective HDAC Inhibitors. *ChemMedChem* **2022,** *17* (9), e202100755.
58. Lauffer, B. E. L.; Mintzer, R.; Fong, R.; Mukund, S.; Tam, C.; Zilberleyb, I.; Flicke, B.; Ritscher, A.; Fedorowicz, G.; Vallero, R.; Ortwine, D. F.; Gunzner, J.; Modrusan, Z.; Neumann, L.; Koth, C. M.; Lupardus, P. J.; Kaminker, J. S.; Heise, C. E.; Steiner, P., Histone Deacetylase (HDAC) Inhibitor Kinetic Rate Constants Correlate with Cellular Histone Acetylation but Not Transcription and Cell Viability. *J. Biol. Chem.* **2013,** *288* (37), 26926-26943.
59. Cross, J. B.; Duca, J. S.; Kaminski, J. J.; Madison, V. S., The Active Site of a Zinc-Dependent Metalloproteinase Influences the Computed pKa of Ligands Coordinated to the Catalytic Zinc Ion. *J. Am. Chem. Soc.* **2002,** *124* (37), 11004-11007.
60. Wang, D.; Helquist, P.; Wiest, O., Zinc Binding in HDAC Inhibitors: A DFT Study. *J. Org. Chem.* **2007,** *72* (14), 5446-5449.
61. Vannini, A.; Volpari, C.; Filocamo, G.; Casavola, E. C.; Brunetti, M.; Renzoni, D.; Chakravarty, P.; Paolini, C.; De Francesco, R.; Gallinari, P.; Steinkühler, C.; Di Marco, S., Crystal structure of a eukaryotic zinc-dependent histone deacetylase, human HDAC8, complexed with a hydroxamic acid inhibitor. *Proceedings of the National Academy of Sciences of the United States of America* **2004,** *101* (42), 15064-15069.

62. Zhou, J.; Wu, R.; Luo, H.-B., Inhibition mechanism of SAHA in HDAC: a revisit. *Phys. Chem. Chem. Phys.* **2015,** *17* (44), 29483-29488.
63. Osko, J. D.; Porter, N. J.; Narayana Reddy, P. A.; Xiao, Y.-C.; Rokka, J.; Jung, M.; Hooker, J. M.; Salvino, J. M.; Christianson, D. W., Exploring Structural Determinants of Inhibitor Affinity and Selectivity in Complexes with Histone Deacetylase 6. *J. Med. Chem.* **2020,** *63* (1), 295-308.
64. Cheshmedzhieva, D.; Toshev, N.; Gerova, M.; Petrov, O.; Dudev, T., Hydroxamic acid derivatives as histone deacetylase inhibitors: a DFT study of their tautomerism and metal affinities/selectivities. *J. Mol. Model.* **2018,** *24* (5), 114.
65. El Yazal, J.; Pang, Y.-P., Novel Stable Configurations and Tautomers of the Neutral and Deprotonated Hydroxamic Acids Predicted from High-Level ab Initio Calculations. *The Journal of Physical Chemistry A* **1999,** *103* (41), 8346-8350.
66. Cheshmedzhieva, D.; Toshev, N.; Gerova, M.; Petrov, O.; Dudev, T., Hydroxamic acid derivatives as histone deacetylase inhibitors: a DFT study of their tautomerism and metal affinities/selectivities. *J. Mol. Model.* **2018,** *24* (5), 114.
67. Porter, N. J.; Mahendran, A.; Breslow, R.; Christianson, D. W., Unusual zinc-binding mode of HDAC6-selective hydroxamate inhibitors. *Proc Natl Acad Sci U S A* **2017,** *114* (51), 13459-13464.
68. Ignatyev, I. S.; Montejo, M.; Rodríguez Ortega, P. G.; González, J. J. L., Quantum chemical study of silanediols as metal binding groups for metalloprotease inhibitors. *J. Mol. Model.* **2013,** *19* (4), 1819-1834.
69. Herbst-Gervasoni, C. J.; Christianson, D. W., Binding of N8-Acetylspermidine Analogues to Histone Deacetylase 10 Reveals Molecular Strategies for Blocking Polyamine Deacetylation. *Biochemistry* **2019,** *58* (49), 4957-4969.
70. Temperini, C.; Innocenti, A.; Guerri, A.; Scozzafava, A.; Rusconi, S.; Supuran, C. T., Phosph(on)ate as a zinc-binding group in metalloenzyme inhibitors: X-ray crystal structure of the antiviral drug foscarnet complexed to human carbonic anhydrase I. *Bioorg. Med. Chem. Lett.* **2007,** *17* (8), 2210-2215.
71. Bartlett, P. A.; Marlowe, C. K., Phosphonamidates as transition-state analogue inhibitors of thermolysin. *Biochemistry* **1983,** *22* (20), 4618-24.
72. Suzuki, N.; Suzuki, T.; Ota, Y.; Nakano, T.; Kurihara, M.; Okuda, H.; Yamori, T.; Tsumoto, H.; Nakagawa, H.; Miyata, N., Design, synthesis, and biological activity of boronic acid-based histone deacetylase inhibitors. *J. Med. Chem.* **2009,** *52* (9), 2909-22.
73. Frey, R. R.; Wada, C. K.; Garland, R. B.; Curtin, M. L.; Michaelides, M. R.; Li, J. L.; Pease, L. J.; Glaser, K. B.; Marcotte, P. A.; Bouska, J. J.; Murphy, S. S.; Davidsen, S. K., Trifluoromethyl ketones as inhibitors of histone deacetylase. *Bioorg. Med. Chem. Lett.* **2002,** *12* (23), 3443-3447.
74. Wada, C. K.; Frey, R. R.; Ji, Z.; Curtin, M. L.; Garland, R. B.; Holms, J. H.; Li, J.; Pease, L. J.; Guo, J.; Glaser, K. B.; Marcotte, P. A.; Richardson, P. L.; Murphy, S. S.; Bouska, J. J.; Tapang, P.; Magoc, T. J.; Albert, D. H.; Davidsen, S. K.; Michaelides, M. R., α-Keto amides as inhibitors of histone deacetylase. *Bioorg. Med. Chem. Lett.* **2003,** *13* (19), 3331-3335.
75. Dai, Y.; Guo, Y.; Curtin, M. L.; Li, J.; Pease, L. J.; Guo, J.; Marcotte, P. A.; Glaser, K. B.; Davidsen, S. K.; Michaelides, M. R., A novel series of histone deacetylase inhibitors incorporating hetero aromatic ring systems as connection units. *Bioorg. Med. Chem. Lett.* **2003,** *13* (21), 3817-3820.
76. Gu, W.; Nusinzon, I.; Smith Jr, R. D.; Horvath, C. M.; Silverman, R. B., Carbonyl- and sulfur-containing analogs of suberoylanilide hydroxamic acid: Potent inhibition of histone deacetylases. *Biorg. Med. Chem.* **2006,** *14* (10), 3320-3329.
77. Suzuki, T.; Miyata, N., Non-hydroxamate histone deacetylase inhibitors. *Curr. Med. Chem.* **2005,** *12* (24), 2867-2880.
78. Suzuki, T.; Kouketsu, A.; Matsuura, A.; Kohara, A.; Ninomiya, S.-i.; Kohda, K.; Miyata, N., Thiol-based SAHA analogues as potent histone deacetylase inhibitors. *Bioorg. Med. Chem. Lett.* **2004,** *14* (12), 3313-3317.
79. Suzuki, T.; Nagano, Y.; Kouketsu, A.; Matsuura, A.; Maruyama, S.; Kurotaki, M.; Nakagawa, H.; Miyata, N., Novel Inhibitors of Human Histone Deacetylases: Design, Synthesis, Enzyme Inhibition,

and Cancer Cell Growth Inhibition of SAHA-Based Non-hydroxamates. *J. Med. Chem.* **2005,** *48* (4), 1019-1032.
80. Wen, J.; Bao, Y.; Niu, Q.; Yang, J.; Fan, Y.; Li, J.; Jing, Y.; Zhao, L.; Liu, D., Identification of N-(6-mercaptohexyl)-3-(4-pyridyl)-1H-pyrazole-5-carboxamide and its disulfide prodrug as potent histone deacetylase inhibitors with in vitro and in vivo anti-tumor efficacy. *Eur. J. Med. Chem.* **2016,** *109*, 350-359.
81. Wenwen Cheng, D. Z., Qiang Zheng, Zhongjun Li, Xiangbao Meng, Design, synthesis and biological evaluation of novel HDAC inhibitors: sulphur-containing zinc binding groups. *J. Chin. Pharm. Sci.* **2019,** *28* (6), 408-421.
82. Anandan, S.-K.; Ward, J. S.; Brokx, R. D.; Bray, M. R.; Patel, D. V.; Xiao, X.-X., Mercaptoamide-based non-hydroxamic acid type histone deacetylase inhibitors. *Bioorg. Med. Chem. Lett.* **2005,** *15* (8), 1969-1972.
83. Dehmel, F.; Ciossek, T.; Maier, T.; Weinbrenner, S.; Schmidt, B.; Zoche, M.; Beckers, T., Trithiocarbonates: exploration of a new head group for HDAC inhibitors. *Bioorg. Med. Chem. Lett.* **2007,** *17* (17), 4746-52.
84. Madsen, A. S.; Kristensen, H. M. E.; Lanz, G.; Olsen, C. A., The Effect of Various Zinc Binding Groups on Inhibition of Histone Deacetylases 1–11. *ChemMedChem* **2014,** *9* (3), 614-626.
85. Suzuki, T., Explorative Study on Isoform-Selective Histone Deacetylase Inhibitors. *Chem. Pharm. Bull. (Tokyo)* **2009,** *57* (9), 897-906.
86. Osada, S.; Sano, S.; Ueyama, M.; Chuman, Y.; Kodama, H.; Sakaguchi, K., Fluoroalkene modification of mercaptoacetamide-based histone deacetylase inhibitors. *Biorg. Med. Chem.* **2010,** *18* (2), 605-11.
87. Pun, M. D.; Wu, H.-H.; Olatunji, F. P.; Kesic, B. N.; Peters, J. W.; Berkman, C. E., Phosphorus containing analogues of SAHA as inhibitors of HDACs. *Journal of Enzyme Inhibition and Medicinal Chemistry* **2022,** *37* (1), 1315-1319.
88. Hanessian, S.; Vinci, V.; Auzzas, L.; Marzi, M.; Giannini, G., Exploring alternative Zn-binding groups in the design of HDAC inhibitors: Squaric acid, N-hydroxyurea, and oxazoline analogues of SAHA. *Bioorg. Med. Chem. Lett.* **2006,** *16* (18), 4784-4787.
89. Al-Amily, D. H.; Hassan Mohammed, M., Design, Synthesis, and Docking Study of Acyl Thiourea Derivatives as Possible Histone Deacetylase Inhibitors with a Novel Zinc Binding Group. *Sci. Pharm.* **2019,** *87* (4), 28.
90. Herman, D.; Jenssen, K.; Burnett, R.; Soragni, E.; Perlman, S. L.; Gottesfeld, J. M., Histone deacetylase inhibitors reverse gene silencing in Friedreich's ataxia. *Nat Chem Biol* **2006,** *2* (10), 551-8.
91. Beconi, M.; Aziz, O.; Matthews, K.; Moumné, L.; O'Connell, C.; Yates, D.; Clifton, S.; Pett, H.; Vann, J.; Crowley, L.; Haughan, A. F.; Smith, D. L.; Woodman, B.; Bates, G. P.; Brookfield, F.; Bürli, R. W.; McAllister, G.; Dominguez, C.; Munoz-Sanjuan, I.; Beaumont, V., Oral administration of the pimelic diphenylamide HDAC inhibitor HDACi 4b is unsuitable for chronic inhibition of HDAC activity in the CNS in vivo. *PLoS One* **2012,** *7* (9), e44498.
92. Desai, D.; Salli, U.; Vrana, K. E.; Amin, S., SelSA, Selenium Analogs of SAHA As Potent Histone Deacetylase Inhibitors. *Bioorg. Med. Chem. Lett.* **2010,** *20* (6), 2044-2047.
93. Hanessian, S.; Vinci, V.; Auzzas, L.; Marzi, M.; Giannini, G., Exploring alternative Zn-binding groups in the design of HDAC inhibitors: squaric acid, N-hydroxyurea, and oxazoline analogues of SAHA. *Bioorg Med Chem Lett* **2006,** *16* (18), 4784-4787.
94. Botta, C. B.; Cabri, W.; Cini, E.; De Cesare, L.; Fattorusso, C.; Giannini, G.; Persico, M.; Petrella, A.; Rondinelli, F.; Rodriquez, M.; Russo, A.; Taddei, M., Oxime Amides as a Novel Zinc Binding Group in Histone Deacetylase Inhibitors: Synthesis, Biological Activity, and Computational Evaluation. *J. Med. Chem.* **2011,** *54* (7), 2165-2182.
95. Yue, K.; Qin, M.; Huang, C.; James Chou, C.; Jiang, Y.; Li, X., Comparison of three zinc binding groups for HDAC inhibitors – A potency, selectivity and enzymatic kinetics study. *Bioorg. Med. Chem. Lett.* **2022,** *70*, 128797.

96. Galletti, P.; Quintavalla, A.; Ventrici, C.; Giannini, G.; Cabri, W.; Penco, S.; Gallo, G.; Vincenti, S.; Giacomini, D., Azetidinones as Zinc-Binding Groups to Design Selective HDAC8 Inhibitors. *ChemMedChem* **2009,** *4* (12), 1991-2001.
97. Hanessian, S.; Auzzas, L.; Larsson, A.; Zhang, J.; Giannini, G.; Gallo, G.; Ciacci, A.; Cabri, W., Vorinostat-Like Molecules as Structural, Stereochemical, and Pharmacological Tools. *ACS Med. Chem. Lett.* **2010,** *1* (2), 70-74.
98. Li, X.; Peterson, Y. K.; Inks, E. S.; Himes, R. A.; Li, J.; Zhang, Y.; Kong, X.; Chou, C. J., Class I HDAC Inhibitors Display Different Antitumor Mechanism in Leukemia and Prostatic Cancer Cells Depending on Their p53 Status. *J. Med. Chem.* **2018,** *61* (6), 2589-2603.
99. Vigushin, D. M.; Ali, S.; Pace, P. E.; Mirsaidi, N.; Ito, K.; Adcock, I.; Coombes, R. C., Trichostatin A Is a Histone Deacetylase Inhibitor with Potent Antitumor Activity against Breast Cancer in Vivo1. *Clinical Cancer Research* **2001,** *7* (4), 971-976.
100. Koehler, K. A.; Lienhard, G. E., 2-phenylethaneboronic acid, a possible transition-state analog for chymotrypsin. *Biochemistry* **1971,** *10* (13), 2477-83.
101. Philipp, M.; Bender, M. L., Inhibition of serine proteases by arylboronic acids. *Proc. Natl. Acad. Sci. USA* **1971,** *68* (2), 478-80.
102. Matthews, D. A.; Alden, R. A.; Birktoft, J. J.; Freer, S. T.; Kraut, J., X-ray crystallographic study of boronic acid adducts with subtilisin BPN' (Novo). A model for the catalytic transition state. *J. Biol. Chem.* **1975,** *250* (18), 7120-6.
103. Hiratake, J.; Oda, J. i., Aminophosphonic and Aminoboronic Acids as Key Elements of a Transition State Analogue Inhibitor of Enzymes. *Bioscience, Biotechnology, and Biochemistry* **1997,** *61* (2), 211-218.
104. Silva, M. P.; Saraiva, L.; Pinto, M.; Sousa, M. E., Boronic Acids and Their Derivatives in Medicinal Chemistry: Synthesis and Biological Applications. *Molecules* **2020,** *25* (18), 4323.
105. Adams, J.; Kauffman, M., Development of the Proteasome Inhibitor Velcade™ (Bortezomib). *Cancer Invest.* **2004,** *22* (2), 304-311.
106. Kane, R. C.; Farrell, A. T.; Sridhara, R.; Pazdur, R., United States Food and Drug Administration approval summary: bortezomib for the treatment of progressive multiple myeloma after one prior therapy. *Clin Cancer Res* **2006,** *12* (10), 2955-60.
107. Ballatore, C.; Huryn, D. M.; Smith, A. B., 3rd, Carboxylic acid (bio)isosteres in drug design. *ChemMedChem* **2013,** *8* (3), 385-95.
108. Yang, W.; Gao, X.; Wang, B., Biological and Medicinal Applications of Boronic Acids. In *Boronic Acids*, 2005; pp 481-512.
109. Tan, Y.; Wu, J.; Song, L.; Zhang, M.; Hipolito, C. J.; Wu, C.; Wang, S.; Zhang, Y.; Yin, Y., Merging the Versatile Functionalities of Boronic Acid with Peptides. *Int. J. Mol. Sci.* **2021,** *22* (23), 12958.
110. Brem, J.; Cain, R.; Cahill, S.; McDonough, M. A.; Clifton, I. J.; Jiménez-Castellanos, J.-C.; Avison, M. B.; Spencer, J.; Fishwick, C. W. G.; Schofield, C. J., Structural basis of metallo-β-lactamase, serine-β-lactamase and penicillin-binding protein inhibition by cyclic boronates. *Nat. Commun.* **2016,** *7* (1), 12406.
111. Hall, D. G., Structure, Properties, and Preparation of Boronic Acid Derivatives. Overview of Their Reactions and Applications. In *Boronic Acids*, 2005; pp 1-99.
112. Hall, D., Structure, Properties, and Preparation of Boronic Acid Derivatives. 2011; Vol. 1, pp 1-133.
113. Liu, X.-C.; Hubbard, J. L.; Scouten, W. H., Synthesis and structural investigation of two potential boronate affinity chromatography ligands catechol [2-(diisopropylamino)carbonyl]phenylboronate and catechol [2-(diethylamino)carbonyl, 4-methyl]phenylboronate. *J. Organomet. Chem.* **1995,** *493* (1), 91-94.
114. Springsteen, G.; Wang, B., A detailed examination of boronic acid–diol complexation. *Tetrahedron* **2002,** *58* (26), 5291-5300.

115. Wiskur, S. L.; Lavigne, J. J.; Ait-Haddou, H.; Lynch, V.; Chiu, Y. H.; Canary, J. W.; Anslyn, E. V., pKa Values and Geometries of Secondary and Tertiary Amines Complexed to Boronic AcidsImplications for Sensor Design. *Org. Lett.* **2001,** *3* (9), 1311-1314.
116. Yang, W.; Gao, X.; Wang, B., Boronic acid compounds as potential pharmaceutical agents. *Med. Res. Rev.* **2003,** *23* (3), 346-368.
117. Fu, H.; Fang, H.; Sun, J.; Wang, H.; Liu, A.; Sun, J.; Wu, Z., Boronic acid-based enzyme inhibitors: a review of recent progress. *Curr. Med. Chem.* **2014,** *21* (28), 3271-80.
118. Ness, S.; Martin, R.; Kindler, A. M.; Paetzel, M.; Gold, M.; Jensen, S. E.; Jones, J. B.; Strynadka, N. C. J., Structure-Based Design Guides the Improved Efficacy of Deacylation Transition State Analogue Inhibitors of TEM-1 β-Lactamase. *Biochemistry* **2000,** *39* (18), 5312-5321.
119. Suzuki, N.; Suzuki, T.; Ota, Y.; Nakano, T.; Kurihara, M.; Okuda, H.; Yamori, T.; Tsumoto, H.; Nakagawa, H.; Miyata, N., Design, Synthesis, and Biological Activity of Boronic Acid-Based Histone Deacetylase Inhibitors. *J. Med. Chem.* **2009,** *52* (9), 2909-2922.
120. Islam, M. N.; Islam, M. S.; Hoque, M. A.; Kato, T.; Nishino, N.; Ito, A.; Yoshida, M., Bicyclic tetrapeptide histone deacetylase inhibitors with methoxymethyl ketone and boronic acid zinc-binding groups. *Bioorg. Chem.* **2014,** *57*, 121-126.
121. Geurs, S.; Clarisse, D.; Baele, F.; Franceus, J.; Desmet, T.; De Bosscher, K.; D'hooghe, M., Identification of mercaptoacetamide-based HDAC6 inhibitors via a lean inhibitor strategy: screening, synthesis, and biological evaluation. *Chem. Commun.* **2022,** *58* (42), 6239-6242.
122. Christianson, D. W.; Lipscomb, W. N., Complex between carboxypeptidase A and a possible transition-state analog: mechanistic inferences from high-resolution x-ray structures of enzyme-inhibitor complexes. *J. Am. Chem. Soc.* **1986,** *108* (16), 4998-5003.
123. Suzuki, T.; Miyata, N., Rational design of non-hydroxamate histone deacetylase inhibitors. *Mini Rev. Med. Chem.* **2006,** *6* (5), 515-26.
124. Curtin, M.; Glaser, K., Histone deacetylase inhibitors: The Abbott experience. *Curr. Med. Chem.* **2003,** *10* (22), 2373-2392.
125. Frey, R. R.; Wada, C. K.; Garland, R. B.; Curtin, M. L.; Michaelides, M. R.; Li, J.; Pease, L. J.; Glaser, K. B.; Marcotte, P. A.; Bouska, J. J.; Murphy, S. S.; Davidsen, S. K., Trifluoromethyl ketones as inhibitors of histone deacetylase. *Bioorg Med Chem Lett* **2002,** *12* (23), 3443-7.
126. Trimble, L. A.; Street, I. P.; Perrier, H.; Tremblay, N. M.; Weech, P. K.; Bernstein, M. A., NMR structural studies of the tight complex between a trifluoromethyl ketone inhibitor and the 85-kDa human phospholipase A2. *Biochemistry* **1993,** *32* (47), 12560-12565.
127. Patel, D. V.; Rielly-Gauvin, K.; Ryono, D. E.; Free, C. A.; Smith, S. A.; Petrillo, E. W., Activated ketone based inhibitors of human renin. *J. Med. Chem.* **1993,** *36* (17), 2431-2447.
128. Peet, N. P.; Burkhart, J. P.; Angelastro, M. R.; Giroux, E. L.; Mehdi, S.; Bey, P.; Kolb, M.; Neises, B.; Schirlin, D., Synthesis of peptidyl fluoromethyl ketones and peptidyl .alpha.-keto esters as inhibitors of porcine pancreatic elastase, human neutrophil elastase, and rat and human neutrophil cathepsin G. *J. Med. Chem.* **1990,** *33* (1), 394-407.
129. Boger, D. L.; Sato, H.; Lerner, A. E.; Austin, B. J.; Patterson, J. E.; Patricelli, M. P.; Cravatt, B. F., Trifluoromethyl ketone inhibitors of fatty acid amide hydrolase: A probe of structural and conformational features contributing to inhibition. *Bioorg. Med. Chem. Lett.* **1999,** *9* (2), 265-270.
130. Walter, M. W.; Felici, A.; Galleni, M.; Soto, R. P.; Adlington, R. M.; Baldwin, J. E.; Frère, J.-M.; Gololobov, M.; Schofield, C. J., Trifluoromethyl alcohol and ketone inhibitors of metallo-β-lactamases. *Bioorg. Med. Chem. Lett.* **1996,** *6* (20), 2455-2458.
131. Edwards, P. D.; Andisik, D. W.; Strimpler, A. M.; Gomes, B.; Tuthill, P. A., Nonpeptidic inhibitors of human neutrophil elastase. 7. Design, synthesis, and in vitro activity of a series of pyridopyrimidine trifluoromethyl ketones. *J. Med. Chem.* **1996,** *39* (5), 1112-1124.
132. Veale, C. A.; Bernstein, P. R.; Bohnert, C. M.; Brown, F. J.; Bryant, C.; Damewood, J. R.; Earley, R.; Feeney, S. W.; Edwards, P. D.; Gomes, B.; Hulsizer, J. M.; Kosmider, B. J.; Krell, R. D.; Moore, G.; Salcedo, T. W.; Shaw, A.; Silberstein, D. S.; Steelman, G. B.; Stein, M.; Strimpler, A.; Thomas, R. M.; Vacek, E. P.; Williams, J. C.; Wolanin, D. J.; Woolson, S., Orally Active Trifluoromethyl Ketone Inhibitors of Human Leukocyte Elastase. *J. Med. Chem.* **1997,** *40* (20), 3173-3181.

133. Lechner, S.; Malgapo, M. I. P.; Grätz, C.; Steimbach, R. R.; Baron, A.; Rüther, P.; Nadal, S.; Stumpf, C.; Loos, C.; Ku, X.; Prokofeva, P.; Lautenbacher, L.; Heimburg, T.; Würf, V.; Meng, C.; Wilhelm, M.; Sippl, W.; Kleigrewe, K.; Pauling, J. K.; Kramer, K.; Miller, A. K.; Pfaffl, M. W.; Linder, M. E.; Kuster, B.; Médard, G., Target deconvolution of HDAC pharmacopoeia reveals MBLAC2 as common off-target. *Nature Chemical Biology* **2022,** *18* (8), 812-820.
134. Gong, C.-J.; Gao, A.-H.; Zhang, Y.-M.; Su, M.-B.; Chen, F.; Sheng, L.; Zhou, Y.-B.; Li, J.-Y.; Li, J.; Nan, F.-J., Design, synthesis and biological evaluation of bisthiazole-based trifluoromethyl ketone derivatives as potent HDAC inhibitors with improved cellular efficacy. *Eur. J. Med. Chem.* **2016,** *112*, 81-90.
135. Ontoria, J. M.; Altamura, S.; Di Marco, A.; Ferrigno, F.; Laufer, R.; Muraglia, E.; Palumbi, M. C.; Rowley, M.; Scarpelli, R.; Schultz-Fademrecht, C.; Serafini, S.; Steinkühler, C.; Jones, P., Identification of Novel, Selective, and Stable Inhibitors of Class II Histone Deacetylases. Validation Studies of the Inhibition of the Enzymatic Activity of HDAC4 by Small Molecules as a Novel Approach for Cancer Therapy. *J. Med. Chem.* **2009,** *52* (21), 6782-6789.
136. Jones, P.; Bottomley, M. J.; Carfí, A.; Cecchetti, O.; Ferrigno, F.; Lo Surdo, P.; Ontoria, J. M.; Rowley, M.; Scarpelli, R.; Schultz-Fademrecht, C.; Steinkühler, C., 2-Trifluoroacetylthiophenes, a novel series of potent and selective class II histone deacetylase inhibitors. *Bioorg. Med. Chem. Lett.* **2008,** *18* (11), 3456-3461.
137. Muraglia, E.; Altamura, S.; Branca, D.; Cecchetti, O.; Ferrigno, F.; Orsale, M. V.; Palumbi, M. C.; Rowley, M.; Scarpelli, R.; Steinkühler, C.; Jones, P., 2-Trifluoroacetylthiophene oxadiazoles as potent and selective class II human histone deacetylase inhibitors. *Bioorg. Med. Chem. Lett.* **2008,** *18* (23), 6083-6087.
138. Depetter, Y.; Geurs, S.; Vanden Bussche, F.; De Vreese, R.; Franceus, J.; Desmet, T.; De Wever, O.; D'hooghe, M., Assessment of the trifluoromethyl ketone functionality as an alternative zinc-binding group for selective HDAC6 inhibition. *MedChemComm* **2018,** *9* (6), 1011-1016.
139. Riddhidev, B.; Endri, K.; Sabitri, L.; Kotsull, L. N.; Nishanth, K.; Dragan, I.; Mary Kay H, P.; James, S.; William, T.; L. M. Viranga, T., Rational design of metabolically stable HDAC inhibitors: An overhaul of trifluoromethyl ketones. *Eur. J. Med. Chem.* **2022,** *244*, 114807.
140. Robello, M.; Barresi, E.; Baglini, E.; Salerno, S.; Taliani, S.; Settimo, F. D., The Alpha Keto Amide Moiety as a Privileged Motif in Medicinal Chemistry: Current Insights and Emerging Opportunities. *J. Med. Chem.* **2021,** *64* (7), 3508-3545.
141. Sieburth, S. M.; Nittoli, T.; Mutahi, A. M.; Guo, L., Silanediols: A New Class of Potent Protease Inhibitors. *Angew. Chem. Int. Ed.* **1998,** *37* (6), 812-814.
142. Mutahi, M. w.; Nittoli, T.; Guo, L.; Sieburth, S. M., Silicon-Based Metalloprotease Inhibitors: Synthesis and Evaluation of Silanol and Silanediol Peptide Analogues as Inhibitors of Angiotensin-Converting Enzyme1. *J. Am. Chem. Soc.* **2002,** *124* (25), 7363-7375.
143. Sieburth, S. M.; Chen, C.-A., Silanediol Protease Inhibitors: From Conception to Validation. *European Journal of Organic Chemistry* **2006,** *2006* (2), 311-322.
144. Ortega, P. G. R.; Montejo, M.; González, J. J. L., Study of the chelating properties of Ge(OH)2 functionality as metal binding group for Zn2+ cation in simplified protease-like environments: a DFT analysis. *J. Mol. Model.* **2014,** *20* (9), 2430.
145. Ramesh, R.; Reddy, D. S., Quest for Novel Chemical Entities through Incorporation of Silicon in Drug Scaffolds. *J. Med. Chem.* **2018,** *61* (9), 3779-3798.
146. Davis, D.; Kim, H. M.; Ramphal, J. Y.; Spencer, J. R.; Tai, V. W. F.; Verner, E. J. Silanol derivatives as inhibitors of histone deacetylase. 2006.
147. Traoré, M.; Mietton, F.; Maubon, D.; Peuchmaur, M.; Francisco Hilário, F.; Pereira de Freitas, R.; Bougdour, A.; Curt, A.; Maynadier, M.; Vial, H.; Pelloux, H.; Hakimi, M.-A.; Wong, Y.-S., Flexible Synthesis and Evaluation of Diverse Anti-Apicomplexa Cyclic Peptides. *J. Org. Chem.* **2013,** *78* (8), 3655-3675.
148. Maubon, D.; Bougdour, A.; Wong, Y. S.; Brenier-Pinchart, M. P.; Curt, A.; Hakimi, M. A.; Pelloux, H., Activity of the histone deacetylase inhibitor FR235222 on Toxoplasma gondii: inhibition of

stage conversion of the parasite cyst form and study of new derivative compounds. *Antimicrobial Agents and Chemotherapy* **2010,** *54* (11), 4843-50.
149. Liu, J.; Kelly, J.; Yu, W.; Clausen, D.; Yu, Y.; Kim, H.; Duffy, J. L.; Chung, C. C.; Myers, R. W.; Carroll, S.; Klein, D. J.; Fells, J.; Holloway, M. K.; Wu, J.; Wu, G.; Howell, B. J.; Barnard, R. J. O.; Kozlowski, J. A., Selective Class I HDAC Inhibitors Based on Aryl Ketone Zinc Binding Induce HIV-1 Protein for Clearance. *ACS Med. Chem. Lett.* **2020,** *11* (7), 1476-1483.
150. Porter, N. J.; Christianson, D. W., Binding of the Microbial Cyclic Tetrapeptide Trapoxin A to the Class I Histone Deacetylase HDAC8. *ACS Chem. Biol.* **2017,** *12* (9), 2281-2286.
151. Dhuguru, J.; Zviagin, E.; Skouta, R., FDA-Approved Oximes and Their Significance in Medicinal Chemistry. *Pharmaceuticals (Basel)* **2022,** *15* (1).
152. Quiroga, A. G.; Cubo, L.; de Blas, E.; Aller, P.; Navarro-Ranninger, C., Trans platinum complexes design: one novel water soluble oxime derivative that contains aliphatic amines in trans configuration. *J. Inorg. Biochem.* **2007,** *101* (1), 104-10.
153. Saglam, N.; Colak, A.; Serbest, K.; Dülger, S.; Güner, S.; Karaböcek, S.; Beldüz, A. O., Oxidative cleavage of DNA by homo- and heteronuclear Cu(II)-Mn(II) complexes of an oxime-type ligand. *BioMetals* **2002,** *15* (4), 357-365.
154. Ueda, H.; Nakajima, H.; Hori, Y.; Fujita, T.; Nishimura, M.; Goto, T.; Okuhara, M., FR901228, a novel antitumor bicyclic depsipeptide produced by Chromobacterium violaceum No. 968. I. Taxonomy, fermentation, isolation, physico-chemical and biological properties, and antitumor activity. *J. Antibiot. (Tokyo)* **1994,** *47* (3), 301-10.
155. Ueda, H.; Manda, T.; Matsumoto, S.; Mukumoto, S.; Nishigaki, F.; Kawamura, I.; Shimomura, K., FR901228, a novel antitumor bicyclic depsipeptide produced by Chromobacterium violaceum No. 968. III. Antitumor activities on experimental tumors in mice. *J. Antibiot. (Tokyo)* **1994,** *47* (3), 315-23.
156. Furumai, R.; Matsuyama, A.; Kobashi, N.; Lee, K.-H.; Nishiyama, M.; Nakajima, H.; Tanaka, A.; Komatsu, Y.; Nishino, N.; Yoshida, M.; Horinouchi, S., FK228 (Depsipeptide) as a Natural Prodrug That Inhibits Class I Histone Deacetylases1. *Cancer Res.* **2002,** *62* (17), 4916-4921.
157. Decroos, C.; Clausen, D. J.; Haines, B. E.; Wiest, O.; Williams, R. M.; Christianson, D. W., Variable Active Site Loop Conformations Accommodate the Binding of Macrocyclic Largazole Analogues to HDAC8. *Biochemistry* **2015,** *54* (12), 2126-2135.
158. Cole, K. E.; Dowling, D. P.; Boone, M. A.; Phillips, A. J.; Christianson, D. W., Structural Basis of the Antiproliferative Activity of Largazole, a Depsipeptide Inhibitor of the Histone Deacetylases. *J. Am. Chem. Soc.* **2011,** *133* (32), 12474-12477.
159. Kepp, K. P., A Quantitative Scale of Oxophilicity and Thiophilicity. *Inorg. Chem.* **2016,** *55* (18), 9461-9470.
160. Ondetti, M. A.; Rubin, B.; Cushman, D. W., Design of Specific Inhibitors of Angiotensin-Converting Enzyme: New Class of Orally Active Antihypertensive Agents. *Science* **1977,** *196* (4288), 441-444.
161. Whittaker, M.; Floyd, C. D.; Brown, P.; Gearing, A. J. H., Design and Therapeutic Application of Matrix Metalloproteinase Inhibitors. *Chem. Rev.* **1999,** *99* (9), 2735-2776.
162. Forbes, C.; Shi, Q.; Fisher, J. F.; Lee, M.; Hesek, D.; Llarrull, L. I.; Toth, M.; Gossing, M.; Fridman, R.; Mobashery, S., Active site ring-opening of a thiirane moiety and picomolar inhibition of gelatinases. *Chem. Biol. Drug Des.* **2009,** *74* (6), 527-34.
163. Brown, S.; Bernardo, M. M.; Li, Z.-H.; Kotra, L. P.; Tanaka, Y.; Fridman, R.; Mobashery, S., Potent and Selective Mechanism-Based Inhibition of Gelatinases. *J. Am. Chem. Soc.* **2000,** *122* (28), 6799-6800.
164. Chen, B.; Petukhov, P. A.; Jung, M.; Velena, A.; Eliseeva, E.; Dritschilo, A.; Kozikowski, A. P., Chemistry and biology of mercaptoacetamides as novel histone deacetylase inhibitors. *Bioorg. Med. Chem. Lett.* **2005,** *15* (5), 1389-1392.
165. Kozikowski, A. P.; Chen, Y.; Gaysin, A. M.; Savoy, D. N.; Billadeau, D. D.; Kim, K. H., Chemistry, Biology, and QSAR Studies of Substituted Biaryl Hydroxamates and Mercaptoacetamides as HDAC Inhibitors—Nanomolar-Potency Inhibitors of Pancreatic Cancer Cell Growth. *ChemMedChem* **2008,** *3* (3), 487-501.

166. Kozikowski, A. P.; Chen, Y.; Gaysin, A.; Chen, B.; D'Annibale, M. A.; Suto, C. M.; Langley, B. C., Functional Differences in Epigenetic ModulatorsSuperiority of Mercaptoacetamide-Based Histone Deacetylase Inhibitors Relative to Hydroxamates in Cortical Neuron Neuroprotection Studies. *J. Med. Chem.* **2007,** *50* (13), 3054-3061.
167. Kalin, J. H.; Zhang, H.; Gaudrel-Grosay, S.; Vistoli, G.; Kozikowski, A. P., Chiral mercaptoacetamides display enantioselective inhibition of histone deacetylase 6 and exhibit neuroprotection in cortical neuron models of oxidative stress. *ChemMedChem* **2012,** *7* (3), 425-39.
168. Stolfa, D. A.; Marek, M.; Lancelot, J.; Hauser, A. T.; Walter, A.; Leproult, E.; Melesina, J.; Rumpf, T.; Wurtz, J. M.; Cavarelli, J.; Sippl, W.; Pierce, R. J.; Romier, C.; Jung, M., Molecular basis for the antiparasitic activity of a mercaptoacetamide derivative that inhibits histone deacetylase 8 (HDAC8) from the human pathogen schistosoma mansoni. *Journal of Molecular Biology* **2014,** *426* (20), 3442-53.
169. Lv, W.; Zhang, G.; Barinka, C.; Eubanks, J. H.; Kozikowski, A. P., Design and Synthesis of Mercaptoacetamides as Potent, Selective, and Brain Permeable Histone Deacetylase 6 Inhibitors. *ACS Med. Chem. Lett.* **2017,** *8* (5), 510-515.
170. Tavares, M. T.; Kozikowski, A. P.; Shen, S., Mercaptoacetamide: A promising zinc-binding group for the discovery of selective histone deacetylase 6 inhibitors. *Eur. J. Med. Chem.* **2021,** *209*, 112887.
171. Hassig, C. A.; Symons, K. T.; Guo, X.; Nguyen, P.-M.; Annable, T.; Wash, P. L.; Payne, J. E.; Jenkins, D. A.; Bonnefous, C. l.; Trotter, C.; Wang, Y.; Anzola, J. V.; Milkova, E. L.; Hoffman, T. Z.; Dozier, S. J.; Wiley, B. M.; Saven, A.; Malecha, J. W.; Davis, R. L.; Muhammad, J.; Shiau, A. K.; Noble, S. A.; Rao, T. S.; Smith, N. D.; Hager, J. H., KD5170, a novel mercaptoketone-based histone deacetylase inhibitor that exhibits broad spectrum antitumor activity in vitro and in vivo. *Mol. Cancer Ther.* **2008,** *7* (5), 1054-1065.
172. Marek, M.; Kannan, S.; Hauser, A. T.; Moraes Mourão, M.; Caby, S.; Cura, V.; Stolfa, D. A.; Schmidtkunz, K.; Lancelot, J.; Andrade, L.; Renaud, J. P.; Oliveira, G.; Sippl, W.; Jung, M.; Cavarelli, J.; Pierce, R. J.; Romier, C., Structural basis for the inhibition of histone deacetylase 8 (HDAC8), a key epigenetic player in the blood fluke Schistosoma mansoni. *PLoS Pathog.* **2013,** *9* (9), e1003645.
173. Porter, N. J.; Shen, S.; Barinka, C.; Kozikowski, A. P.; Christianson, D. W., Molecular Basis for the Selective Inhibition of Histone Deacetylase 6 by a Mercaptoacetamide Inhibitor. *ACS Med. Chem. Lett.* **2018,** *9* (12), 1301-1305.
174. Saleh Ahmed, C. C., Scott Cuthill, Graham Dawson, William Gattrell, Mario Lobell, Neil Pegg, Imaad Saba, Simon Swain, Claire Thomas, Graham Wynne Mercaptoamides as histone deacetylase inhibitors. US20060047123A1, 2006.
175. Segretti, M. C. F.; Vallerini, G. P.; Brochier, C.; Langley, B.; Wang, L.; Hancock, W. W.; Kozikowski, A. P., Thiol-Based Potent and Selective HDAC6 Inhibitors Promote Tubulin Acetylation and T-Regulatory Cell Suppressive Function. *ACS Med. Chem. Lett.* **2015,** *6* (11), 1156-1161.
176. Dehmel, F.; Weinbrenner, S.; Julius, H.; Ciossek, T.; Maier, T.; Stengel, T.; Fettis, K.; Burkhardt, C.; Wieland, H.; Beckers, T., Trithiocarbonates as a novel class of HDAC inhibitors: SAR studies, isoenzyme selectivity, and pharmacological profiles. *J. Med. Chem.* **2008,** *51* (13), 3985-4001.
177. Moree, W. J.; van der Marel, G. A.; Liskamp, R. M. J., Peptides containing a sulfinamide or a sulfonamide moiety: New transition-state analogues. *Tetrahedron Letters* **1991,** *32* (3), 409-412.
178. Allmendinger, T.; Felder, E.; Hungarbühler, E., Fluoroolefin dipeptide isosteres -II.: Enantioselectlve synthesis of both antipodes of the phe-gly dlpeptide mimic. *Tetrahedron Letters* **1990,** *31* (50), 7301-7304.
179. Morand, S.; Jubault, P.; Bouillon, J.-P.; Couve-Bonnaire, S., gem-Heteroatom-Substituted Fluoroalkenes as Mimics of Amide Derivatives or Phosphates: A Comprehensive Review. *Chem. Eur. J.* **2021,** *27* (69), 17273-17292.
180. Abraham, R. J.; Ellison, S. L. R.; Schonholzer, P.; Thomas, W. A., A theoretical and crystallographic study of the geometries and conformations of fluoro-olefins as peptide analogues. *Tetrahedron* **1986,** *42* (7), 2101-2110.

181. Cieplak, P.; Kollman, P. A.; Radomski, J. P., Molecular Design of Fluorine-Containing Peptide Mimetics. In *Biomedical Frontiers of Fluorine Chemistry*, American Chemical Society: 1996; Vol. 639, pp 143-156.
182. Jacobsen, N. E.; Bartlett, P. A., A phosphonamidate dipeptide analog as an inhibitor of carboxypeptidase A. *J. Am. Chem. Soc.* **1981,** *103* (3), 654-657.
183. Vanommeslaeghe, K.; Loverix, S.; Geerlings, P.; Tourwé, D., DFT-based ranking of zinc-binding groups in histone deacetylase inhibitors. *Biorg. Med. Chem.* **2005,** *13* (21), 6070-6082.
184. Nkabyo, H. A.; Barnard, I.; Koch, K. R.; Luckay, R. C., Recent advances in the coordination and supramolecular chemistry of monopodal and bipodal acylthiourea-based ligands. *Coord. Chem. Rev.* **2021,** *427*, 213588.
185. Haggarty, S. J.; Koeller, K. M.; Wong, J. C.; Butcher, R. A.; Schreiber, S. L., Multidimensional Chemical Genetic Analysis of Diversity-Oriented Synthesis-Derived Deacetylase Inhibitors Using Cell-Based Assays. *Chem. Biol.* **2003,** *10* (5), 383-396.
186. Wong, J. C.; Hong, R.; Schreiber, S. L., Structural Biasing Elements for In-Cell Histone Deacetylase Paralog Selectivity. *J. Am. Chem. Soc.* **2003,** *125* (19), 5586-5587.
187. Stockwell, B.; Haggarty, S.; Schreiber, S., High-throughput screening of small molecules in miniaturized mammalian cell-based assays involving post-translational modifications. *Chem. Biol.* **1999,** *6*, 71-83.
188. Wagner, F. F.; Weïwer, M.; Lewis, M. C.; Holson, E. B., Small Molecule Inhibitors of Zinc-dependent Histone Deacetylases. *Neurotherapeutics* **2013,** *10* (4), 589-604.
189. Rai, M.; Soragni, E.; Chou, C. J.; Barnes, G.; Jones, S.; Rusche, J. R.; Gottesfeld, J. M.; Pandolfo, M., Two new pimelic diphenylamide HDAC inhibitors induce sustained frataxin upregulation in cells from Friedreich's ataxia patients and in a mouse model. *PLoS One* **2010,** *5* (1), e8825.
190. Hildmann, C.; Wegener, D.; Riester, D.; Hempel, R.; Schober, A.; Merana, J.; Giurato, L.; Guccione, S.; Nielsen, T. K.; Ficner, R.; Schwienhorst, A., Substrate and inhibitor specificity of class 1 and class 2 histone deacetylases. *J. Biotechnol.* **2006,** *124* (1), 258-270.
191. Thaler, F.; Mercurio, C., Towards Selective Inhibition of Histone Deacetylase Isoforms: What Has Been Achieved, Where We Are and What Will Be Next. *Chemmedchem* **2014,** *9* (3), 523-536.
192. Bressi, J. C.; Jennings, A. J.; Skene, R.; Wu, Y.; Melkus, R.; Jong, R. D.; O'Connell, S.; Grimshaw, C. E.; Navre, M.; Gangloff, A. R., Exploration of the HDAC2 foot pocket: Synthesis and SAR of substituted N-(2-aminophenyl)benzamides. *Bioorg. Med. Chem. Lett.* **2010,** *20* (10), 3142-3145.
193. Rai, M.; Soragni, E.; Jenssen, K.; Burnett, R.; Herman, D.; Coppola, G.; Geschwind, D. H.; Gottesfeld, J. M.; Pandolfo, M., HDAC inhibitors correct frataxin deficiency in a Friedreich ataxia mouse model. *PLoS One* **2008,** *3* (4), e1958.
194. Thomas, E. A.; Coppola, G.; Desplats, P. A.; Tang, B.; Soragni, E.; Burnett, R.; Gao, F.; Fitzgerald, K. M.; Borok, J. F.; Herman, D.; Geschwind, D. H.; Gottesfeld, J. M., The HDAC inhibitor 4b ameliorates the disease phenotype and transcriptional abnormalities in Huntington's disease transgenic mice. *Proc Natl Acad Sci U S A* **2008,** *105* (40), 15564-9.
195. Chou, C. J.; Herman, D.; Gottesfeld, J. M., Pimelic diphenylamide 106 is a slow, tight-binding inhibitor of class I histone deacetylases. *J Biol Chem* **2008,** *283* (51), 35402-9.
196. Wang, Y.; Stowe, Ryan L.; Pinello, Christie E.; Tian, G.; Madoux, F.; Li, D.; Zhao, Lisa Y.; Li, J.-L.; Wang, Y.; Wang, Y.; Ma, H.; Hodder, P.; Roush, William R.; Liao, D., Identification of Histone Deacetylase Inhibitors with Benzoylhydrazide Scaffold that Selectively Inhibit Class I Histone Deacetylases. *Chem. Biol.* **2015,** *22* (2), 273-284.
197. Li, X.; Jiang, Y.; Peterson, Y. K.; Xu, T.; Himes, R. A.; Luo, X.; Yin, G.; Inks, E. S.; Dolloff, N.; Halene, S.; Chan, S. S. L.; Chou, C. J., Design of Hydrazide-Bearing HDACIs Based on Panobinostat and Their p53 and FLT3-ITD Dependency in Antileukemia Activity. *J. Med. Chem.* **2020,** *63* (10), 5501-5525.
198. Nelson, S. D.; Mitchell, J. R.; Snodgrass, W. R.; Timbrell, J. A., Hepatotoxicity and metabolism of iproniazid and isopropylhydrazine. *Journal of Pharmacology and Experimental Therapeutics* **1978,** *206* (3), 574-85.
199. Gowda, R.; Madhunapantula, S. V.; Desai, D.; Amin, S.; Robertson, G. P., Selenium-containing histone deacetylase inhibitors for melanoma management. *Cancer Biol. Ther.* **2012,** *13* (9), 756-765.

200. Karelia, N.; Desai, D.; Hengst, J. A.; Amin, S.; Rudrabhatla, S. V.; Yun, J., Selenium-containing analogs of SAHA induce cytotoxicity in lung cancer cells. *Bioorg. Med. Chem. Lett.* **2010,** *20* (22), 6816-6819.
201. Cook, G. R.; Manivannan, E.; Underdahl, T.; Lukacova, V.; Zhang, Y.; Balaz, S., Synthesis and evaluation of novel oxazoline MMP inhibitors. *Bioorg. Med. Chem. Lett.* **2004,** *14* (19), 4935-4939.
202. Oh, S.; Jung, J.-C.; Avery, M. A., Synthesis of New β-Lactam Analogs and Evaluation of Their Histone Deacetylase (HDAC) Activity. *Zeitschrift für Naturforschung B* **2007,** *62* (11), 1459-1464.
203. Decuyper, L.; Jukič, M.; Sosič, I.; Žula, A.; D'hooghe, M.; Gobec, S., Antibacterial and β-Lactamase Inhibitory Activity of Monocyclic β-Lactams. *Med. Res. Rev.* **2018,** *38* (2), 426-503.
204. Cainelli, G.; Galletti, P.; Garbisa, S.; Giacomini, D.; Sartor, L.; Quintavalla, A., 4-Alkyliden-β-lactams conjugated to polyphenols: Synthesis and inhibitory activity. *Biorg. Med. Chem.* **2005,** *13* (22), 6120-6132.
205. Schwartz, L. M.; Howard, L. O., Conductance study of squaric acid aqueous dissociation. *J. Phys. Chem.* **1971,** *75* (12), 1798-1803.
206. Onaran, M. B.; Comeau, A. B.; Seto, C. T., Squaric Acid-Based Peptidic Inhibitors of Matrix Metalloprotease-1. *J. Org. Chem.* **2005,** *70* (26), 10792-10802.
207. Elliott, T.; Slowey, A.; Ye, Y.; Conway, S., The use of phosphate bioisosteres in medicinal chemistry and chemical biology. *MedChemComm* **2012,** *3*.
208. Chasák, J.; Šlachtová, V.; Urban, M.; Brulíková, L., Squaric acid analogues in medicinal chemistry. *Eur. J. Med. Chem.* **2021,** *209*, 112872.
209. Agnew-Francis, K. A.; Williams, C. M., Squaramides as Bioisosteres in Contemporary Drug Design. *Chem. Rev.* **2020,** *120* (20), 11616-11650.
210. Lim, N. C.; Morton, M. D.; Jenkins, H. A.; Brückner, C., Squaric Acid N-Hydroxylamides: Synthesis, Structure, and Properties of Vinylogous Hydroxamic Acid Analogues. *J. Org. Chem.* **2003,** *68* (24), 9233-9241.
211. Moreno-Yruela, C.; Fass, D. M.; Cheng, C.; Herz, J.; Olsen, C. A.; Haggarty, S. J., Kinetic Tuning of HDAC Inhibitors Affords Potent Inducers of Progranulin Expression. *ACS Chem. Neurosci.* **2019,** *10* (8), 3769-3777.
212. Kitir, B.; Maolanon, A. R.; Ohm, R. G.; Colaço, A. R.; Fristrup, P.; Madsen, A. S.; Olsen, C. A., Chemical Editing of Macrocyclic Natural Products and Kinetic Profiling Reveal Slow, Tight-Binding Histone Deacetylase Inhibitors with Picomolar Affinities. *Biochemistry* **2017,** *56* (38), 5134-5146.
213. Beshore, D. C.; Adam, G. C.; Barnard, R. J. O.; Burlein, C.; Gallicchio, S. N.; Holloway, M. K.; Krosky, D.; Lemaire, W.; Myers, R. W.; Patel, S.; Plotkin, M. A.; Powell, D. A.; Rada, V.; Cox, C. D.; Coleman, P. J.; Klein, D. J.; Wolkenberg, S. E., Redefining the Histone Deacetylase Inhibitor Pharmacophore: High Potency with No Zinc Cofactor Interaction. *ACS Med. Chem. Lett.* **2021,** *12* (4), 540-547.
214. Borgonetti, V.; Governa, P.; Manetti, F.; Galeotti, N., Zingiberene, a non-zinc-binding class I HDAC inhibitor: A novel strategy for the management of neuropathic pain. *Phytomedicine* **2023,** *111*, 154670.
215. Wagner, F. F.; Olson, D. E.; Gale, J. P.; Kaya, T.; Weïwer, M.; Aidoud, N.; Thomas, M.; Davoine, E. L.; Lemercier, B. C.; Zhang, Y.-L.; Holson, E. B., Potent and Selective Inhibition of Histone Deacetylase 6 (HDAC6) Does Not Require a Surface-Binding Motif. *J. Med. Chem.* **2013,** *56* (4), 1772-1776.
216. Liu, J.; Yu, Y.; Kelly, J.; Sha, D.; Alhassan, A.-B.; Yu, W.; Maletic, M. M.; Duffy, J. L.; Klein, D. J.; Holloway, M. K.; Carroll, S.; Howell, B. J.; Barnard, R. J. O.; Wolkenberg, S.; Kozlowski, J. A., Discovery of Highly Selective and Potent HDAC3 Inhibitors Based on a 2-Substituted Benzamide Zinc Binding Group. *ACS Med. Chem. Lett.* **2020,** *11* (12), 2476-2483.
217. Cellupica, E.; Caprini, G.; Cordella, P.; Cukier, C.; Fossati, G.; Marchini, M.; Rocchio, I.; Sandrone, G.; Vanoni, M. A.; Vergani, B.; Źrubek, K.; Stevenazzi, A.; Steinkühler, C., Difluoromethyl-1,3,4-oxadiazoles are slow-binding substrate analog inhibitors of histone deacetylase 6 with unprecedented isotype selectivity. *J. Biol. Chem.* **2023,** *299* (1), 102800.

218. Faridoon; Zha, Y.; Zhang, G.; Li, J., Medicinal chemistry insights into non-hydroxamate HDAC6 selective inhibitors. *Med. Chem. Res.* **2022,** *32*, 1-14.